



# UNIVERSITÀ DEGLI STUDI DI PALERMO

PhD Course in Biomedicine and Neuroscience

Dipartimento di Biomedicina, Neuroscienze e Diagnostica avanzata

(BiND) SSD BIO/10

**Effects of 5-Azacidine on Dnmt2/Trdmt1 expression and  
reticulum endoplasmic stress induction in cellular models of  
insulinoma.**

**LA CANDIDATA**

**Dott.ssa Kamila Filip**

**IL COORDINATORE**

**Prof. Fabio Bucchieri**

**TUTOR**

**Prof.ssa Marianna Lauricella**

**Co-tutor**

**Prof.ssa Claudia Campanella**

**XXXIII CYCLE**

**ACHIEVEMENT YEAR TITLE 2020/2021**

# List of contents

Abstract.....	4
1. Introduction.....	7
1.1 The pancreas .....	8
1.2 Insulin: synthesis and functions .....	9
1.3 Pancreatic diseases – contemporary hassle and the approach to cope with it.....	14
1.4 Endoplasmic reticulum (ER) .....	20
1.5 Trdmt1 and tRNA methylation.....	27
1.6 Aging and cell senescence.....	30
2. Aim of the study .....	33
3. Materials and methods .....	36
3.1 Cell lines and in vitro cell culture methods .....	37
3.2 Cytotoxicity .....	38
3.3 Apoptosis .....	39
3.4 Senescence-associated $\beta$ -galactosidase activity (SA- $\beta$ -gal) .....	39
3.5 Cell cycle.....	40
3.6 Oxidative stress .....	40
3.7 Nitrosative stress.....	41
3.9 Cell lysates and protein concentration evaluation.....	43
3.10 Western blotting .....	43
3.11 Protein aggregation .....	44
3.12 Flow cytometry .....	44
3.13 Laser-based confocal imaging .....	45
3.14 Confocal imaging .....	46
3.15 Statistical analysis.....	46
4. Results .....	47

<b>4.1</b>	<b>HP and 5-AzaC treatment induce changes in senescence and cell cycle inhibition in pancreatic <math>\beta</math>-cells .....</b>	<b>48</b>
<b>4.2</b>	<b>Characterization of an oxidative and nitrosative stress.....</b>	<b>51</b>
<b>4.2.1</b>	<b>Oxidative stress.....</b>	<b>51</b>
<b>4.2.2</b>	<b>FOXO3a elevated level after stress induction and methylation inhibition .</b>	<b>52</b>
<b>4.2.3</b>	<b>Nitrosative stress .....</b>	<b>56</b>
<b>4.3</b>	<b>HP and 5-AzaC induced apoptosis in pancreatic <math>\beta</math>-cells.....</b>	<b>58</b>
<b>4.4</b>	<b>5-Azacidine mediated alterations in protein production and localization in pancreatic <math>\beta</math>-cells .....</b>	<b>60</b>
<b>4.4.1</b>	<b>5-AzaC mediated activation of ER stress pathway and prevents creating protein aggregates in insulinoma.....</b>	<b>60</b>
<b>4.4.2</b>	<b>Autophagy mediated cell death activation in NIT-1 cell line upon HP and 5-AzaC treatment .....</b>	<b>63</b>
<b>4.4.3</b>	<b>HP and 5-AzaC mediated Phospho-S6 downregulation .....</b>	<b>65</b>
<b>4.4.4</b>	<b>Changes in Trdmt1 expression and localization in pancreatic <math>\beta</math>-cells .....</b>	<b>68</b>
<b>4.4.5</b>	<b>Increased colocalization of Dnmt2/Trdmt1 and p-eiF2<math>\alpha</math> in pancreatic <math>\beta</math>-cells under HP mediated cellular stress and tRNA methylation inhibition .....</b>	<b>70</b>
<b>4.4.6</b>	<b>Trdmt1 does not localize in an endoplasmic reticulum .....</b>	<b>72</b>
<b>4.4.7</b>	<b>5-Azac treatment increases insulin production in pancreatic <math>\beta</math>-cells .....</b>	<b>73</b>
<b>5.</b>	<b>Discussion.....</b>	<b>76</b>
	<b>Conclusions.....</b>	<b>85</b>
	<b>Literature.....</b>	<b>86</b>

# Abstract

Diabetes mellitus affects people all over the world of all ages or social groups making it a worldwide healthcare challenge. Moreover, untreated or badly treated diabetes carries a risk of serious complications including premature death (IDF Diabetes Atlas 9th edition, 2019). The main symptom of diabetes is insulin secretion and/or action disorder leading to hyperglycemia what results in impaired carbohydrate, fat, and protein metabolism (“Diagnosis and Classification of Diabetes Mellitus,” 2013).

Dnmt2/Trdmt1 in its structure and sequence is similar to DNA methyltransferases, however, it has been shown that mainly methylates aspartic acid transfer RNA, specifically at the cytosine-38 residue (Goll et al., 2006; Okano et al., 1998). tRNA methylation ensures accurate protein synthesis, tRNA structure stabilization, codon-anticodon interaction strengthening, and prevention from any mistakes in a frameshift (Hori, 2014). Different tRNA deficiency and various enzymes modifying ribonucleotides in tRNAs can disturb ER function. In the presented study we wanted to explore the potential role of 5-Azacytidine and Dnmt2/Trdmt1 in pancreatic  $\beta$ -cells.

To investigate Trdmt1, ER stress, senescence, and aging and potential implications in diabetes insulin production and but also possible promotion of senescent cells elimination, insulinoma pancreatic  $\beta$ -cells were treated with two compounds: hydrogen peroxide, a well-known pro-oxidant inducing aging, and SISP, and 5-Azacytidine, an inhibitor of DNA methylation and tRNA methylation suppressor at C38 position which is a major Trdmt1 target (Lewinska et al., 2018; Schaefer et al., 2009).

In the presented study two insulin secreting pancreatic  $\beta$ -cell lines were treated with hydrogen peroxide and 5-Azacytidine. NIT-1 is an insulinoma cell line established from NOD/Lt (nonobese diabetic) mice and transgenic for the SV40 T-antigen. BetaTC6 is derived from insulinoma transgenic mice expressing SV40 T-antigen. Both cell lines secrete insulin in a response to the presence of glucose in the medium. Moreover, NIT-1 spontaneously develops type 1 diabetes what makes it a good model to understand T1D pathogenesis and treatment (Pearson et al., 2016; Poirout et al., 1995).

Presented results indicate 5-AzaC mediated endoplasmic reticulum stress in pancreatic  $\beta$ -cells thus UPR and UPS activation. 5-AzaC induced tRNA methylation inhibition at the Trdmt1 target site in T1D representative leads to ER stress mediated autophagy pathway which prevents apoptosis and maintains proliferation rate. Furthermore, 5-AzaC boosted

insulin production in the non-obese diabetic cell line. It has been shown that BetaTC6 cells are more vulnerable to stress and HP induced excessive NO production, ER stress, and related activation of apoptotic cell death pathway and decreased proliferation. Moreover, HP mediated premature senescence, signaling inhibition, and proliferation blockage of senescent cells indicates its senostatic activity and HP/5-AzaC mediated selective elimination of senescent cells treatment demonstrates senolytic activity. Additionally, Trdmt1 may help to cope with the cellular stress induction either by augmented translocation to the cytoplasm or increased biosynthesis. 5-AzaC modulates insulin secretion by senescent insulinoma cells and enhanced insulin production in the NOD cell line may be considered as a factor preventing T1D. The combined therapy of prooxidants and 5-AzaC can be studied as a promising candidate for insulinoma treatment.

## **Acknowledgments**

*I would like to acknowledge all the people who were an important part of my Ph.D. journey at the University of Palermo, Italy. I wish to thank Prof. Marianna Lauricella, Prof. Claudia Campanella as my thesis tutors and responsible for my research activity. I would like to mention Prof. Francesco Cappello for giving me the opportunity to be a part of Unipa. Here, I would like to send my warmest thanks to Prof. Antonella Marino-Gamazza for mentoring me during my research and being very supportive.*

*The experimental part of the Ph.D. thesis (about the role of Dnmt2/Trdmt1 in insulinoma cells) was partly supported by OPUS 13 Grant number UMO-2017/25/B/NZ2/01983 from National Science Center (Poland) within scientific collaboration with Prof. Maciej Wnuk Lab (University of Rzeszow, Poland) to whom I would like to express my special thanks. I would like to acknowledge given me the possibility to realize most of the experimental part at the University of Poland, for the support, and all the precious scientific advice. I would like to thank the entire Polish laboratory team, especially Prof. Anna Lewinska and Dr. Jagoda Adamczyk-Grochala for all the help.*

*To my family, my parents and sister but also my best friends I made in Palermo, Konstantinos Mantalovas, Iain Dunn, and in particular Ronald Roberts who was my great support when things seemed to be hopeless.*

# **1. Introduction**

## 1.1 The pancreas

The pancreas is a dual-function gland combining two glands in one: an exocrine and an endocrine. The location of the pancreas is directly dictated by its significant role in the digestion process. The pancreas lies in the upper part of the abdomen behind the stomach (Yuan et al., 2021). It is an elongated organ whose widest left part called the head lies against the C-shaped duodenum. The next short part of the pancreas connecting the head with the body is the neck. The tapered body of the pancreas goes slightly upward and as the last part narrows till the end is called the tail and is located close to the spleen (Longnecker, 2021; *The Pancreas: An Integrated Textbook of Basic Science, Medicine, and Surgery*, n.d.). From the front, it is separated from the stomach by the omental bursa. Only the anterior part and the tail of the pancreas are covered with peritoneum but posteriorly is uncovered with peritoneum. The main pancreatic duct (Wirsung) goes through the entire pancreas from the tail to the head where it connects with the bile duct creating the hepatopancreatic duct (the ampulla of Vater). The accessory duct connects with the main duct at the level of the pancreatic neck and opens into the duodenum at the minor duodenal papilla (Beger et al., 2009; Yuan et al., 2021). The main pancreatic mass is an exocrine part which contains distributed throughout the parenchyma an endocrine part. The exocrine pancreas responsible for digestion is composed out of acinar cells secreting digestive enzymes like proteinases, lipases, and amylases. A secreted liquid containing a mix of digestive enzymes, also called pancreatic juice, flows through the pancreatic duct to a duodenum. The endocrine portion grouped into islets (Langerhans islets) represents only 3 % of the total pancreatic mass (Figure 1). Islets are mainly located near the center of the lobule and each of them contains approximately 1 – 3 thousand cells although there have been also found very small islets containing about 10 cells or even a single cell distributed among glandular vesicles. Both islets and surrounding exocrine pancreatic lobules are penetrated by fenestrated capillaries that allow the release of the hormones. Pancreatic islets are composed out of a mix of 5 different types of cells ( $\alpha$ ,  $\beta$ ,  $\delta$ ,  $\epsilon$ , and PP cells). The endocrine pancreas synthesizes and secretes into the bloodstream a hormone GHREL ( $\epsilon$ -cells) and 4 hormones responsible for maintaining the glucose level in the blood: glucagon ( $\alpha$ -cells), insulin ( $\beta$ -cells), somatostatin ( $\delta$ -cells), and 36-amino-acid linear polypeptide called pancreatic polypeptide (PP cells). The most common cells present in the Langerhans islands are insulin-secreting  $\beta$ -cells. The total content of those cells among all pancreatic endocrine cells reaches 80 %. Those cells are mostly found in the center of the islets (Haschek et al., 2009).



All of the cells in the mammalian organism have insulin receptors on their membrane.

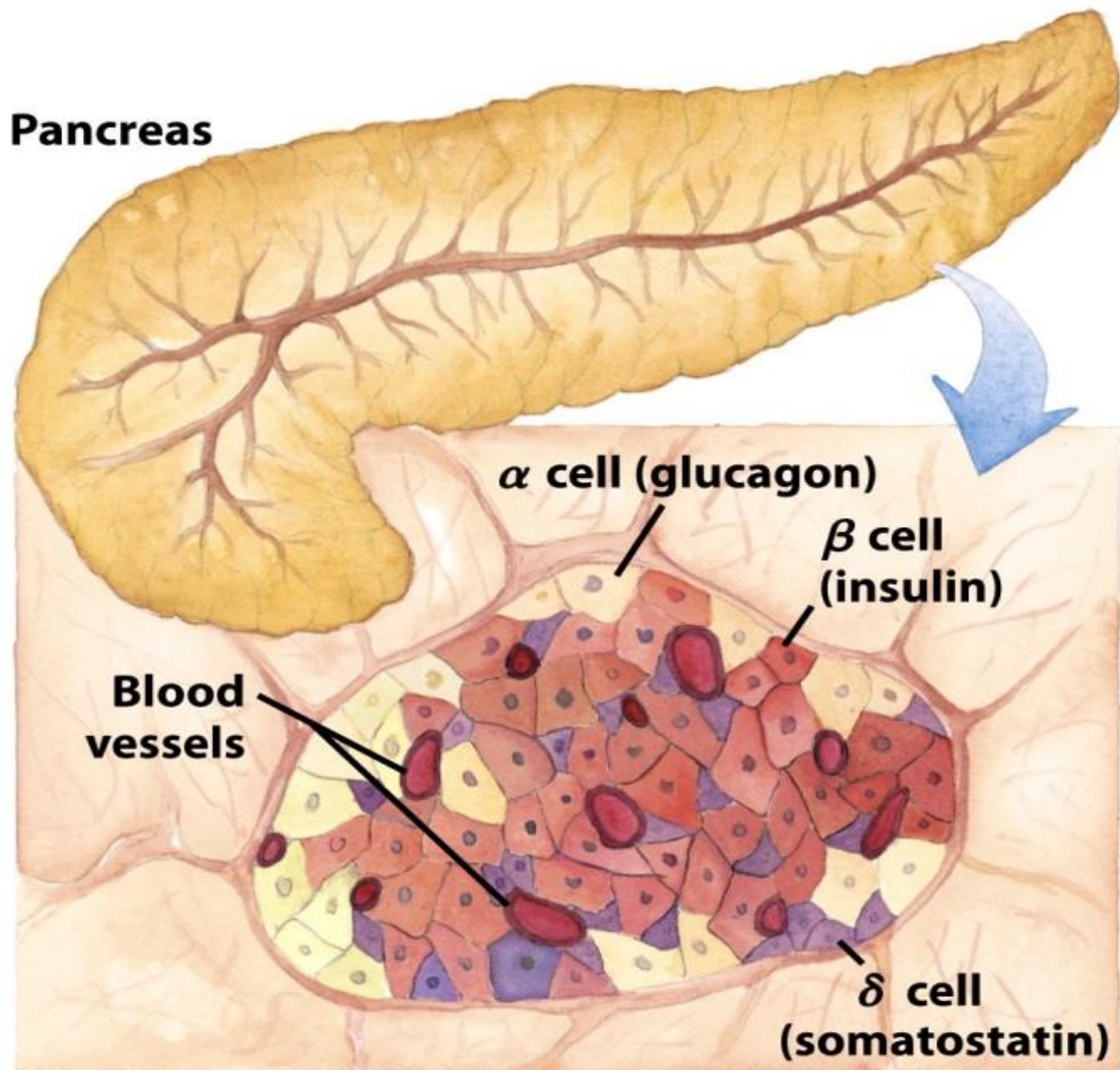


**Figure 23-27**  
*Lehninger Principles of Biochemistry, Fifth Edition*  
© 2008 W. H. Freeman and Company

**Figure 1. Langerhans islets of the pancreas (Nelson 1942-, 2005).**

### **1.2 Insulin: synthesis and functions**

Insulin is a small peptide hormone composed of 51 amino acids divided into two chains: an A chain (21 amino acids) and a B chain (30 amino acids) bounded by disulfide bonds. At first, it is translated from mRNA in the cytosol as a 110 amino-acids long single chain pre-proinsulin. During translocation into the endoplasmic reticulum, the signal peptide is removed what gives a rise to proinsulin. Formed prohormone has an extra C chain and a total content of 74 amino-acids. C chain is detached from the proinsulin molecule in the

endoplasmic reticulum of  $\beta$ -cells then A, and B chains are linked together forming the active hormone – insulin (Weiss et al., 2000) (Robert D. Utiger, 2020) (Figure 2).

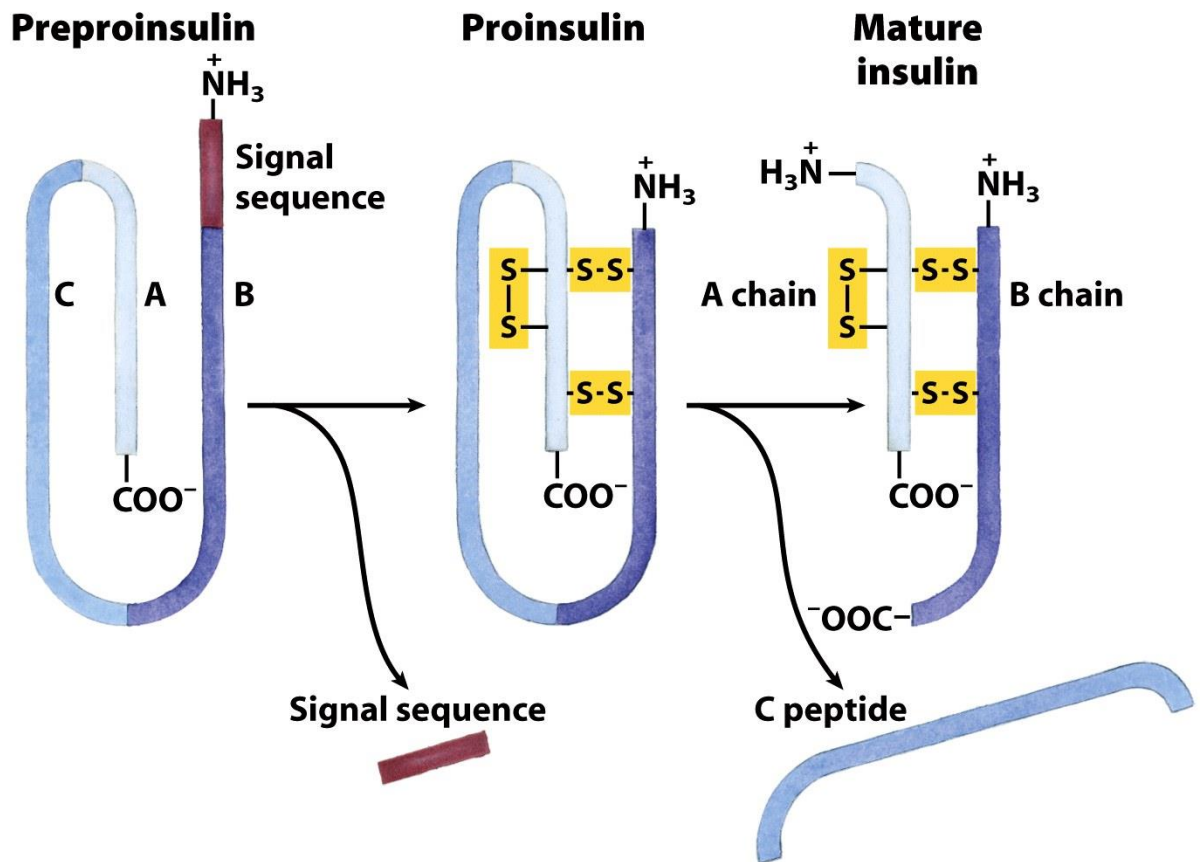


**Figure 23-5**  
*Lehninger Principles of Biochemistry, Fifth Edition*  
 © 2008 W.H. Freeman and Company

**Figure 2. Insulin synthesis (Nelson 1942-, 2005).**

Insulin acts as a hypoglycemic hormone. The glucose level in the blood is regulated by insulin which concentration in the blood changes in parallel. Hyperglycaemia increases insulin production by pancreatic  $\beta$ -cells what quickly leads to hypoglycemia. Changes in insulin release are coupled to changes in  $\beta$ -cells metabolism via metabolic regulation of the activity of the ATP-sensitive potassium (KATP) channel. When glucose levels rise, the oxidation of glucose by  $\beta$ -cells increases the cellular ATP levels. This causes closure of KATP channels, which leads to membrane depolarization, activation of voltage-dependent  $Ca^{+2}$  channels,  $Ca^{+2}$  entry which triggers insulin secretion (Freeman, 2006) (Figure 3).

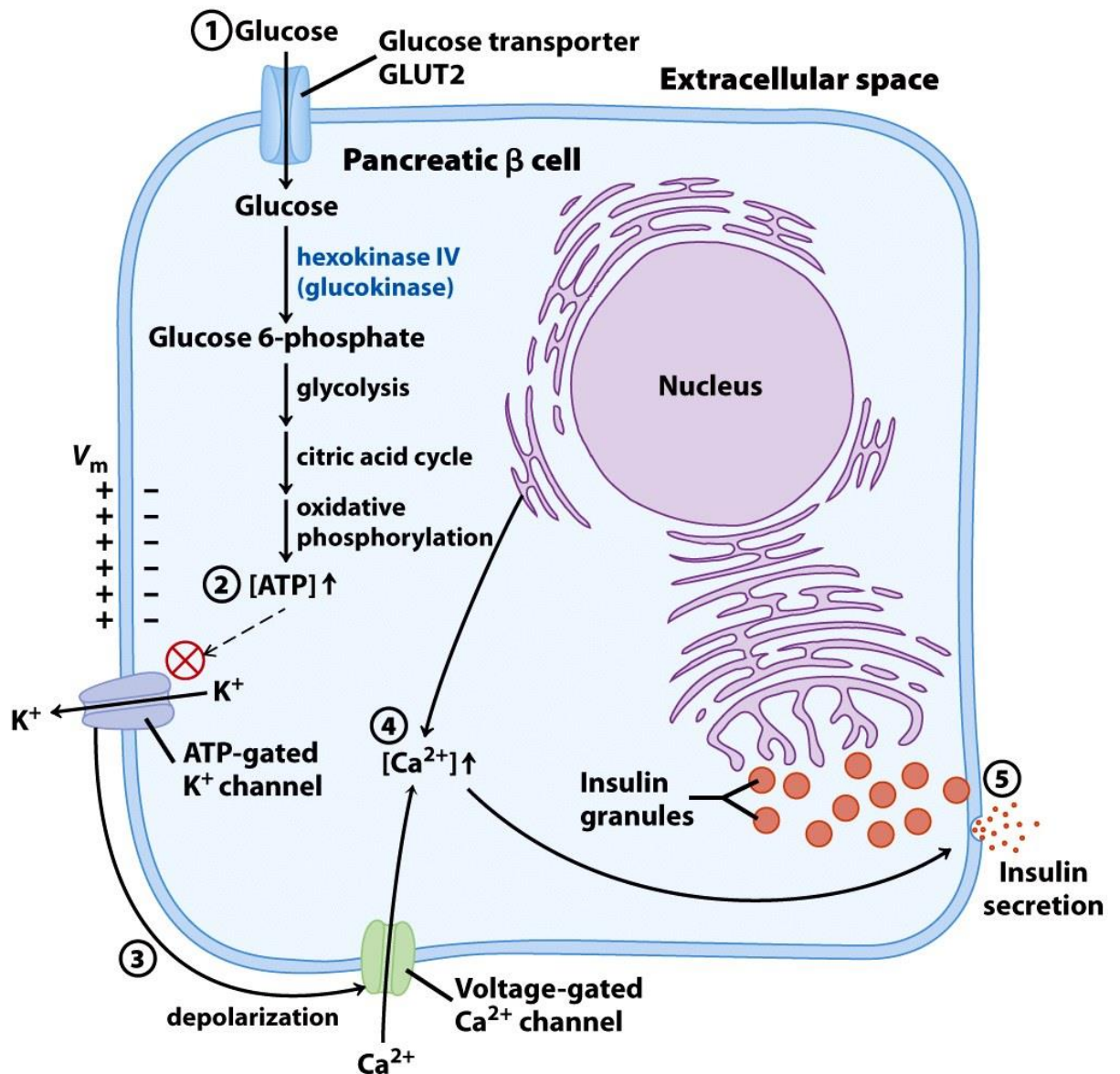


**Figure 23-28**  
*Lehninger Principles of Biochemistry, Fifth Edition*  
 © 2008 W.H. Freeman and Company

**Figure 3. Mechanism of glucose-stimulated insulin secretion in pancreatic β-cells (Nelson 1942-, 2005).**

Insulin secretion is not regulated only by glucose but also other substances like amino acids, free fatty acids, glucagon or secretin activate its secretion, and for instance, adrenalin and noradrenalin which decrease insulin secretion. Insulin is an antagonist of another pancreatic hormone – glucagon whose production is stimulated by hypoglycemia and inhibited by increased glucose level in blood (Murray et al., 2015; Popkin, 2015).

Insulin does not have a direct impact on glucose penetration into the cells, except for adipocytes and muscle cells where it increases glucose uptake. Insulin decreases the blood glucose level promoting glycolysis, glycogen synthesis, and the pentose phosphate pathway. Furthermore, insulin stimulates different anabolic processes, like lipogenesis and protein synthesis. The effect of insulin is exerted in particular in three tissues: muscle, liver, and adipose tissue. In the muscle, insulin stimulates glycogen synthesis and protein synthesis. In the liver, insulin promotes glycolysis, glycogen synthesis, and the conversion of glucose into lipids, which are then distributed to all cells in the form of lipoproteins. In white adipocyte insulin enhances lipogenesis and suppresses lipolysis (Murray et al., 2015; Watanabe et al., 1998). (Figure 4)

<b>TABLE 23-3</b>		<b>Effects of Insulin on Blood Glucose: Uptake of Glucose by Cells and Storage as Triacylglycerols and Glycogen</b>	
<b>Metabolic effect</b>		<b>Target enzyme</b>	
↑ <b>Glucose uptake (muscle, adipose)</b>		↑ <b>Glucose transporter (GLUT4)</b>	
↑ <b>Glucose uptake (liver)</b>		↑ <b>Glucokinase (increased expression)</b>	
↑ <b>Glycogen synthesis (liver, muscle)</b>		↑ <b>Glycogen synthase</b>	
↓ <b>Glycogen breakdown (liver, muscle)</b>		↓ <b>Glycogen phosphorylase</b>	
↑ <b>Glycolysis, acetyl-CoA production (liver, muscle)</b>		↑ <b>PFK-1 (by ↑ PFK-2)</b> ↑ <b>Pyruvate dehydrogenase complex</b>	
↑ <b>Fatty acid synthesis (liver)</b>		↑ <b>Acetyl-CoA carboxylase</b>	
↑ <b>Triacylglycerol synthesis (adipose tissue)</b>		↑ <b>Lipoprotein lipase</b>	

**Table 23-3**  
*Lehninger Principles of Biochemistry, Fifth Edition*  
 © 2008 W. H. Freeman and Company

**Figure 4. Hypoglycemic effects of insulin (Nelson 1942-, 2005).**

The insulin receptor is a heterotetrameric glycoprotein present on the outer cell membrane containing two extracellular  $\alpha$ -subunits and two transmembrane  $\beta$ -subunits. Side chains of both the A- and B-chain of insulin mediate binding with an  $\alpha$ -subunits of the receptor (Kahn & White, 1988; Weiss et al., 2000). The intracellular part of the receptor contains a tyrosine kinase domain, inactive in the absence of a ligand. In the presence of ligand bound to the extracellular domain, the insulin receptor becomes an activated dimer. The kinase domains come in contact and are activated by transphosphorylation, resulting in phosphorylation of specific Tyr residues in the intracellular part of the receptor outside the kinase domain. The

active receptor recruits the intracellular insulin receptor substrate (IRS) proteins, which are subsequently tyrosine-phosphorylated. While the phosphorylation of specific tyrosine residues activates IRS, there are serine phosphorylation sites that inactivate IRS by causing their dissociation from the IR and decreasing tyrosine phosphorylation (Copps & White, 2012). The binding of insulin to the IR can activate two distinct branches of insulin signaling: the Ras-mitogen-activated protein kinase (MAPK) and PI3K-Akt pathways (Hubbard, 2013), which mediate the different effects of insulin (Figure 5).

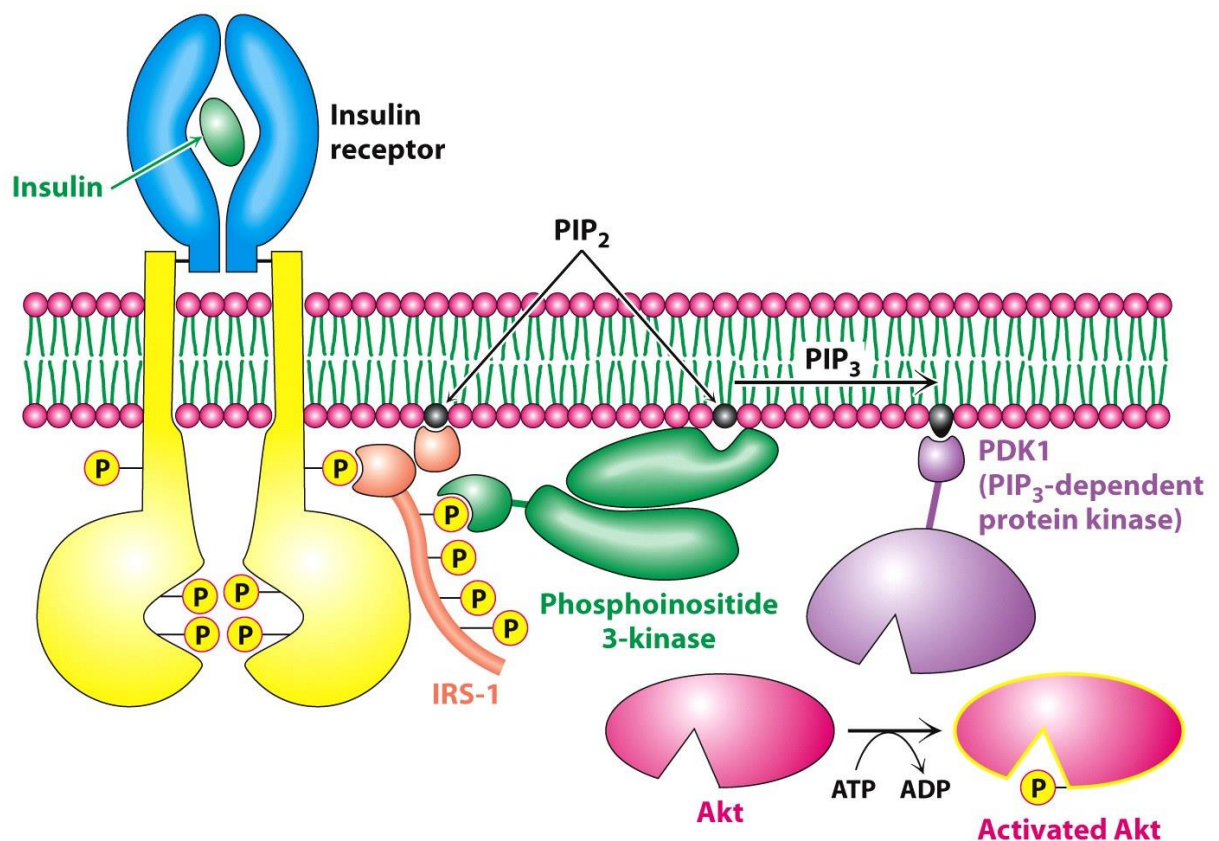


**Figure 14.21**  
*Biochemistry, Seventh Edition*  
 © 2012 W. H. Freeman and Company

**Figure 5. Insulin receptor and mechanism of signalling (Nelson 1942-, 2005).**

PI3K-Akt pathway metabolic effects of insulin are activated by binding of the p85 or p55 to the IRS leading to conversion phosphatidylinositol (3,4)-bisphosphate (PIP<sub>2</sub>) into phosphatidylinositol (3,4,5)-trisphosphate (PIP<sub>3</sub>). This translocates Akt-kinase to the cell membrane. Akt is completely activated after phosphorylation of threonine 308 by phosphoinositide-dependent protein kinase 1 (PDK1) and then phosphorylation of serine 273 by mTOR complex 2. PI3K-Akt pathway regulates metabolic effects of insulin-like glucose

homeostasis, lipid metabolism, protein synthesis but also cell survival and proliferation (Gabbouj et al., 2019; Huang et al., 2018).

The complex of insulin receptor and IRS binds to another docking protein Shc (Src homology 2 domain-containing) activating signaling pathway. Shc activation triggers GRB2 and SOS complex thus activating the Ras-MAPK pathway. Induced in this pathway ERK 1 and 2 kinases directly impact cell proliferation, differentiation through gene expression control (Boucher et al., 2014).

### **1.3 Pancreatic diseases – contemporary hassle and the approach to cope with it**

Diabetes mellitus is one of the greatest challenges in nowadays medicine. It affects people of all ages, communities, and all continents what makes it a worldwide issue. The International Diabetes Federation (IDF) reports that 1 in 11 adults suffers from diabetes which is approximately 463 million people and half of them are not diagnosed. The other great problem is up to 80 % of people with diabetes live in low- and middle-income countries which additionally increases the risk of possible complications that untreated or ineffectively treated diabetes carries. Even 90 % of all premature deaths related to diabetes occur in poor countries (IDF Diabetes Atlas 9th edition, 2019).

Diabetes is a chronic metabolic disease in which the main symptom is increased glucose level in the blood. Hyperglycemia is caused by a failure in insulin secretion and/or action what leads to implications in the functioning of several organs including eyes, kidneys, and heart. It is a consequence of impairment in carbohydrate, fat, and protein metabolism. Two main types of diabetes are distinguished: insulin-dependent type 1 diabetes (T1D) and insulin resistance type 2 diabetes (T2D) (“Diagnosis and Classification of Diabetes Mellitus,” 2013).

Type 1 Diabetes (T1D) is an autoimmune disease characterized by a deficit or absence of insulin resulting from T cell-mediated destruction of  $\beta$ -cells of the pancreas (Bottazzo et al., 1974). The reduced production of insulin is responsible for the presence of high blood sugar levels. In addition to hypoinsulinaemia and hyperglycaemia other classic symptoms of T1D include polyuria, polydipsia, weight loss, and fatigue, which, if untreated, can lead to a coma and ultimately to death. Furthermore, T1D patients are characterized by the presence in serum of auto-antibodies against  $\beta$ -cell auto-antigens. Islet cell antibodies (ICA) were the first auto-antibodies identified in T1D patients (Bottazzo et al., 1974). In addition to ICA,

other auto-antibodies associated with T1D are autoantibodies to insulin (IAA) (Palmer et al., 1983), glutamic acid decarboxylase (GADA) (Baekkeskov et al., 1990), and protein tyrosine phosphatase like protein (IA2) (Clayton, 2009). The highest incidence rate of T1D is found in adolescents, although it is widely accepted that adults can also develop the disease. T1D is a multifactorial disease where both genetic and environmental factors contribute to the pathogenesis. In genetically predisposed individuals, multiple and different environmental factors trigger an autoimmune response that causes the destruction of pancreatic  $\beta$ -cells. Several genome screens, in combination with family-based association studies, have shown that the most important genes responsible for the development of diabetes are those related to the Human Leukocyte Antigen (HLA), the locus of the genes that encode proteins, which facilitate the presentation of antigens to T lymphocytes. HLA is a group of polymorphic genes consisting of 30 units, located in humans on the short arm of chromosome 6. Approximately 50% of the genetic risk of T1D is correlated with the HLA class II region and the presence of haplotypes HLA-DR3-DQ2 and HLA-DR4-DQ8 is the strongest determinants of diabetes susceptibility (Pociot & Lernmark, 2016). Other genetic polymorphisms that have also been associated with T1D development include those for the Insulin gene (INS) (Bell et al., 1984), IL-2 receptor  $\alpha$  (Vella et al., 2005), Cytotoxic T lymphocyte antigen (CTLA4) (Nisticò et al., 1996), Protein tyrosine phosphatase non-receptor 22 (PTPN22) (Bottini et al., 2004) and Intercellular adhesion molecule 1 (ICAM1) (Nishimura et al., 2000). In addition to genetic components, many environmental factors have been associated with increased susceptibility to T1D, although, to date, none have been confirmed as a clear causative agent of T1D. The main environmental factors include viral factors especially infections with enteroviruses, e.g. children whose mothers during pregnancy were infected with an enterovirus have a higher risk to develop T1D. Additionally, the other environmental factors provoking the autoimmune attack are: diet, insufficiency of vitamin D, or even exaggerated hygiene what leads to the underdevelopment of the immune system.

Patients suffering from T1D are very likely to develop several long-term complications like blindness, neuropathy, end-stage renal disease and their quality of life is relatively poor. Those people need to watch their diet, ensure regular physical activity, check-ups with the doctor, and the most importantly a therapy for insulin replacement. (DiMeglio et al., 2018) (Lucier, Weinstock, 2020). The increasing number of diabetic patients increases the need for the production of insulin which is an essential and basic medicine in diabetes treatment.

Insulin is produced with the usage of recombinant DNA technology. In these biotechnological methods, organisms are used to express genes that normally do not occur in them by combining DNA molecules from different organisms. First heterologous proteins were produced in bacteria *Escherichia coli* but already in 1977 started to use a eukaryotic alternative which was baker's yeast *Saccharomyces cerevisiae* that was considered a better option for a human use protein production. In 1982 recombinant insulin called humulin was produced. It was the very first therapeutic biotechnology product. Ever since various numbers of new, improved homologs have been created like produced in *S. cerevisiae* Novolin. Another example may be the Humalog produced in *E. coli* a fast-acting analog of insulin in which the order Pro28 and Lys29 at the C-terminus in the B chain have been reversed increasing its availability to function. Those changes were based on the insulin-like growth factor 1 (IGF-1) sequence and structure to decrease dimerization of the B subunit (Sandow et al., 2015). The vast majority of biopharmaceuticals are being produced in mammalian cell lines but recent studies show plant molecular farming as another possibility in human therapeutic protein production, including insulin. In 2005 insulin was produced by transgenic *Arabidopsis thaliana* plant. Genetic modification was designed at the accumulation of expressed insulin in the storage organelles present in seeds called the oilbodies (Nykiforuk et al., 2006). Using transgenic plants in plant molecular farming is very promising in a low cost, effective, and biologically active insulin production that can be administrated orally or as an injection (Baeshen et al., 2014; Yao et al., 2015). Numerous plant-based compounds mimic insulin action and have been used through years in folk medicine for diabetes treatment. Insulin-like proteins extracted from different parts of plants like leaves, fruits, and seeds have a great perspective to be used as a main or at least supporting medicine for diabetic patients. Mechanisms of insulin-like proteins actions are similar to insulin biochemical pathways what include insulin resistance modulation or controlling the level of glucose. The plants from which derived peptides activate insulin-mediated pathways can include *Glycine max* (soybean), *Pisum sativum* (peas), *Costus igneus* (costus), or *Moringa oleifera* (moringa) (Costa et al., 2020; Paula et al., 2017).

Type 2 diabetes (T2D) is the most known and most frequent type of diabetes, which typically affects subjects of mature age. (T2D) is a meaningful problem affecting millions of people worldwide. The main issue is a constantly increasing number of patients suffering from T2D. This type of diabetes is also the cause of premature mortality and complications



like cardiovascular disease, blindness, limb amputation, or kidney dysfunction (Małecki, 2006; Reed & Scribner, 1999).

T2D is characterized by weakening insulin secretion and chronic insulin resistance in tissues (e.g. muscles, heart, liver). Usually, the original background of T2D is insulin resistance leading to increased production of insulin and in the late event function of burden pancreatic  $\beta$ -cell is declined. (Małecki, 2006). Insulin resistance is related to some defects of insulin receptors (IR) or insulin signaling-transduction. The pancreas of insulin-insensitive patients produce greater amounts of insulin to compensate for this state what results in  $\beta$ -cell damage. 6Even though IRs are present on the membrane of all mammalian cells the major role plays the ones located on adipocytes, hepatocytes, and myocytes of skeletal muscle what indicates that mainly those three cell types are affected by insulin resistance.

As for T1D, genetics and environmental factors are important disease determinants in T2D. Over 40 genes have been associated with T2D including peroxisome proliferator-activated receptor gamma (PPAR $\gamma$ ), ATP binding cassette subfamily C member 8 (ABCC8), and potassium voltage-gated channel subfamily J member 11 (KCNJ11). (Kooner et al., 2011). The environmental causes that have a big impact on the expansion of diabetes are lack of physical activity and bad diet what is observed mainly in developing countries. Food, poor in nutrients and rich in calories combined with sitting lifestyle increases body mass index and obesity level, the main cause of T2D development (Popkin, 2015). Adipose tissue is capable of producing and releasing pro-inflammatory cytokines, such as TNF $\alpha$ , IL-6, IL-1 $\beta$ , and the chemotactic protein of monocytes (MCP-1) (Coelho et al., 2013; Ruvinsky et al., 2005). Macrophages associated with adipose tissue are mainly responsible for the synthesis of pro-inflammatory cytokines. The adipose tissue of the obese subject is characterized by a latent inflammatory state and by an infiltration of macrophages, which actively participate in the onset of an inflammatory condition of the adipose tissue itself. In obesity, the expansion of adipose tissue leads to hypertrophy of the adipocytes. The release of chemokines induces the recruitment of macrophages from the bloodstream. Once penetrated into the adipose tissue and activated locally, the macrophages, in synergy with the adipocytes and other cells, trigger and perpetuate a vicious circle of recruitment of other macrophages and the production of pro-inflammatory cytokines. The visceral adipose tissue, compared to the subcutaneous adipose tissue, produces a greater quantity of pro-inflammatory cytokines and is characterized by a greater lipolytic activity, with greater release into the circulation of free fatty acids compared to the subcutaneous adipose tissue. The increased circulating level

of  $\text{TNF}\alpha$  and IL-6 is closely associated with insulin resistance and the development of type II diabetes (Greenberg & Obin, 2006). Insulin resistance is partly justified by the reduced level of adiponectin resulting from the increased secretion of  $\text{TNF}\alpha$ . In addition to the effects of  $\text{TNF}\alpha$  on adiponectin repression, pro-inflammatory cytokines directly alter insulin sensitivity by inhibition of the insulin signal.  $\text{TNF}\alpha$  and IL-6, activate intracellular signals that lead to activation of serine kinases such as JNK and the transcription factor NF- $\kappa$ B. The activation of JNK involves the phosphorylation and inactivation of the substrate of the insulin receptor (IRS) and consequent shutdown of the insulin signal. These effects result in an increased production of glucose by the liver (by means of gluconeogenesis and glycogenolysis). At the muscle level, glucose intake is reduced. At the level of adipose tissue, glucose intake is reduced and the release of fatty acids increases. These events lead to an increase in the circulation of glucose and fatty acids and, subsequently, an increase in insulin resistance. Furthermore, NF- $\kappa$ B activates the transcription of pro-inflammatory genes that increase the release of inflammatory cytokines by amplifying the inflammatory state (Figure 6).

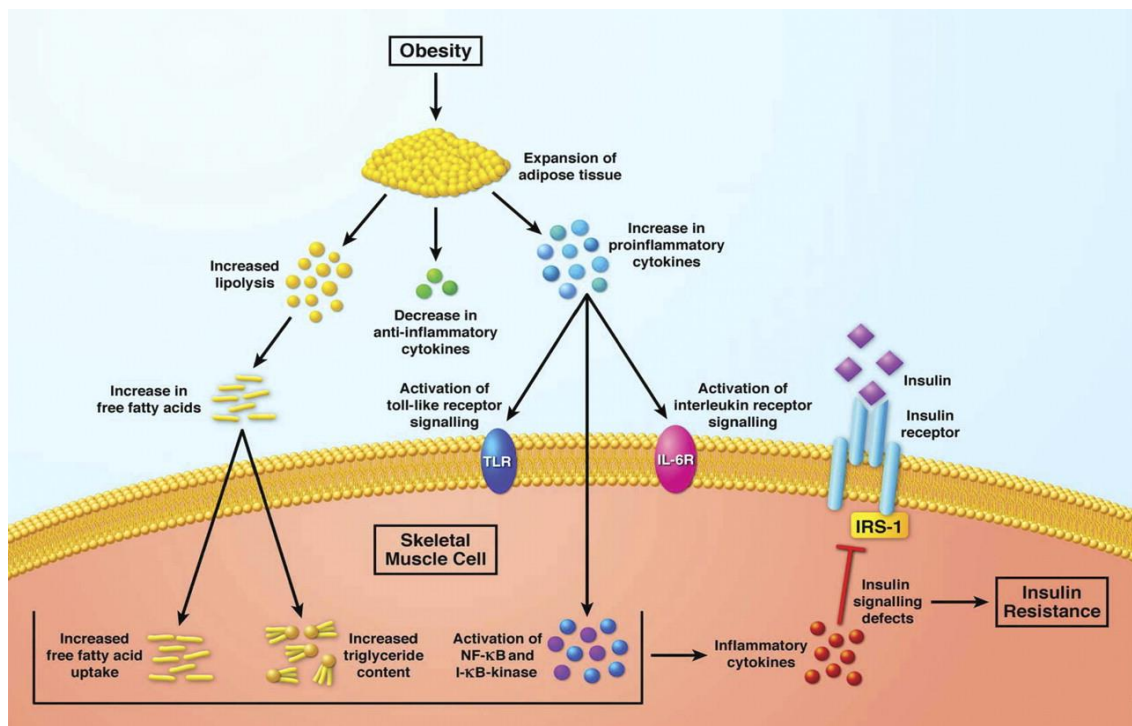


**Figure 6. Obesity as a determinant of insulin resistance (Nelson 1942-, 2005).**

However, poor insulin sensitivity, even with already developed T2D, can be reversed by caloric restriction (CR), weight loss, or intermittent fasting (IF) (Barnosky et al., 2014;

Furmler et al., 2018). Nevertheless, in some cases, studies show that the response to IF increased or even induced in non-T2D cases of insulin resistance. Those data indicate limitations in this approach for diabetes treatment (Horne et al., 2020; B. Liu et al., 2020; Park et al., 2017). In opposite to that CR is for sure one of the most effective approaches in the T2D treatment. CR is a long-term change of eating habits focusing on the reduction of consummated calories but not below the basal caloric metabolism to avoid starvation. Lowering calorie intake decreases glucose level, regulates gene expression of proteins involved in the insulin signaling pathway, and increases insulin sensitivity (Wiesenborn et al., 2014). CR leads to the reduction of adipose tissue and lowers circulating fatty acids that are the main inflammatory mediators thus decreasing inflammation states related to a higher risk of insulin resistance development. One of the insulin resistance triggers is obesity followed by oxidative stress; thus CR reduces weight loss and lessens free radicals restoring normal redox state. Furthermore, CR not only helps to cope with already existing T2D but also prevents from developing it as well as other diseases (cancer, cardiovascular disease) and promotes longevity by inhibiting aging processes (Anderson & Weindruch, 2012; B. Liu et al., 2020; Molino et al., 2010; Soare et al., 2014; Yaribeygi et al., 2019).

One of the genetic factors associated with the development of T2D is genetic variations in the Cdk5 regulator associated protein 1-like 1 (*cdk11*). Studies showed that *Cdk11* was a mammalian methylthiotransferase, which specifically synthesizes 2-methylthio-N (6)-threonylcarbamoyladenine (ms(2)t(6)A) at position 37 of tRNA(Lys)(UUU). *Cdk11* is an ER-localizing protein that is functionally associated with Cdk5/p35. Deficiency of *Cdk11* in  $\beta$  cells plays a significant role causes glucose intolerance, induction aberrant proinsulin synthesis, ER stress in  $\beta$  cells, enhanced susceptibility to high-fat diet stress. But the molecular function of Cdk5 is still unknown (Wei & Tomizawa, 2011, 2012). ER stress is caused by a mistranslation of Lys codon in Proinsulin and reduces the concentration of mature insulin in  $\beta$  cells. It results in lower insulin secretion and glucose intolerance. Additionally, ER stress links the molecular level of obesity, the collapse of insulin action, and progress of T2D (Wei et al., 2011).

Diabetes mellitus may be developed as well as a secondary disease after insulinoma treatment. Insulinoma is a rare pancreatic neuroendocrine tumor affecting  $\beta$ -cell islets what leads to an excessive amount of insulin production resulting in hypoglycemia. Conversely, diabetic patients rarely develop insulinoma. However, as a consequence of symptomatic hypoglycemia insulinomas do not always produce an adequate amount of insulin.

Furthermore, insulinoma may not be detected in diabetic patients due to antidiabetic medication being a misleading factor of a decreased blood glucose level (Nastos et al., 2020). Insulinoma diagnosis can be difficult due to symptoms similar to other diseases. Small and evenly distributed insulinoma tumors can be detected with ultrasonography or computer tomography (Grant, 2005). Moreover, the biochemical diagnosis includes plasma glucose, insulin, C-peptide, and proinsulin levels detection. Most of the time it can be cured by surgical resection. Whenever this approach is not possible insulinoma treatment focuses on permanent glucose level monitoring and medical treatment normalizing blood glucose level like octreotide or diazoxide administration (Okabayashi et al., 2013). At the basis of insulinoma, pathogenesis lies in accumulated genetic and epigenetic changes (Nastos et al., 2020). The molecular alternations responsible for insulinoma development include increased proliferation and cell cycle dysregulation via overexpression of growth signals proteins like cyclin D1, Akt1, or ghrelin, inhibited apoptosis related to c-Myc, and Bcl-X<sub>L</sub> dysregulation, or angiogenesis (Jonkers et al., 2007). Moreover, insulinomas exhibit greater levels of phosphorylated mTOR signaling pathway proteins like p-mTOR and p-P70S6K. Those are involved in autophagy inhibition and cell growth, and proliferation regulation (Zhan et al., 2012). It has been also shown that the presence of a genetic syndrome leading to the expanding of hormonal glands called multiple neoplasia type 1 (MEN-1 syndrome) puts patients at a higher risk of insulinoma development. *MEN1* gene localized on chromosome 11q13 encodes menin, a protein interacting with various nuclear and cytosol proteins correlated to tumor formation (Shin et al., 2010).

#### **1.4 Endoplasmic reticulum (ER)**

The endoplasmic reticulum (ER) is an organelle made out of cisternae and tubules closed with a membrane. There are two forms of ER so-called smooth (SER) and rough (RER). Each of them is specialized in different actions and occurs in different proportions depending on the cell function. SER is associated with glycogen metabolism and lipids synthesis. RER, further simply named ER, is rich in ribosomes and is a place in a cell where proteins are synthesized, folded, post-translational modified, and transported to different destinies (Kilarski, 2005). Since from the ER only properly folded proteins are being transmitted, ER assures multiple mechanisms of quality control to prevent dangerous consequences of

incorrect protein release. All proteins containing any types of defects are either kept in the ER for completing folding or are degraded (Ellgaard et al., 1999).

Disruptions in the ER structure or function as well as an overload of the folding machinery by increased expression of wild-type proteins lead to ER stress and activates a signaling pathway called unfolded protein response (UPR). The main task of UPR is to arrest protein translation to decrease the load within the ER and increase the degradation of misfolded proteins (Flamment et al., 2012; Lindholm et al., 2006). ER stress may be triggered to develop several disorders like neurodegenerative diseases (Alzheimer disease, Parkinson disease, Huntington disease), bipolar disorder, atherosclerosis, inflammation, ischemia, heart diseases, liver diseases, kidney diseases, viral infection, and hereditary tyrosinemia type I. There are four chemicals evoking ER stress: glycosylation inhibitors,  $\text{Ca}^{2+}$  metabolism disruptors, reducing agents, or hypoxia. ER stress response consists of four mechanisms: translational attenuation, expression of ER chaperones, enhanced ERAD (ER-associated degradation), and apoptosis (Yoshida, 2007). ER stress possibly plays also an important role in the regulation of insulin pathways and thereby contributes to insulin resistance in hepatic, muscle, and adipose cells. One of the examples showing connecting ER stress and hepatic insulin resistance is ER stress induced by, lipid accumulation disrupting insulin signaling. Activated by ER stress SREBP-1c, XBP1 and NRF2 transcription factors induce lipogenesis. In the response to that collected lipid metabolites can interfere with the insulin signaling pathway (Flamment et al., 2012).

Misfolded or unfolded proteins undergo a complex ERAD process consisting of four main steps. At first, with the help of molecular chaperones and lectin-like proteins, aberrant proteins are recognized and then retrotranslocated from the ER lumen into the cytosol. Next retrotranslocated proteins are ubiquitinated and degraded by the proteasome (Erbaykent Tepedelen & Ballar Kirmizibayrak, 2019). Before retrotranslocation and ubiquitination glycan chain that may interrupt entrance into the proteasome through the pores are removed from the proteins by peptide-N-glycanase. Proteins are marked with ubiquitin thanks to the short 40 - 50 amino acids ubiquitin-binding domains (UBA) present in the bigger proteins so-called ubiquitin adaptors. Marked proteins are derived to the proteasome by the AAA-ATPase p97/Cdc48 complex (Hoseki et al., 2010; Raasi & Wolf, 2007). Ubiquitylated proteins are degraded by 26S proteasome made out of the two types of complexes, one molecule of catalytic core 20S complex and two molecules of regulatory 19S complex. The 19S particle is responsible for ubiquitylated proteins recognition in an ATP-dependent

binding step, ubiquitin removal, and targeting the protein into the 20S complex where proteins are degraded into smaller oligopeptides 3 – 15 amino acid long and hydrolyzed to amino acids (Pickart, 1997). In pancreatic  $\beta$ -cells, ERAD dysfunction may be an administrative factor of diabetes development by disruption of proinsulin maturation in the ER. Studies on the rat insulinoma cell line INS-1 with impaired ERAD pathway revealed decreased glucose stimulated insulin secretion (GSIS), mitochondrial membrane potential reduced  $\text{Ca}^{2+}$  level, and escalated ROS production (Hu et al., 2019).

One of the cellular responses helping restore ER homeostasis during the ER stress caused by the accumulation of misfolded proteins in the ER lumen is UPR. This mechanism increases the capacity of the ER to fold proteins by enhancing the production of molecular chaperones and foldases and decreasing protein biosynthesis. If the ER stress may be mitigated by the UPR pathway cell will survive and will be prepared for eventual future ER stress events. Whereas if ER stress is unbearable and UPR fails to restore homeostasis cell death promoting pathway is activated. As mentioned previously there are some quality control mechanisms in the ER that secure proper protein folding. For example, protein folding processes are supported by several types of machinery consisting of molecular chaperones like Hsp70 chaperones BiP/GRP78/Kar2p and Lhs1p/GRP170/ORP150, Hsp90 chaperone GRP90, and the lectin chaperones calnexin, calreticulin, and calmeglin (Schröder, 2008). One of the most abundant and thus major chaperones in the ER stress is GRP78/BiP (78 kDa glucose regulated protein/binding-immunoglobulin protein). GRP78 is an ATP-dependent protein that belongs to the HSP70 family with 60% homology and conserved two domains, at the N-terminal site ATP binding domain (ABD) and a substrate binding domain (SBD) at the C-terminal site. GRP78 plays a crucial role in the embryonic development, tumor growth, transport of synthesized polypeptides, folding and assembly of proteins, ERAD pathway activation by binding with the SBD to misfolded proteins, calcium homeostasis regulation, apoptosis inhibition, and activation of transmembrane ER stress sensors (IRE1, PERK, and ATF6) (Ibrahim et al., 2019; Inageda, 2010; Jeon et al., 2016; Lee et al., 2006). GRP78 is regulated by insulin/IGF-1 signaling pathways. It has been shown that IGF-1R (IGF-1 receptor) activation induces PI3K/AKT/mTOR pathway thus leading to increased transcription level of *Grp78* (Ha & Lee, 2020). Moreover, insulin and IGF-1 upregulate GRP78 expression what protects the cell from ER-stress mediated apoptotic cell death (Inageda, 2010; Novosyadlyy et al., 2008). In normal cell GRP78 binds to activating transcription factor (ATF6), protein kinase RNA-like endoplasmic reticulum kinase

(PERK), Inositol-requiring enzyme 1 (IRE1), and ER-associated caspases, like murine caspase-12/human caspase 4. When the cell is under a stress condition caused by aberrant protein accumulation GRP78 is gradually dissociated from ER-stress sensors what activates UPR (Miao Wang et al., 2009). After that PERK is autophosphorylated what transits it into an active state. Activated PERK phosphorylates the  $\alpha$  subunit of a eukaryotic translation initiation factor (eIF2 $\alpha$ ) which role focuses on the reduction of translation and therefore decreasing protein synthesis. However, eIF2 $\alpha$  may also selectively increase the translation of activation transcription factor 4 (ATF4) by increasing mRNA translation containing upstream reading frame (uORF) (Harding et al., 2000; Lu et al., 2004). ATF4 induces activation of a pro-apoptotic CCAAT-enhancer-binding protein homologous protein (CHOP) (Huber et al., 2013). Furthermore, ATF6 released from the GRP78 is translocated to the Golgi apparatus and cleaved. After that, the cleaved ATF6 is transported to the nucleus where acts as an active transcription factor and increases the synthesis of proteins responsible for folding capacity, like GRP78 or GRP94 (Shen et al., 2002). Another transmembrane ER stress sensor that is activated by GRP78 release is IRE1. This transmembrane protein consists of an N-terminal luminal domain (LD), single pass transmembrane domain, and on the cytosolic site a C-terminal tail acting as a protein kinase and ribonuclease. IRE1 LD is dimerized/oligomerized after direct binding with misfolded proteins and the cytosolic domain is autophosphorylated in trans (Adams et al., 2019). An active form demonstrates endoribonuclease activity and splices a small 26-base intron from the mRNA encoding the transcription factor X-box binding protein 1 (XBP-1) responsible for activation of protein degradation on ERAD signaling pathway and ER stress chaperones thus increasing folding capacity (Yamamoto et al., 2007; Yoshida et al., 2001). Overexpression of IRE1 under ER stress triggered by chronic hyperglycaemia leads to suppression of insulin gene expression and insulin mRNA degradation in pancreatic  $\beta$ -cells (Lipson et al., 2006, 2008). In another study cyclopiazonic acid (CPA) induced ER stress in  $\beta$ -cells resulted in the degradation of insulin-1 (Ins1) and insulin-2 (Ins2) mRNA (P. Pirot et al., 2007).

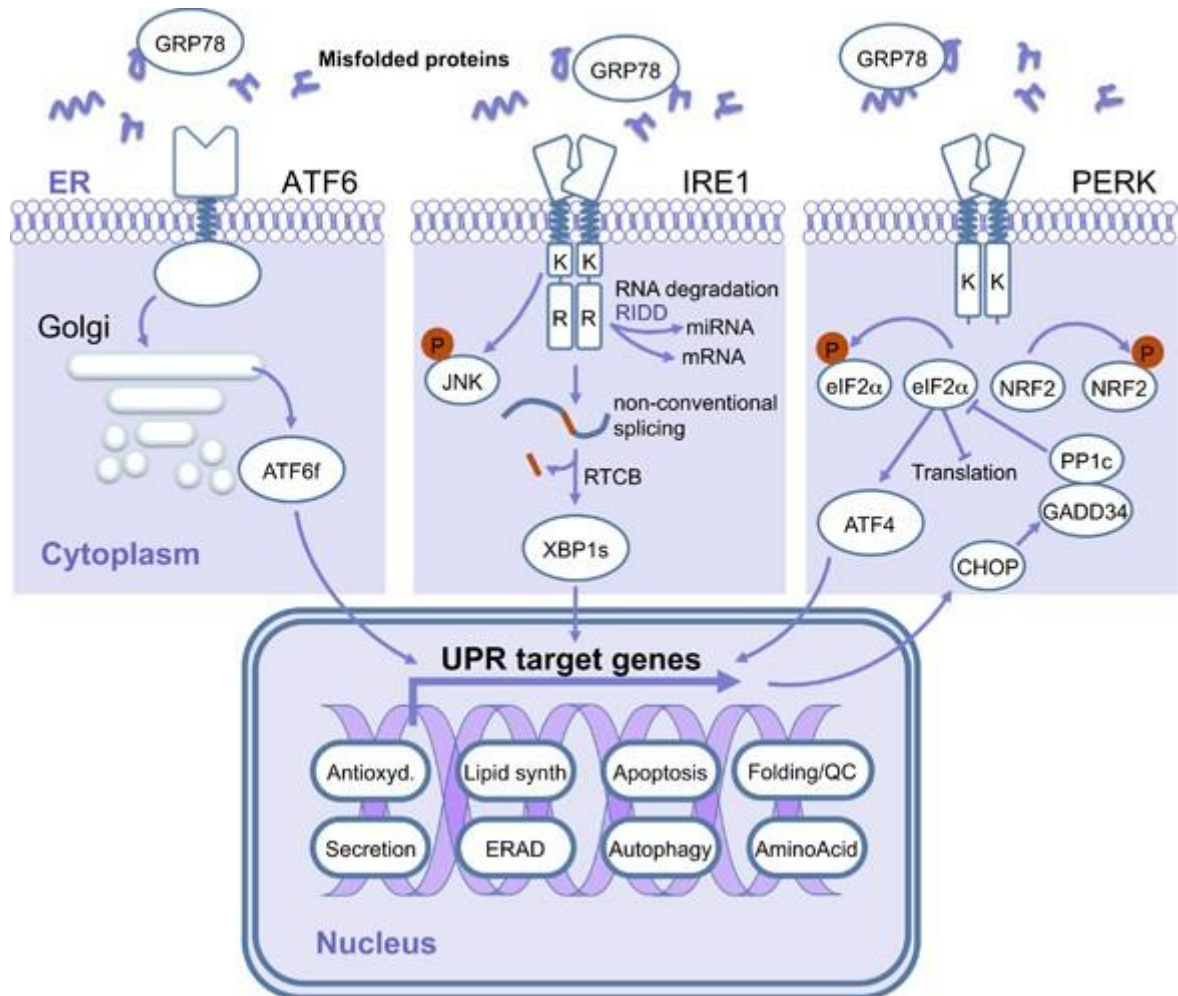


**Figure. 7 UPR pathway in a response to ER stress (Avril et al., 2017).**

Cell under the ER stress conditions will activate several pathways including translation inhibition, protein degradation, or increasing folding capacity by increasing ER size and induction of ER chaperones what in the late event should lead to cell survival. However, if the stress is too big to handle cell has to be executed via apoptosis. It is a process of programmed cell death occurring when the damages in the cell cannot be removed or "healed". In opposite to necrosis, it is a fully controlled cell death that does not lead to any inflammation. This specific suicide of a cell is a relevant pathway for maintaining balance in the organism by the elimination of unwanted or potentially dangerous cells. Regulated IRE1-dependent decay of mRNA (RIDD) leads to the reduction of mRNA localized in the ER what if it lasts for too long may induce cell death (Hollien et al., 2009; Sano & Reed, 2013). ER stress-mediated cell death mechanisms include IRE1 mediated stimulation of Apoptotic-Signaling Kinase-1 (ASK1) downstream of stress kinases Jun-N-terminal kinase



(JNK). The C-terminus domain of IRE1 binds with an adaptor protein TNF receptor-associated factor 2 (TRAF2) which activates JNK. IRE1 activates apoptosis also via ASK1 and MKK6/7 activation of p38/MAPK (mitogen-activated protein kinase) signaling pathway. Besides, activated JNK attenuate BCL2 responsible for apoptosis inhibition (R. Li et al., 2020; Urano et al., 2000). Furthermore, it has been shown that p38/MAPK dependent phosphorylation activates pro-apoptotic CHOP and induces autophagy (Kim et al., 2010), an alternative survival mechanism activated during ER stress. Autophagy, what from Greek means “self-eating”, is a process of lysosomal degradation of damaged organelles, cell compartments, or impaired proteins by an organelle called autophagosomes. Autophagy activation helps to cope with ER stress and lowers apoptosis. Lysosome-mediated protein degradation during ER stress is the secondary response to the accumulation of aberrant proteins right after the ERAD pathway. The double-membrane vesicle fuses with the lysosome where carried cargo is lysed. Elongation of the vesicles happens thanks to two ubiquitin-like conjugation systems, an autophagy gene (ATG)-related proteins ATG5/ATG12, microtubule-associated protein light chain 3 (LC3)/ATG8 and class III PI3-kinase complex. (Runwal et al., 2019). To the family of LC3 proteins belong LC3A, LC3B, and LC3C. The best studied form is LC3B which during autophagy is cleaved forming a cytosolic LC3B-I and then at the carboxyterminal glycine phosphatidylethanolamine (PE) is conjugated and the membrane-bound variant LC3B-II is formed. Located in the membrane LC3B-II is responsible for collecting the cargo. LC3B-II is further associated with the phagophore by the Atg5-Atg12-Atg16L complex which plays a crucial role in the autophagophore formation (Noda et al., 2009). The phagophore membrane sac encloses a portion of cytoplasm and organelles creating a double-membrane autophagosome vesicle. Formed autophagosome fuses with the lysosome and contained it hydrolases degrade carried cargo in the lysis process (Mizushima, 2007; Xie & Klionsky, 2007). Lysed content is recycled as well as an LC3-I protein. For that, the PE is removed from the LC3-II by Atg4B and cytosolic LC3-I is restored (Tanida, 2011). Conversion of LC3-I to LC3-II is correlated with the number of autophagosomes and thus is used as a marker of autophagy. Induction of ER stress activates IRE1/JNK/beclin-1 mediated autophagy induction accompanied by increased apoptosis (Cheng et al., 2014; Zheng et al., 2019). Even though the activation of the IRE1-JNK pathway is essential for an ER stress-mediated autophagy induction but it is not exclusive (Ogata et al., 2006). However, sometimes proteins are directly transitioned into the lysosome in a process called chaperone-mediated autophagy (CMA). This kind of

autophagy allows degrading only specific proteins occurring in the cytoplasm. Incorrect proteins are recognized and bound by a heat shock-cognate protein of 70 KDa (Hsc70), then transferred to the lysosome where interact with the cytosolic part of lysosome-associated membrane protein type 2A (LAMP-2A) and enter the lysosome where are completely degraded (Cuervo & Wong, 2014; Dice, 2007). It has been shown that ER stress mediates CMA via activating UPR proteins (EIF2/PERK) and the p38 MAPK signal transduction (W. Li et al., 2017, 2018). Furthermore, study on a pancreatic cancer cells revealed ER stress induction, CMA, and apoptosis activation through downregulation of a selective autophagy receptor called optineurin (OPTN) which usually is upregulated in a pancreatic cancer cells (Ali et al., 2019). Increased autophagosome formation as a response to the ER stress may be next to an ERAD pathway an extra system helping to cope with the excess of misfolded proteins to promote cell survival. The crosstalk between apoptosis and autophagy suggest that induction of one of this pathway inactivates the other. In the situation when the ER stress is at approximately a low level autophagy pathway is activated. However at a high level of ER stress at first autophagy may be activated and then be inhibited and apoptosis is initiated instead (Holczer et al., 2015). Autophagy-apoptosis crosstalk seems to be very complex as both pathways can inhibit and activate each other depending on the stress level, cell type, and condition. At the acute level of ER stress autophagy switch to apoptosis pathway is already irreversible (Zhu, 2020). Autophagy can inhibit apoptotic cell death via abnormal proteins removal, inhibition of apoptotic caspases activation (caspase-8), or SQSTM1/p62 autophagy-specific substrate exclusion. However, under ER stress autophagy activates apoptotic cell death. ER stress results in the increased release of  $Ca^{2+}$  to the cytoplasm from the ER what stimulates autophagy via protein kinase C (PKC) and apoptosis via  $Ca^{2+}$ -mediated mitochondrial cell death. Increased release of  $Ca^{2+}$  from ER results in autophagy activation through CaMKK- $\beta$ , AMPK, and mTOR pathway (Høyer-Hansen & Jäättelä, 2007; Sano & Reed, 2013; Song et al., 2017). Furthermore, calcium transfer by an inositol 1,4,5-trisphosphate (IP3) receptor (IP3R), one of the main calcium channels in ER, stimulates apoptosis and inhibits autophagy. Moreover, studies have shown that IP3R inhibition triggers the autophagy pathway (Kania et al., 2017; Vicencio et al., 2009). As mentioned before upon the ER stress ATF4 activates CHOP leading to the apoptosis induction by Bcl-2 reduction and death receptor activation 5 (DR5). Also, Bcl-2 phosphorylation mediated by a JNK pathway leads to autophagy activation. Moreover, ATF4 also stimulates numerous ATG genes thus activating autophagy (Song et al., 2017).

### 1.5 Trdmt1 and tRNA methylation

DNMT2/TRDMT1 is a methyltransferase (tRNA (cytosine(C38)-C(5))-methyltransferase). Dnmt2/Trdmt1 and its homologs are widely expressed in different organisms *Homo sapiens*, *Mus musculus*, *Drosophila melanogaster*, *Schizosaccharomyces pombe*, or *Arabidopsis thaliana*, but the genomes of *Saccharomyces cerevisiae* or *Caenorhabditis elegans* do not contain related sequences (Dong et al., 2001; Raddatz et al., 2013; Shanmugam et al., 2014b). Dnmt2 enzyme was initially considered as only a homolog of the DNA methyltransferases and indeed Dnmt2/Trdmt1 is a highly conserved protein belonging to the DNA methyltransferase family with residual DNA-cytosine-C5 methyltransferase activity. However, despite Trdmt1 structure and sequence similarity to DNA methyltransferases, studies show that Trdmt1 mainly methylates aspartic acid transfer RNA, specifically at the cytosine-38 residue. Trdmt1 contains conserved methyltransferase motifs, thus likely encoding a functional cytosine methyltransferase (Goll et al., 2006; Jurkowski et al., 2008; Okano et al., 1998). Transfer RNA (tRNA) is a short RNA adaptor molecule that decodes a specific codon of a messenger RNA (mRNA) sequence into a protein by transferring a specific amino acid to the end of a newly synthesized protein chain in a ribosome. tRNA methylation is a post-transcriptional modification essential for proper and effective protein synthesis, tRNA structure stabilization, codon-anticodon interaction strengthening, and prevention from any mistakes in a frameshift (Hori, 2014). Most of the methyltransferases, including Trdmt1, use S-adenosyl-L-methionine (AdoMet) as a donor of a methyl group. tRNA methyltransferases recognize the local structure around the target site of a tRNA strand what allows them to work very precisely modifying an exact nucleoside at an exact tRNA position. Two animal 5-methylcytosine ( $m^5C$ ) methyltransferases, Trdmt1 and Nsun2, can modify specific tRNAs. It has been shown that mice with deficient Nsun2 and Trdmt1 lose cytosine-C5 methylation. The lack of methyl groups at cytosine-5 tRNA interferes with tRNA folding and stability, codon-anticodon interactions, and reading frame maintenance. Research also shows that Trdmt1 most often methylates tRNA at C38 what protects tRNA against cleavage by the ribonuclease angiogenin and suggests the role of Trdmt1 in the regulation of protein translation (Ghanbarian et al., 2016; Tuorto et al., 2015). Mechanism of the DNA  $m^5C$  methyltransferases is based on an initial nucleophilic attack on Cys in motif IV but RNA  $m^5C$  methyltransferases instead of Cys from motif VI use the one from motif

IV. It is fascinating that amino acid sequence motifs in Trdmt1 protein are similar to DNA cytosine C5 thus Trdmt1 for RNA methylation uses a mechanism typical for DNA methyltransferases. It has been postulated that m<sup>5</sup>C RNA methyltransferases are the result of the merge of m<sup>5</sup>C DNA and m<sup>5</sup>U RNA methyltransferases (Bujnicki et al., 2004; Y. Liu et al., 2000). Dnmt2 proteins hold residues characteristic for DNA m<sup>5</sup>C methyltransferases and methylate RNA in a DNA methyltransferase catalytic mechanism (Jurkowski et al., 2008).

Dnmt2-mediated methylation varies between different organisms, thus for example it in *M. musculus* and *D. melanogaster* seems to be restricted to only three tRNAs: <sup>Gly</sup>GCC, <sup>Asp</sup>GTC, and <sup>Val</sup>AAC (Jeltsch et al., 2017). Additionally, Trdmt1 homolog GsDnmt2 has been found in bacteria *Geobacter* species in which methylates mainly tRNA<sup>Glu</sup>UUC but tRNA<sup>Asp</sup>GTC only with weak activity (Shanmugam et al., 2014a). The role of DNMT2/TRDMT1 has been postulated in organ differentiation, regulation of protein translation, aging, and longevity as well as in signaling pathways maintaining genomic stability, and regulating antiviral response (Schaefer & Lyko, 2010). A Trdmt1-mediated stress response is based on cytosine 38 methylation in the anticodon loop of tRNA Asp. Moreover, Lewinska et al., have observed decreased telomerase activity and telomere length in NH3T3 mouse fibroblasts (continuous cell line) and increased DNA damage level with decreased levels of Dnmt2 (Lewinska et al., 2017). However, plants and flies without functional Trdmt1 protein do not show any morphological differences compared to the wild-type (Goll et al., 2006). The reverse situation is in zebrafish which reduced the size of the morphants by half and specifically affected liver, retina, and brain development due to a failure to conduct late differentiation (Rai et al., 2007). The other studies on Trdmt1 mutant mice show that tRNA methyltransferase Trdmt1 is required for accurate polypeptide synthesis during haematopoiesis (Tuorto et al., 2015). Interestingly, the authors did not show the impact of lack of Trdmt1 on the insulin pathway because there is know that insulin can regulate haematopoiesis too. Moreover, some authors show that Trdmt1 regulates life span and stress resistance and adaptation (Blanco & Frye, 2014; Lewinska et al., 2017). Trdmt1 knockdown may also lead to changes in mRNA m<sup>5</sup>C methylation and its expression profile what affects for example insulin signaling pathway, insulin resistance, or ubiquitin-mediated proteolysis (Xue et al., 2019). In the study on wild type and Trdmt1 deficient mice, the substantial role of C38 tRNA methylation during haematopoiesis was revealed. C38 tRNA methylation ensures accuracy in tRNA<sup>Glu</sup> and tRNA<sup>Asp</sup> codons recognition. Lack of the Trdmt1 mediated

tRNA methylation generated errors in protein translation and eventually the development of aberrant phenotype (Tuorto et al., 2015). A very specific and rapid tRNA methylation suppression at C38 position can be achieved with a 5-Azacitidine (5-AzaC). 5-AzaC at first was described and used as an inhibitor of DNA methylation, however later on it has been found that 5-AzaC also inhibits Trdmt1 mediated tRNA methylation (Schaefer et al., 2009). 5-AzaC is a chemical analog of pyrimidine nucleoside, cytidine synthesized for the first time by Piskala and Sorm in 1964 (Piskala & Šorm, 1964). This drug is widely used in haematologic malignancies treatment or acute  $\beta$ -thalassemia. 5-AzaC demonstrates several activities like immunosuppressive, antimitotic, radioprotective, antitumor, or mutagenic. More importantly, inhibits DNA methyltransferase leading to de- or hemi-methylation what allows the transcription factor to bind to DNA and thus changing gene expression (Christman, 2002; Müller & Florek, 2010). However, as mentioned before, it has been also discovered that 5-AzaC inhibits RNA methyltransferase Trdmt1 (Figure 8). Schaefer et al. observed hypomethylation of tRNA<sup>Asp</sup> cytosine residue C38 which is a major Trdmt1 target. 5-AzaC is widely tested on leukemia cells. 5-AzaC incorporation into the RNA in leukemic cells leads to inhibition of RNA synthesis, a decrease of total RNA stability, and downregulation of ribonucleotide reductase subunit 2 (RRM2) responsible for providing deoxyribonucleotides for DNA synthesis and repair (Aimiwu et al., 2012). It has been shown that 5-AzaC only a small portion incorporates into DNA and mainly incorporates into RNA what results in reduced protein synthesis, cell cycle inhibition in all phases, and apoptosis induction (Hollenbach et al., 2010; L. H. Li et al., 1970).

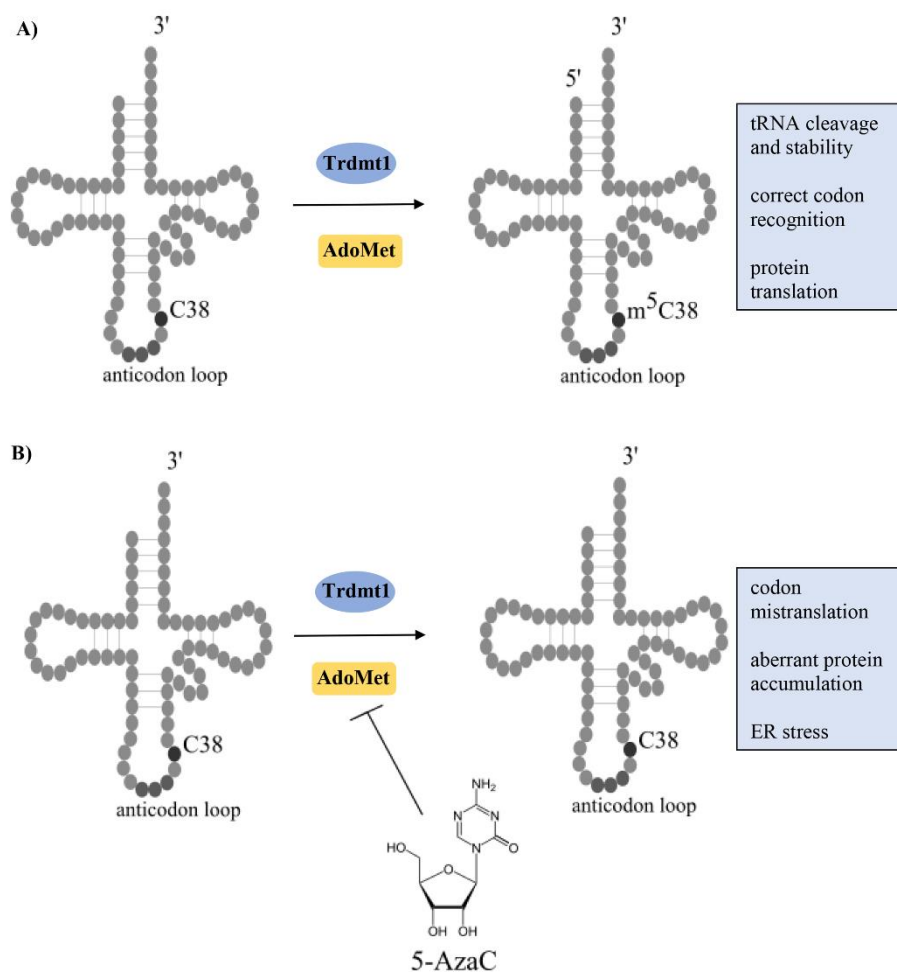


**Figure 8. Model illustrating the role of Trdm1 and 5-AzaC in tRNA methylation.**

### 1.6 Aging and cell senescence

According to the Hayflick limit presented by Leonard Hayflick and Paul Moorhead in 1961, the number of possible cell divisions is restricted, and after that time cells enter the irreversible growth arrest (Hayflick & Moorhead, 1961). It is defined as cellular senescence, where cells are still alive and metabolically active but do not proliferate. Except that senescent cells demonstrate changes in the morphology, chromatin organization, and alterations in protein expression and secretion like increased levels of pro-inflammatory cytokines. All of those changes taken together give so-called senescence-associated secretory phenotype (SASP) (Coppé et al., 2008; Pazolli et al., 2012). Cellular senescence is highly related to aging and consider as one of its mechanisms. At the base of aging lies the accumulation with the lifetime of aberrant alterations in the body on a tissue, cell, and molecular level. All of those modifications are the side effects of the metabolism enhanced

by an unhealthy lifestyle and toxic compounds found in the environment (Rae et al., 2010). Major hallmarks of aging are DNA damages, epigenetic and gene expression changes, telomere shortening, stress vulnerability, loss of protein homeostasis, or disruption in cell to cell communication (Carmona & Michan, 2016; López-Otín et al., 2013). The difference between aging and senescence is that aging is a progressive process of decline in cell functions and senescence occurs throughout the lifespan. However, the number of senescent cells increases with age.

Cell senescence is characterized by a stable cell cycle arrest which means that those cells do not respond to any growth-promoting stimuli and will not re-enter the cell cycle. The main triggers of cell proliferation arrest induction are p53/p21CIP1 and p16Ink4a/phospho-Rb tumor suppressor pathways. One of the widely used senescence markers is mentioned p16Ink4a which upregulation has been very commonly observed in senescent cells both in vitro and in vivo (J. Y. Liu et al., 2019; Serrano et al., 1997). In a pancreatic  $\beta$ -cells expression of p16Ink4a increases glucose-stimulated insulin secretion (GSIS) and thus surprisingly improves glucose homeostasis in diabetic mice. Similar features have been found in human  $\beta$ -cells: senescent cells express p16Ink4a and insulin secretion is enhanced (Helman et al., 2016). A marker involved in aging in pancreatic  $\beta$ -cells is also insulin-like growth factor IGFR1. Its expression is correlated with senescence, disruption in the secretion of insulin, and expression of age-related markers (p16Ink4A and p53BP1). Furthermore, pancreatic cells show a high level of heterogeneity within and between islets in their age (Aguayo-Mazzucato et al., 2017). It is worth mentioning that exposure to many subcytotoxic stresses is causative of another type of senescence called stress-induced premature senescence (SIPS). Cells undergoing SIPS are characterized with senescence-like morphology, alterations associated with senescence gene expression, and usually irreversible cell cycle arrest. The difference between replicative senescence and SIPS is that the first one is programmed, related to the Hayflick limit, and the second one is induced by cellular stresses. The stressors leading to SIPS development include hydrogen peroxide, hyperoxia, ethanol, UV, homocysteine, ionizing radiation, etc (Suzuki & Boothman, n.d.; O. Toussaint et al., 2000; Olivier Toussaint et al., 2002).

Dysregulation in apoptosis is strongly connected with the aging process. Aging increases apoptosis events but also it has been postulated that age-related higher possibility of failure in apoptosis pathway is one of the main cancer-promoting factors. Apoptosis and also cell cycle arrest are controlled by p53 which collapse increasing with age may be a link between

age and higher cancer rate. Furthermore, various studies indicate apoptosis activation as a promising anticancer therapy (Reinhardt & Schumacher, 2012; Rodier et al., 2007).

It is suggested that changes in the expression profile of apoptosis-related proteins in senescent cells may be the reason for their resistance to programmed cell death and thus escalation of the number of senescent cells with age. Baar et al. studies have shown that FOXO4 is a key factor in senescent cell viability and that perturbations of FOXO4 and p53 interaction lead to activation of apoptosis pathway and thereby homeostasis restore (Baar et al., 2017). It has been also reported that microRNAs are involved in the aging process, e.g. miR-434-3p regulates apoptosis in aged skeletal muscle cells by targeting eIF5A1, and aging mice demonstrate a low level of miR-434-3p in skeletal muscle (Chen et al., 2010; Pardo et al., 2017).

Age-related disorders in cellular activity include decreased expression and function of several ER chaperones what is correlated with its age-related increasing oxidation. Nuss et al. have shown ER stress activation due to decreased functioning of the two ER chaperones, protein disulfide isomerase (PDI) and immunoglobulin heavy chain binding protein (BiP). The decline was a result of age-dependent oxidative stress (Nuss et al., 2008). The process of aging affects not only UPR chaperones but also UPR enzymes and ER structure. The study on chondrocytes from aged articular cartilage revealed downregulation of molecular chaperones and elevated levels of ER stress markers like phospho-IRE-1, XBP-1, ATF4, or CHOP and also elevated levels of markers characteristic for apoptosis (Nupr1 and TRB3) (Tan et al., 2020). The risk of T2D development increases with age due to insulin resistance, glucose intolerance, and weakened insulin secretion. The factors of this state are co-existing age-related diseases and changes in the organism like greater body fat. The obesity state induces ROS production by adipocytes and thus stimulating inflammation and insulin resistance (Ahima, 2009; Halim & Halim, 2019).



## **2. Aim of the study**

Collected material suggests that ER function may be affected by different tRNA deficiency as well as various enzymes modifying ribonucleotides in tRNAs. In a present study, we wanted to determine the potential consequences of 5-AzaC treatment on insulin production, Dnmt2/Trdmt1 expression levels, and endoplasmic reticulum stress in cellular models of insulinoma via 5-AzaC mediated tRNA methylation disruption at the Dnmt2/Trdmt1 target site (Figure 9) (Schaefer et al., 2009). How the Trdmt1 mediated methylation regulates cellular senescence of pancreatic  $\beta$ -cells? Does insulin level depend on cellular senescence regulated by Trdmt1? Do alternations in the redox pathway impacts Trdmt1 expression? Does a pro-oxidant accelerates cellular aging and is it associated with levels of Trdmt1 and insulin? Does oxidative stress enhance ER stress? Is ER stress associated with changes in the level and localization of Trdmt1? Does the 5-AzaC mediated methyltransferase inhibition may lead to ER stress and modify insulin production? Can 5-AzaC promote the elimination of old pancreatic  $\beta$ -cells? Does senotherapy may be used in insulinoma treatment and does Trdmt1 can be a target in this therapy?

We hypothesized that 5-AzaC demonstrates senolytic activity on SIPS insulinoma cells by decreasing Dnmt2/Trdmt1 activity and ER stress related UPR and/or ERAD pathways activation.

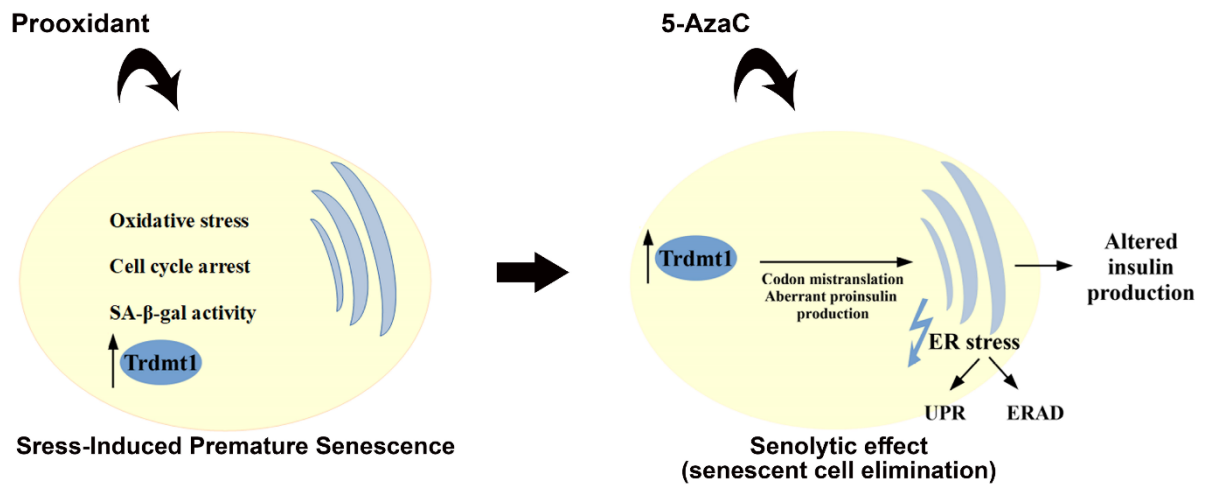


**Figure 9. Model illustrating the assumption of stress-induced premature senescent insulinoma cells treated with 5-AzaC and Trdmt1 related changes.** 5-AzaC mediated Dnmt2/Trdmt1 upregulation and decreased activity leads to Asp, Gly, and Val codons mistranslation and eventually to aberrant proinsulin production. Accumulation of misfolded proteins results in ER stress and is related to alternations in insulin production. To cope with the stress caused by the protein translation perturbations ERAD and UPR pathways are activated.

### **3. Materials and methods**

### **3.1 Cell lines and in vitro cell culture methods**

Established from insulinoma SV40 T-antigen transgenic mice cell lines NIT-1 and BetaTC6 were purchased from ATCC (Menassas, VA, USA). Moreover, NIT-1 was established from a transgenic NOD/Lt (nonobese diabetic) mouse. It is a widely used model for type I diabetes insulin-dependent diabetes mellitus. Cells at all of the steps of the experimental scheme were cultured at 37°C in the presence of 5 % CO<sub>2</sub> in DMEM with 4,5 g/L glucose, L-glutamine, and sodium pyruvate (Corning REF 10-013-CV) enriched with 15 % FBS (Corning) and antibiotics antimycotic solution (100 U/ml penicillin, 0.1 mg/ml streptomycin and 0.25 µg/ml amphotericin B) (Corning REF 30-004-CI). Cells were passaged by detaching with the trypsin-EDTA solution (Sigma-Aldrich) according to the manufacturer instructions. Firstly cells were rinsed with Ca<sup>+2</sup> and Mg<sup>+2</sup>-free DPBS and then 1X trypsin-EDTA solution was added in the amount needed to completely cover the cells in the vessel. Cells were incubated for approximately 2 minutes at 37°C in the presence of 5 % CO<sub>2</sub>. Both cell lines were cultured up approximately 70 - 80% confluency. At this point the culture medium was enriched with either 100 µM hydrogen peroxide (HP) (Sigma-Aldrich) for oxidative stress induction or 1 µM 5-Azacytidine (5-AzaC) (Sigma-Aldrich) for methylation inhibition and incubated for following 24 h and then collected for further experiments. In the third experimental system cells were treated with 100 µM hydrogen peroxide for 24 h and then media was replaced and cells were treated with 1 µM 5-AzaC for the following 24 h. The experimental scheme has been shown in figure 10.

After treatment, both cell lines were analyzed to find out if ER stress was induced and if it was, what was its relation with DNMT2 in pancreatic beta cells.

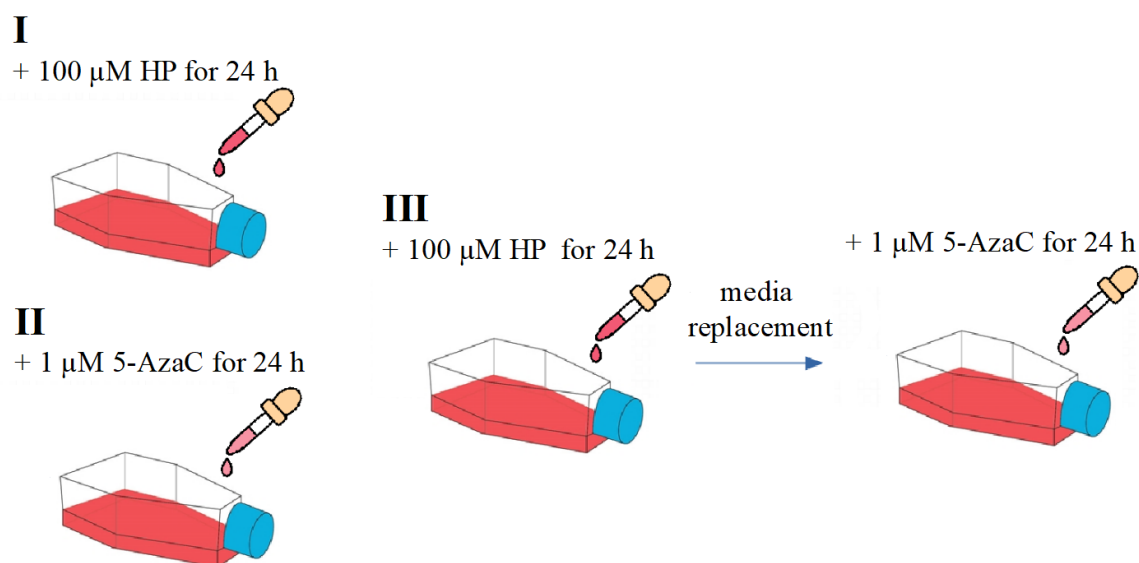


**Figure 10.** Schematic overview of the experimental design of the cell culture. Pancreatic  $\beta$ -cells NIT-1 and BetaTC6 were seeded in the cell culture flasks and cultivated till 70-80% confluency. At this point, old media was replaced with fresh DMEM containing 100  $\mu$ M HP (I) and 1  $\mu$ M 5-AzaC (II) and incubated for 24 hours. After that time cells were collected for further experiments. In a third flask (III) cells at 70-80% confluency were first cultured in DMEM with 100  $\mu$ M HP for 24 hours. Later on, for another 24 hours, media was replaced with DMEM containing 1  $\mu$ M 5-AzaC.

### 3.2 Cytotoxicity

Hydrogen peroxide is well known cellular stress inducer that may also increase the production of TRDMT1 (Lewinska et al., 2018). HP also belongs to a group of stressors triggering SIPS arising (O. Toussaint et al., 2000). Cytotoxicity of hydrogen peroxide was evaluated by conducting an MTT assay. This colorimetric assay uses the ability of enzymes present only in metabolically active cells to convert a yellow tetrazolium salt (3-[4,5-dimethylthiazol-2-yl]-2,5-diphenyl-tetrazolium bromide, MTT) to a purple formazan (Cole, 1986). Cells were seeded onto a 96-well plate at density  $1 \times 10^4$  cells per well and grown for 24 hours. In the next step, media was removed and cells were cultured in media containing 200  $\mu$ M, 100  $\mu$ M, 50  $\mu$ M, and 25  $\mu$ M HP for 15 minutes, 1 hour, and 24 hours. After that time cells were incubated with MTT solution for 4 hours at 37°C and created formazan crystals were dissolved in dimethyl sulfoxide (DMSO) (Sigma-Aldrich). Cell metabolic activity was measured by reading the absorbance at 570 nm using microplate reader (Titertek Multiskan MCC/340, Flow Laboratories, Basel, Switzerland). Based on this test the 100  $\mu$ M concentration was chosen for further analysis.

### 3.3 Apoptosis

The percentage of apoptotic cells was measured by Annexin V detection which was assayed using Muse™ Cell Analyzer and Muse™ Annexin V and Dead Cell Assay Kit (Merck Millipore, Warsaw, Poland). As a dead cell marker used a fluorescent DNA dye 7-aminoactinomycin D (7-AAD) which is an indicator of cell membrane structural integrity. Quantitative cell analysis performed on The Muse Cell Analyzer is based on fluorescence detection and microcapillary technology. For performing the assay NIT-1 and BetaTC6 cells treated with HP, 5-AzaC, HP, and 5-AzaC and also untreated cells were dissociated with trypsin and suspended in a fresh medium. 100 µl of Muse™ Annexin V & Dead Cell Reagent warmed up to room temperature was dispensed into tubes. 100 µl of cells in suspension was added to each tube, mixed by pipetting, and incubated for 20 minutes at room temperature in the dark. After that time each sample was loaded on the instrument and analyzed by the instrument. Four populations of cells were identified in the performed assay:

- non-apoptotic cells: Annexin V (-) and 7-AAD (-)
- early apoptotic cells: Annexin V (+) and 7-AAD (-)
- late-stage apoptotic and dead cells: Annexin V (+) and 7-AAD (+)
- mostly nuclear debris: Annexin V (-) and 7-AAD (+).

All of the results were shown using Muse™ Annexin V and the Dead Cell software module. All of the calculations were performed automatically. The obtained Annexin V profile was presented as dot plots.

### 3.4 Senescence-associated $\beta$ -galactosidase activity (SA- $\beta$ -gal)

Pancreatic  $\beta$ -cells NIT-1 and BetaTC6 were treated with HP and 5-AzaC as described above and cultured for the following 7 days. After that time cells were fixed at room temperature in the darkness with a solution of 2 % formaldehyde and 0,2 % glutaraldehyde in PBS (Sigma-Aldrich), then washed in PBS and incubated overnight at 37°C in a solution of 1 mg/ml 5-bromo-4chloro-3-indolyl- $\beta$ -D-galactopyranoside, 5 mM potassium ferrocyanide, 5 mM potassium ferricyanide, 150 mM NaCl, 2 mM MgCl<sub>2</sub> and 40 mM citratephosphate buffer, pH 6.0 (Sigma–Aldrich). Cells were assayed with the usage of an Olympus BX71

light inverted microscope with a DP72 CCD camera and an analysis system CellB (Shinjuku, Tokyo, Japan).

### **3.5 Cell cycle**

One of the oldest applications of flow cytometry is cell cycle assay by DNA content quantitation. Cells treated with HP, 5-AzaC, and a combination of both were fixed in 4 % paraformaldehyde (PFA) for 20 minutes at room temperature. In the next step, cells were centrifugated at 300 g for 5 minutes, washed in DPBS, resuspended in 70 % ethanol, and incubated for 20 minutes on the ice. For nucleus visualization analyzed cells were incubated with propidium iodide (PI) for 10 minutes protected from light. Thus the percentage of cells in particular cell cycle phases G<sub>0</sub>/G<sub>1</sub>, S, and G<sub>2</sub>/M was analyzed using IDEAS® Software FlowSight Cytometry Imaging.

### **3.6 Oxidative stress**

After HP, 5-AzaC, HP, and 5-AzaC treatment changes in the levels of reactive oxygen species (ROS) were analyzed using flow cytometry and Muse™. The Muse® Oxidative Stress Kit (Merck Milipore) detects superoxide radicals basing on dihydroethidium (DHE) as a fluorescent probe. DHE can be oxidized by cellular superoxide to ethidium bromide fluorophore (Etd<sup>+</sup>) that intercalates into DNA resulting in red fluorescence (Q. Wang & Zou, 2018). All the reagents were prepared according to the protocol provided by the manufacturer. Muse® Oxidative Stress Reagent stock solution was diluted 1:100 in 1X Assay Buffer and this way obtained Muse® Oxidative Stress Reagent intermediate solution was diluted 1:80 in 1X Assay Buffer. Received Working Solution was used in the further assay. All of the reagents were prepared freshly right before use, stored at room temperature, and protected from the light. Cell suspension of treated and untreated cells was prepared by cell dissociation from cell culture flask as described above and suspended in a 1X Assay Buffer to a final concentration of 1 x 10<sup>6</sup> cells/ml. Muse® Oxidative Stress Reagent and 1X Assay Buffer were warmed up to room temperature. Into each tube, 10 µl of cells in suspension were added and 190 µl of Muse Oxidative Stress Reagent and mixed thoroughly by pipetting up and down. Prepared samples were incubated for 30 minutes at 37°C and then loaded on the instrument to run the assay. Two groups of cells were recognized:

- M1: negative cells ROS (–)



- M2: cells with ROS activity, ROS (+).

All of the results were shown using Muse™ Oxidative Stress software module. All of the calculations were performed automatically. Obtained ROS profiles were displayed on a histogram.

### **3.7 Nitrosative stress**

Levels of nitric oxide in pancreatic  $\beta$ -cells of NIT-1 and BetaTC6 cell line after HP, 5-AzaC, HP, and 5-AzaC treatment and without treatment were measured using Muse™ Nitric Oxide KIT (Merck Milipore). Used kit includes two main components: The Muse Nitric Oxide Reagent (DAX-J2 Orange) and a dead cell marker 7-amino-actinomycin D (7-AAD). DAX-J2 Orange is a cell-permeable reagent which oxidation upon NO inside the living cell results in the production of a highly fluorescent product. The second compound of the kit is a DNA dye 7-AAD. This dead cell marker allows recognizing cells with a disrupted membrane structure like apoptotic or necrotic cells where membrane integrity is lost (Schmid et al., 2007). All the reagents were warmed up to room temperature before use. Muse Nitric Oxide Reagent stock was diluted 1:1000 in 1X Assay Buffer. Obtained Muse® Nitric Oxide working solution was used right after preparation and stored in the dark at room temperature. Muse® 7-AAD working solution was prepared by diluting the Muse 7-AAD stock solution 1:45 in 1X Assay Buffer and stored on ice in the dark. NIT-1 and BetaTC6 cell lines treated with HP, 5-AzaC, HP, and 5-AzaC and untreated were detached from cell culture flask with trypsin. Cells were washed in DPBS and resuspended in 1X Assay Buffer to final concentration approximately  $1 \times 10^5$  cells/ml. Into each tube added 10  $\mu$ l of cells in suspension and 100  $\mu$ l of Muse® Nitric Oxide working solution. The content of the tubes was mixed thoroughly by pipetting up and down and incubated for 30 minutes in the 37° incubator with 5% CO<sub>2</sub>. After incubation added to each tube 90  $\mu$ l of Muse 7-AAD working solution mixed thoroughly by pipetting up and down and incubated for 5 minutes at room temperature in the dark. Ready samples loaded on the instrument to run the assay. In performed analysis four populations were distinguished:

- Viable Cells with no Nitric Oxide Activity (negative): Nitric Oxide (-) and 7-AAD (-)
- Live Cells with Nitric Oxide Activity: Nitric Oxide (+) and 7-AAD (-)
- Dead Cells with Nitric Oxide Activity: Nitric Oxide (+) and 7-AAD (+)
- Dead Cells with no Nitric Oxide Activity: Nitric Oxide (-) and 7-AAD (+)

All of the results were displayed using Muse™ Nitric Oxide software module. All of the calculations were performed automatically. Obtained results were presented as dot plots.

### **3.8 Protein carbonylation**

At first, proteins were separated in sodium dodecyl sulfate (SDS) gel electrophoresis. In the next step separated proteins were transferred to a membrane and incubated with anti-DNP antibody and then with a secondary antibody conjugated with horseradish peroxidase. The level of protein carbonylation was detected with a chemiluminescent reaction. In this project, protein carbonylation was analyzed using OxyBlot™ Protein Oxidation Detection Kit (Merck Milipore). Protein lysates of pancreatic  $\beta$ -cells NIT-1 and BetaTC6 cell lines treated with HP, 5-AzaC, both HP, and 5-AzaC and untreated were prepared as described previously. For derivatization of the protein mixture, 5  $\mu$ l of protein sample was transferred into 2 Eppendorf tubes (one for derivatization and the other one for a negative control) and denaturated by adding 5  $\mu$ l of 12% SDS. Samples were derivatized by adding 10  $\mu$ l of 1X DNPH solution to one of the tubes. To the other tube serving as a negative control added 10  $\mu$ l of 1X Derivatization-Control Solution. Tubes were incubated for 15 minutes at room temperature. After incubation 7.5  $\mu$ l of Neutralization Solution was added to both tubes. With prepared, this way samples proceeded to electrophoresis and Western blotting. 2.5  $\mu$ l molecular weight standard was mixed with DNP residues and 20  $\mu$ l of 1X Gel Loading Buffer. Samples were loaded into the gel.

After electrophoresis proteins were transferred to a membrane. Unspecific signals were blocked by incubating the membrane in a blocking solution of 1 % BSA for 1 hour at room temperature with gentle shaking. Later, the membrane was incubated in a primary antibody diluted in a blocking solution in ratio 1:150 for 1 hour at room temperature with gentle agitation. Membrane washed 3 times 5 minutes each with 1X TBS-T at room temperature. The secondary antibody was diluted 1:300 in 1 % BSA and the membrane was incubated in it for 1 hour at room temperature with gentle agitation. After incubation with the antibody, the membrane was washed as previously, 3 times 5 minutes each in TBS-T. The membrane was placed on a plastic sheet and exactly covered with chemiluminescent reagent Clarity™ Western ECL Blotting Substrate (BioRad) mixed in proportion 1:1 right before use and incubated for 4 minutes in the dark. Signal was detected using a G:BOX imaging system (Syngene, Cambridge, UK) according to the manufacturer's instructions.

### **3.9 Cell lysates and protein concentration evaluation**

For preparing the whole-cell extracts cells treated with HP and/or 5-AzaC as described above, and non-treated cells, as a control, were collected, washed in 1 ml of DPBS (Corning), and centrifuged at 2000 rpm for 5 minutes at room temperature. Cell pellet was resuspended in cold RIPA buffer (50 mM Tris-HCl pH 7.5, 1 % NP40, 0.5 % sodium deoxycholate, 0.1 % SDS, 150 mM NaCl, 1 mM EDTA, 1X protease inhibitor cocktail, 1 mM PMSF), incubated on ice for 30 minutes and vortexed every 10 minutes. For further cell disruption tubes were placed into the thermomixer and incubated at 4°C for 30 minutes with maximum speed. Cell lysates were centrifuged at 12000 g for 15 minutes at 4°C. The supernatant containing whole protein extract was transferred into the fresh tubes. The concentration of proteins in obtained extracts was evaluated with the BCA (Bicinchoninic Acid) protein assay. In this method, Cu<sup>2+</sup> ions are reduced by proteins to Cu<sup>+</sup> in an alkaline pH. Responsible for this are peptide bonds present in amino acid residues of cysteine, cystine, tyrosine, and tryptophan. Reduced copper ions react with bicinchoninic acid creating a purple complex. To perform BCA assay protein lysates were loaded into a 96-well plate in three repetitions, 12.5 µl per well. For a standard curve used BSA (Sigma Aldrich) diluted in RIPA buffer in following concentrations: 0 mg/ml, 0.1 mg/ml, 0.2 mg/ml, 0.5 mg/ml and 1 mg/ml. Loaded into the 96-well plate in the same manner as samples. To each well containing samples and BSA added 100 µl of a prepared working solution containing BCA and copper (II) sulfate (Sigma Aldrich) mixed in a proportion 50:1. The plate was incubated at 37°C for 30 minutes and after that time absorbance was measured on TECAN Plate Reader at 562 nm wavelength.

### **3.10 Western blotting**

Mice pancreatic β-cells NIT-1 and BetaTC6 cultivated in media containing 100 µM HP and/or 1 µM 5-AzaC and untreated cells were lysed and levels of proteins were measured using Western blot assay. Samples with whole protein content were loaded into the 10 % gel and separated in SDS-PAGE. Into the first well loaded protein standard Spectra™ Multicolor Broad Range Protein Ladder (Thermo Fisher Scientific). Proteins were separated at 80 V for approximately 30 minutes (stacking gel) and at 120 V till samples reached the end of the gel (resolving gel). Separated proteins were transferred from the gel to a nitrocellulose membrane using a wet-tank method. The transfer was performed in a Towbin buffer (0.25M

Tris, 1.92 M glycine, 20% methanol) in a cold room at 100 V for 100 minutes. Membranes were blocked in a 1% BSA solution in TBS-T for 1 hour at room temperature. In the next step, membranes were incubated overnight at 4°C with agitation in primary antibodies diluted in blocking solution. After incubation in primary antibodies membranes were washed in TBS-T 3 times 5 minutes each and incubated in secondary antibodies anti-rabbit IgG conjugated to horseradish peroxidase for 1 hour at room temperature. Signals of searched proteins were detected using a Clarity™ Western ECL Blotting Substrate (BioRad) and G:BOX imaging system (Syngene, Cambridge, UK) according to the manufacturer's instructions. All results were normalized to a GAPDH.

### **3.11 Protein aggregation**

Abnormal, misfolded, or unfolded proteins are degraded in the ubiquitin-proteasome pathway. However, any perturbations in the pathway of removing incorrect proteins lead to the accumulation of protein aggregates (Ge et al., 2007). In protein extracts pancreatic  $\beta$ -cells cell lines the amount of peptide and protein aggregates was detected with the usage of PROTEOSTAT® Protein aggregation assay (Enzo Life Sciences) which detection range is between 1  $\mu$ l/ml and 10 mg/ml of protein. As a positive and negative control used lyophilized native and aggregated protein was provided by the manufacturer. Into each well of 96-well plate dispensed 98  $\mu$ l of protein and 2  $\mu$ l of PROTEOSTAT Detection Reagent previously diluted in 10x Assay Buffer and water. After 15 minutes of incubation in the dark measured the absorbance on TECAN Plate Reader at an excitation setting 550 nm and an emission filter at 600 nm.

### **3.12 Flow cytometry**

HP and/or 5-AzaC treated and untreated cells were collected from the cell culture washed in DPBS and fixed in 4 % paraformaldehyde (PFA) for 20 minutes at room temperature. In the next step, cells were centrifugated at 300 g for 5 minutes, washed in DPBS, resuspended in 70 % ethanol, and incubated for 20 minutes on the ice. Cells were centrifugated at 300g for 5 minutes washed twice in 1% BSA diluted in DPBS and incubated in blocking solution (1% BSA in DPBS) for 30 minutes at room temperature. After blocking cells were incubated with primary antibody anti-DNMT2 (1:100) (Santa Cruz Biotechnology) and secondary antibody anti-mouse (1:500) (Lifetechnologies) conjugated with FITC and nuclei were stained with

propidium iodide (PI) for 10 minutes at room temperature in the dark. In another set fixed cells were subjected to incubation with primary antibodies anti-DNMT2 (1:500) (Santa Cruz Biotechnology), anti-peIF2 Ser 52 (1:100) (Invitrogen) for 1 hour, and a secondary antibodies goat anti-rabbit (1:500) (Invitrogen) conjugated with Cy5 and goat anti-mouse (1:500) (Life Technologies) conjugated with FITC. All antibodies were diluted in 1 % BSA and incubations were carried on for 1 hour at room temperature. During incubation with secondary antibody, samples had to be also protected from light. Nucleus staining with PI was performed for 10 minutes at room temperature in the dark. Using Amnis FlowSight Imaging Flow Cytometer Trdmt1/Dnmt2 and peIF2 $\alpha$  levels and co-localization were analyzed.

For autophagy analysis treated and fixed cells as described above were incubated with LC3b antibody (1:100) (Cell Signalling) and with secondary antibody anti-rabbit (1:500) conjugated with Alexa Fluor 488 donkey rabbit IgG (H+L) (Thermo Fisher Scientific).

### **3.13 Laser-based confocal imaging**

Cells were seeded into 96-well plate in density  $3 \times 10^3$  cells/well treated with HP and/or 5-AzaC and for control untreated. Cells were incubated with fixing solution (DPBS, Triton X-100 0,01% and formaldehyde 3,7%), next blocked with 1 % BSA solution in DPBS with Triton X-100. Fixed and blocked cells were incubated overnight with the primary antibodies anti-FOXO3a (1:200) (Thermo Fisher Scientific), anti-F-actin, and for 1 hour with a secondary antibodies anti-mouse (1:200) conjugated with Texas Red, anti-rabbit (1:1000) conjugated with FITC (Thermo Fisher Scientific), and nuclei were stained with Hoechst solution diluted in DPBS to a final concentration 1  $\mu$ g/ml.

Cells were seeded into 96-well plate in density  $3 \times 10^3$  cells/well treated with HP and/or 5-AzaC and for control untreated. Cells were incubated with fixing solution (DPBS, Triton X-100 0,01% and formaldehyde 3,7%), next blocked with 1 % BSA solution in DPBS with Triton X-100. Fixed and blocked cells were incubated overnight with the primary antibody phospho-S6 (Ser235, Ser236) (Thermo Fisher Scientific) (1:100) and for 1 hour with the secondary antibody anti-rabbit (1:200) conjugated with Texas Red.

For endoplasmic reticulum visualization living cells were stained with ER-Tracker Blue White DPX (Thermo Fisher Scientific). Staining was performed in staining solution diluted to final concentration of 1  $\mu$ M in Hank's Balanced Salt Solution for 30 minutes at 37°C and

5 % CO<sub>2</sub>. In the next step, cells were incubated with a primary antibody anti-DNMT2 (1:100) (Thermo Fisher Scientific) and for 1 hour with a secondary antibody anti-mouse (1:200) (Thermo Fisher Scientific) conjugated with Texas Red, the nucleus was stained with Hoechst solution diluted in DPBS to a final concentration 1 µg/ml.

Proteasome activity was performed according to the protocol provided by the manufacturer. All of the samples were analyzed using HCA system IN Cell Analyzer 6500 HS and IN Carta software.

### **3.14 Confocal imaging**

In the 6-well plate, sterile glass coverslips were placed at the bottom of each well, and cells were seeded in DMEM and cultured until approximately 80 % confluency. After that time pancreatic β-cells were treated with HP, 5-AzaC, HP, and 5-AzaC as described previously. As a control used untreated cells. Treated and untreated cells were washed 2 times with DPBS (Thermo Fisher Scientific) 5 minutes each and then incubated in 0.1 M sodium citrate buffer for 10 minutes. After that time cells were rinsed once again with PBS twice 5 minutes each and incubated in dissolved in DPBS 3 % BSA for 30 minutes to block unspecific signals. Then coverslips with attached cells were incubated with diluted in PBS primary antibody anti-insulin (1:50) (Santa Cruz Biotechnology) overnight at 4°C. Cells were washed with DPBS two times 5 minutes each and incubated with diluted in DPBS secondary antibody anti-rabbit (brand) conjugated with FITC for 1 hour at room temperature. After incubation cells were washed two times with PBS for 5 minutes each and stained with diluted in PBS DAPI (brand) (1:1000) for 15 minutes at room temperature for visualization of the nucleus. After rinsing cells with DPBS like described before, coverslips were transferred to glass slides with a drop of PBS and placed on those face down. Ready samples were analyzed with a confocal microscope (brand) under 40x magnification.

### **3.15 Statistical analysis**

Statistical analysis was performed with GraphPadPrism. Bars indicate SD, n = 3, \*\*\*p < 0.001, \*\*p < 0.01, \*p < 0.05 compared to the control (ANOVA and Dunnett's a posteriori test).

## **4. Results**

#### **4.1 HP and 5-AzaC treatment induce changes in senescence and cell cycle inhibition in pancreatic $\beta$ -cells**

Two insulin secreting pancreatic  $\beta$ -cell lines were treated with hydrogen peroxide and 5-Azacytidine. NIT-1 is an insulinoma cell line established from NOD/Lt (nonobese diabetic) mice and transgenic for the SV40 T-antigen. Insulin is secreted by NIT-1 in a response to the presence of glucose in the medium (Hamaguchi et al., 1991). Moreover, NIT-1 spontaneously develops type 1 diabetes what makes it a good model to understand T1D pathogenesis and treatment (Pearson et al., 2016). The other cell line, BetaTC6 is derived from insulinoma transgenic mice expressing SV40 T-antigen. This cell line contains small amounts of glucagon and somatostatin and an abundant amount of insulin which is secreted in a response to glucose (Poitout et al., 1995).

Hydrogen peroxide used in this study induces cellular stress and, as has been shown on human fibroblasts, may increase the production of Trdmt1 (Lewinska et al., 2018). One of the cell responses to cell stress and aging is senescence and thus loss of the proliferation capability. HP is a stressor that induces premature senescence of cells (SIPS), and therefore senescent-like morphology and cell growth arrest (Olivier Toussaint et al., 2002). To identify senescence cells and detect possible changes as a result of cellular stress induction by HP and 5-AzaC used SA- $\beta$ -gal assay. Senescence-associated- $\beta$ -galactosidase (SA- $\beta$ -gal) is a lysosomal enzyme which activity is enhanced with increased pH from optimal pH 4, found in young cells, to suboptimal pH 6 in senescent cells. That is why the expression level of SA- $\beta$ -gal is commonly used as a biomarker of senescence and aging in cell cultures. The content of SA- $\beta$ -gal may be measured by histochemical staining with X-gal used as a substrate which cleavage stains cells blue (Dimri et al., 1995; Itahana et al., 2013; Shlush et al., 2011). As shown in figure 11 A SA- $\beta$ -gal staining revealed the level of senescent cells after HP and 5-AzaC treatment. HP treatment leads to premature senescence which indicates its senostatic activity – inhibits signaling and blocks proliferation of senescent cells. What was observed is a change in morphology of  $\beta$ -cells after combined treatment with HP and 5-AzaC. Cells of both cell lines did not aged, did not proliferate but were not also dead what indicates senolytic activity (Figure 11 C). All senescent cells were killed and the cell cycle of others was inhibited. Proliferation profile of NIT-1 and BetaTC6 cell lines treated with HP and/or 5-AzaC. HP significantly decreased the number of cells in the culture. BetaTC6 cell line has shown higher vulnerability for oxidative stress induction.



The cell cycle is a process in which a cell gets prepared and then undergoes division into two new cells. The four main stages that can be recognized in the cell cycle are the phase of preparation for division (G1), DNA complete copy synthesis (S), organization and condensation genetic material for division (G2), and a phase of formation of two actual daughter cells called mitosis (M). The order and accuracy of each step during the cell cycle are monitored through the entire process by multiple checkpoints (Barnum & O'Connell, 2014; J. M. Mitchison, 1972). This mechanism guarantees precise cell division and protects from any dangerous disturbances that may lead to for example to cancer development. A cell can stop the cycle to repair the damage and go back to the cycle, or if the harm is too big cell is eliminated via apoptosis. ROS is responsible for a DNA damage induction thus may stimulate cell cycle arrest (Shackelford et al., 2000). The research on human fibroblasts has shown that HP induced oxidative stress causes results in cell cycle arrest of cells primarily in the G1 or G2/M phase or apoptosis of cells in the S phase. Moreover after one week of treatment developed senescence-like growth arrest (CHEN et al., 2000).

In this study, HP mediated cell cycle inhibition was observed in both cell lines NIT-1 and BetaTC6 during the G2/M phase. but also in the S phase. 5-AzaC and HP treatment induced cell cycle arrest on the S phase. S phase substantial inhibition of cell cycle in BetaTC6 cell line upon cellular stress induced by HP was also detected. 5-AzaC and HP only slight increase in the number of cells in the S phase (Figure 11 B). In both cell lines, 5-AzaC seems to weakens HP mediated cell cycle inhibition.

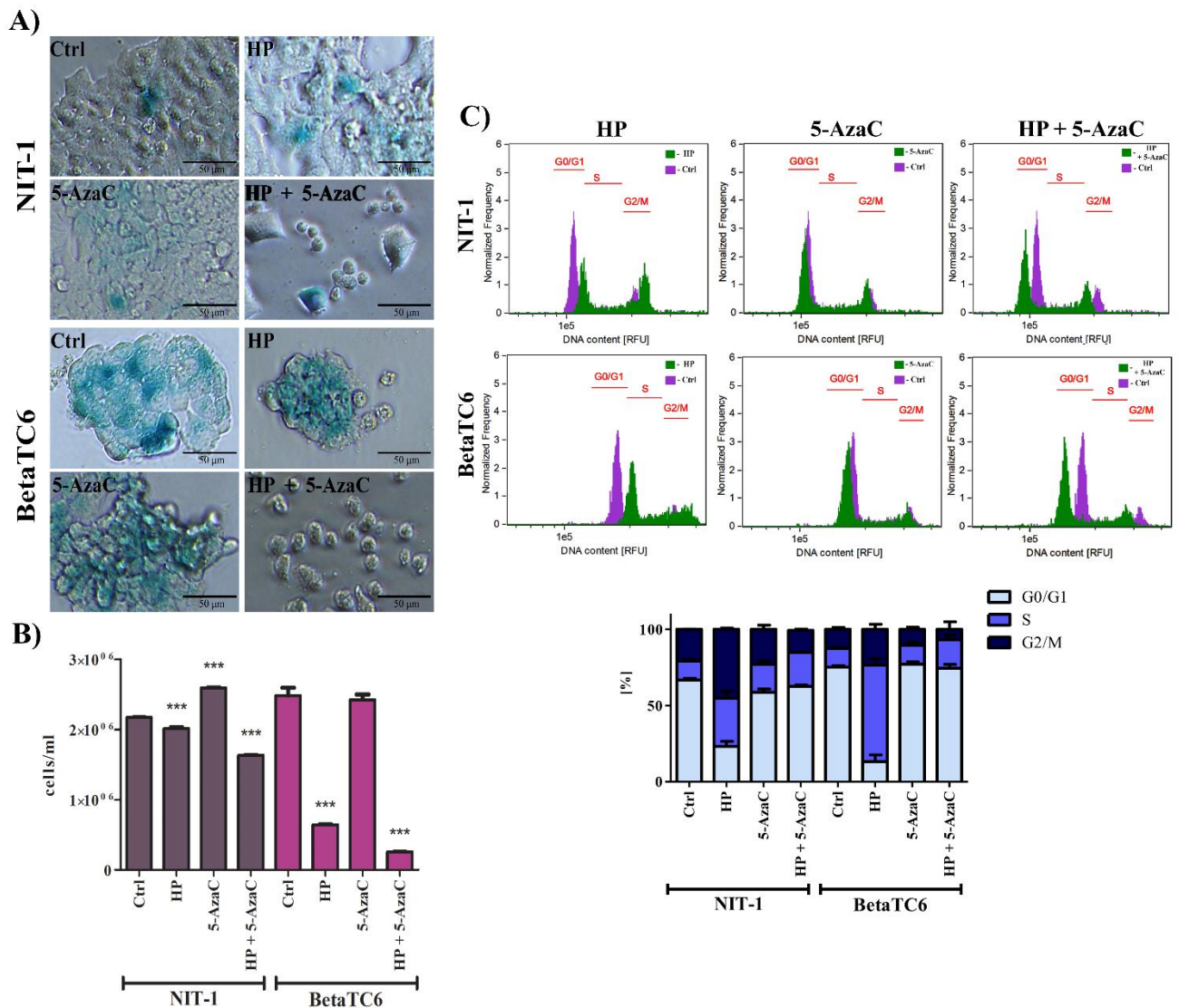


**Figure 11. HP and 5-AzaC cell senescence induction and cell cycle inhibition in G2/M phase after oxidative stress induction.** (A) SA- $\beta$ -gal staining revealed level of senescent cells after HP and 5-AzaC treatment: **NIT-1** Ctrl 70-80 %, HP < 80 %, 5-AzaC < 80 %, HP + 5-AzaC > 20%; **BetaTC6** Ctrl < 90 %, HP < 90 %, 5-AzaC < 90 %, HP + 5-AzaC 0%. (B) Proliferation profile of NIT-1 and BetaTC6 cell lines treated with HP and/or 5-AzaC. (C) The cell cycle phase was estimated with flow cytometric analysis of cell DNA content. In this study for the cell cycle evaluation used an Amnis® FlowSight® imaging flow cytometer and nuclei were stained with a DNA binding dye propidium iodide (PI). On the figure presented histograms with the DNA content of NIT-1 and BetaTC6 cells treated with HP and/or 5-AzaC overlapped on the untreated controls. Statistical analysis was performed with GraphPadPrism. Bars indicate SD, n = 3, \*\*\*p < 0.001, \*\*p < 0.01, \*p < 0.05 compared to the control (ANOVA and Dunnett's *a posteriori* test).

## 4.2 Characterization of an oxidative and nitrosative stress

### 4.2.1 Oxidative stress

Oxidative stress is described as a disproportion between antioxidants and reactive oxygen species (ROS). Excess of oxygen free radicals and other reactive species is a cause of many perturbations in a cell including damage of nucleic acids, proteins, and lipids (Halliwell & Aruoma, 1991; T. Hamilton, 2012). Free superoxide radicals can be eliminated by a Cu/Zn superoxide dismutase 1 (SOD1) preventing cells from damage and developing several diseases in organisms, like diabetes, cancer, or inflammation. SOD1 upregulation may be triggered by various chemical and biological factors including heat shock, HP, nitric oxide, or heavy metals (Zelko et al., 2002). Conducted analysis showed elevated levels of ROS in both cell lines after treatment with HP and combined treatment with HP and 5-AzaC (figure 12 A). However, NIT-1 cell line turned out to be more vulnerable to oxidative stress induction by both HP and 5-AzaC in comparison to BetaTC6. Moreover, as shown in figure 12 B, Western blot analysis of SOD1 level in pancreatic  $\beta$  cells revealed the superior response of NIT-1 cell line to ROS via higher expression of the protein under HP induced cellular stress and also after methylation inhibition with 5-AzaC. In BetaTC6 protein expression analysis showed downregulation of SOD1 after HP and 5-AzaC treatment, and small upregulation after combined HP and 5-AzaC treatment.

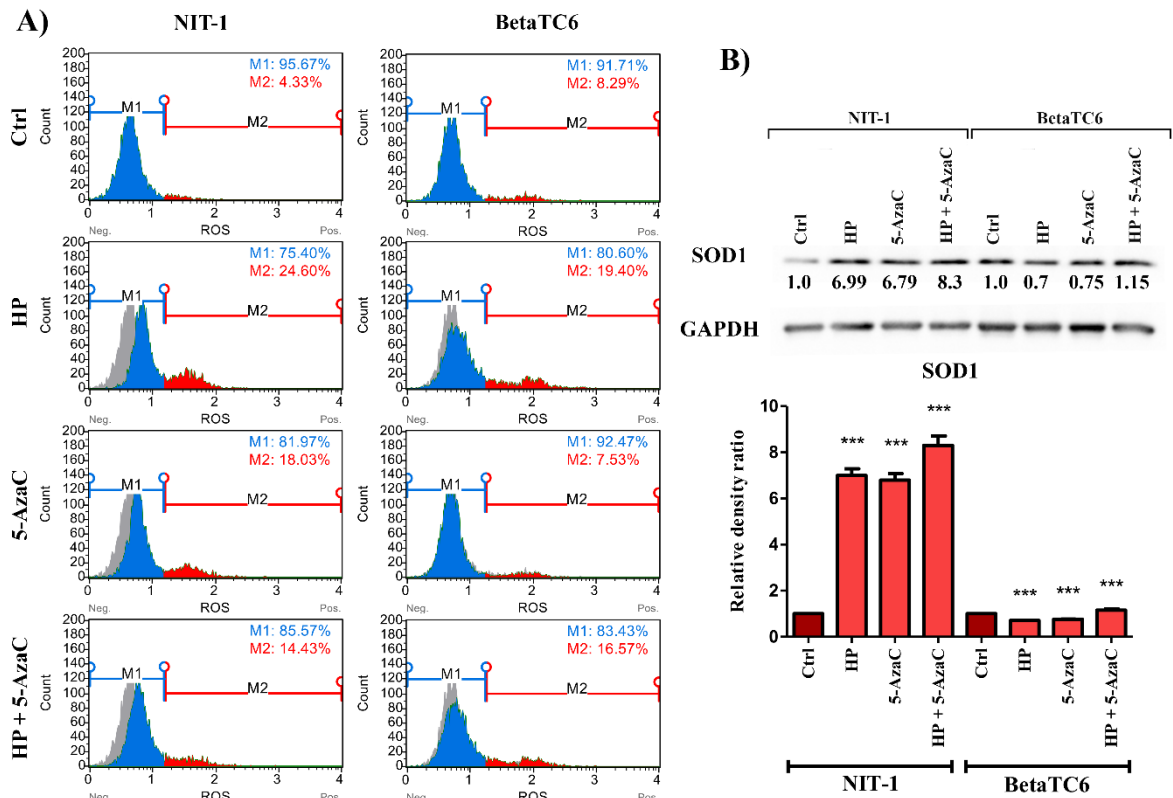


**Figure 12. NIT-1 cell line is more vulnerable to oxidative stress induction.** (A) The oxidative stress level was measured by superoxide detection with Muse® Oxidative Stress Kit. On presented graphs displayed population M1: Negative cells (ROS<sup>-</sup>) and population M2: Cells with ROS activity (ROS<sup>+</sup>). Results are overlaid on a histogram with the negative control (grey). The number of cells/ml in a stained cell sample and the percentage of each population were measured and calculated automatically with the Muse™ Oxidative Stress software module. (B) The graph presented gel quantitation measured with GelQantNET program statistical analysis done with GraphPadPrism. SOD1 level was normalized to GAPDH. Bars indicate SD, n = 3, \*\*\*p < 0.001, \*\*p < 0.01, \*p < 0.05 compared to the control (ANOVA and Dunnett's *a posteriori* test).

#### 4.2.2 FOXO3a elevated level after stress induction and methylation inhibition

FOXO3a belongs to the mammalian forkhead members of the class O (FOXO) transcription factors family. FOXO proteins are related to the regulation of the cell cycle, apoptosis, autophagy, response to stress, or DNA repair. Some cellular stressors including oxidative stress may impact FOXO activity by stimulation actions like translocation from the cytoplasm to the nucleus or several posttranslational modifications like acetylation-deacetylation, phosphorylation, and ubiquitination. The best known FOXO3a modification is phosphorylation. Akt mediated phosphorylation inhibits FOXO3a transcriptional activity

and FOXO3a is translocated to the cytoplasm where binds to 14-3-3 protein what stimulates degradation of FOXO3a by a proteasome. FOXO3a activation is regulated by a protein phosphatase-2A (PP2A) which is necessary for its translocation to the nucleus and dephosphorylation allowing FOXO3a target genes regulation (Nho, 2014). Acetylation-deacetylation of FOXO3a is stimulated by oxidative stress what has an impact on its localization (Furukawa-Hibi et al., 2005). FOXO3a in mice skeletal muscle is translocated to the nucleus, dephosphorylated, and then via binding and thus activation of the genes like ATG12 and GABARAP1L, promotes autophagy (Zhao et al., 2007).

In a presented study Western blot analysis of FOXO3a expression level from the whole cell lysates showed increased production by HP treated NIT-1 cell line and a substantial increase in HP and 5-AzaC treated cells (Figure 13 B). It is worth noticing that the basal level of FOXO3a in control, untreated NIT-1 cells is already relatively high compare with untreated BetaTC6 cells. However, as shown in figure 13 A, immunofluorescent analysis of NIT-1 has not revealed any significant translocation to the nucleus. At the same time, HP induced cellular stress leads to decreased production of FOXO3a in BetaTC6 (Figure 14 B) and slightly increased after HP/5-AzaC treatment. HP and HP/5-AzaC treatment lead to FOXO3a translocation to the nucleus to compare with untreated cells what may be sufficient as a response to increased oxidative stress (Figure 14 A).

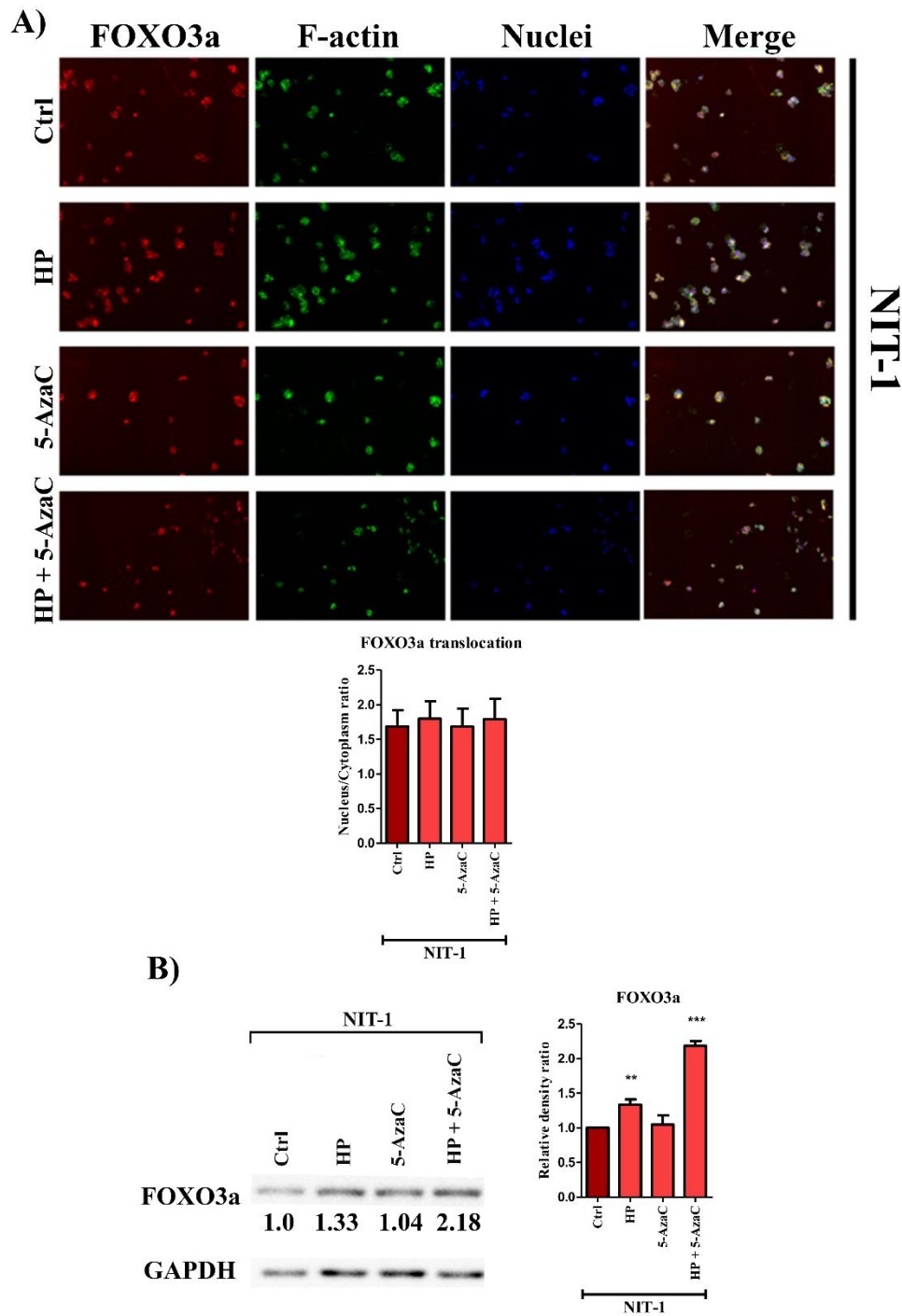


**Figure 13. Increased expression of FOXO3a in NIT-1 cell line and no translocation to the nucleus.** (A) Representative images of FOXO3a staining (red fluorescence), F-actin (green fluorescence), and nuclei (blue fluorescence). Digital pictures were taken with IN Cell Analyzer 6500 HS, quantitative analysis was performed with HCA system IN Cell Analyzer 6500 HS and IN Carta software. Statistical analysis was done with GraphPadPrism. Bars indicate SD,  $n = 3$ ,  $***p < 0.001$ ,  $**p < 0.01$ ,  $*p < 0.05$  compared to the control (ANOVA and Dunnett's *a posteriori* test). (B) Gel quantitation was performed with GelQantNET program and statistical analysis was done with GraphPadPrism. Levels of all proteins were normalized to GAPDH. Bars indicate SD,  $n = 3$ ,  $***p < 0.001$ ,  $**p < 0.01$ ,  $*p < 0.05$  compared to the control (ANOVA and Dunnett's *a posteriori* test).

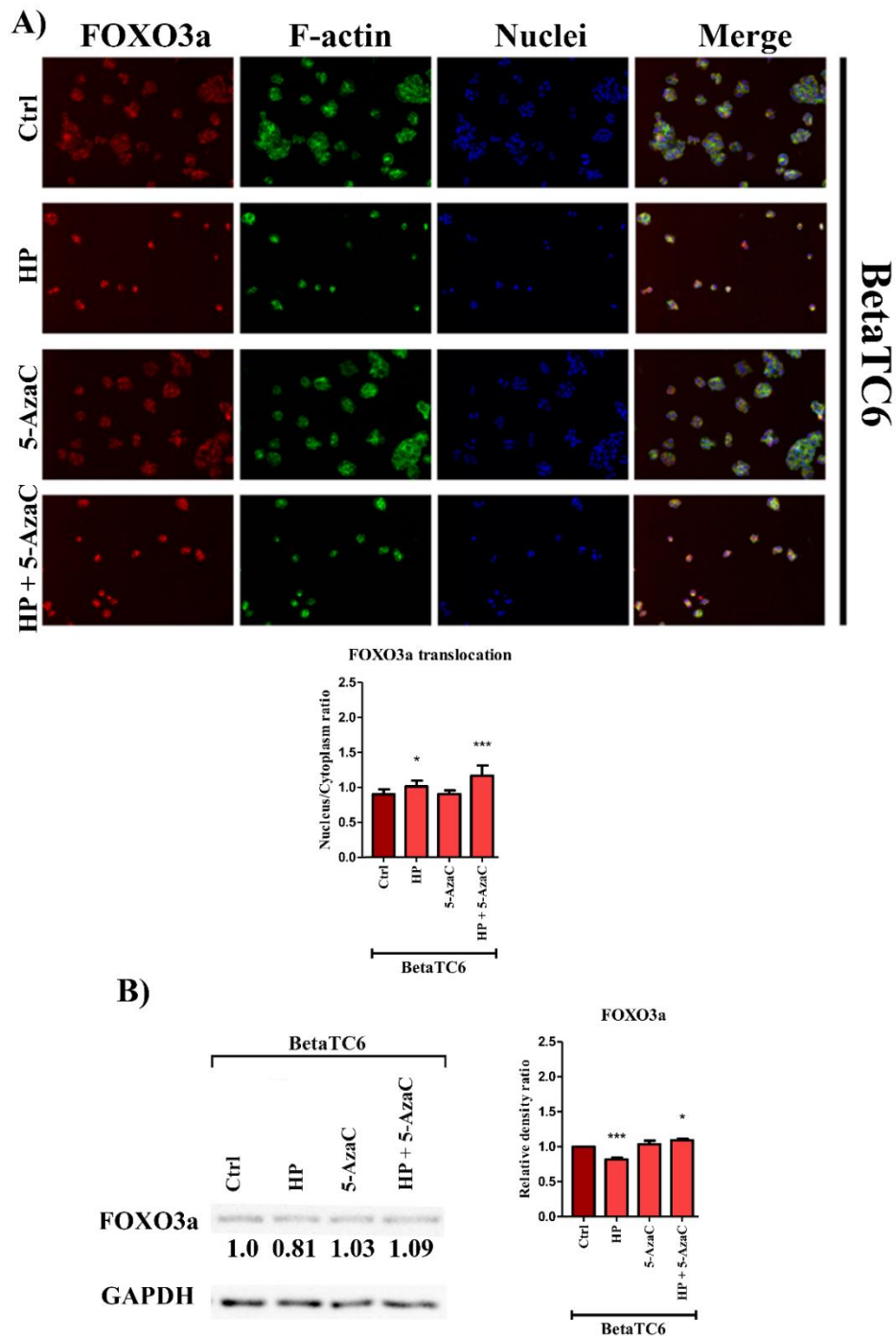


**Figure 14. Changes in the expression of FOXO3a in the BetaTC6 cell line and translocation to the nucleus.** (A) Representative images of FOXO3a staining (red fluorescence), F-actin (green fluorescence), and nuclei (blue fluorescence). Digital pictures were taken with IN Cell Analyzer 6500 HS, quantitative analysis was performed with HCA system IN Cell Analyzer 6500 HS, and IN Carta software. and statistical analysis was done with GraphPadPrism. Bars indicate SD,  $n = 3$ , \*\*\* $p < 0.001$ , \*\* $p < 0.01$ , \* $p < 0.05$  compared to the control (ANOVA and Dunnett's *a posteriori* test). (B) Gel quantitation was performed with GelQantNET program and statistical analysis was done with GraphPadPrism. Levels of all proteins were normalized to GAPDH. Bars indicate SD,  $n = 3$ , \*\*\* $p < 0.001$ , \*\* $p < 0.01$ , \* $p < 0.05$  compared to the control (ANOVA and Dunnett's *a posteriori* test).

### **4.2.3 Nitrosative stress**

Oxidative stress is a premise by the growth of nitric oxide (NO) levels and thus the occurrence of nitrosative and nitrative stress (Cipak Gasparovic et al., 2017). NO takes part in numerous biological mechanisms including apoptosis, cell cycle, or inflammation (Bruckdorfer, 2005). NO signaling plays an important role in the modulation of skeletal muscle metabolism and insulin signaling. Deficit of NO may have serious implications in an organism like cell senescence, insulin resistance, or T2D (Levine et al., 2012). As shown in figure 15 A, hydrogen peroxide leads to increased levels of NO in BetaTC6 and caused no changes in the NIT-1 cell line. The greatest escalation of NO production was observed in the BetaTC6 cell line treated with HP and 5-AzaC.

One of the main targets of reactive oxygen species including oxygen-free radicals is proteins. In the oxidative reactions of proteins carbonyl (CO) groups are inserted into their side chains. If the carbonyl groups are present in the protein side-chain may be verified by a very sensitive reaction with 2,4-dinitrophenylhydrazine (DNPH). The CO groups are derivatized with DNPH to DNP-hydrazone product what can be detected by Western blotting (Dalle-Donne et al., 2003). That is why the present study used this phenomenon to determine the level of carbonylated proteins with the help of the OxyBlot™ Protein Oxidation Detection Kit. Figure 15 B shows increased protein carbonylation was observed in the NIT-1 cell line. In this cell line methylation inhibition in stressed cells lead to explicit augment of CO groups inserted into protein side chain. BetaTC6 has responded the opposite way where depletion of carbonylation was observed.



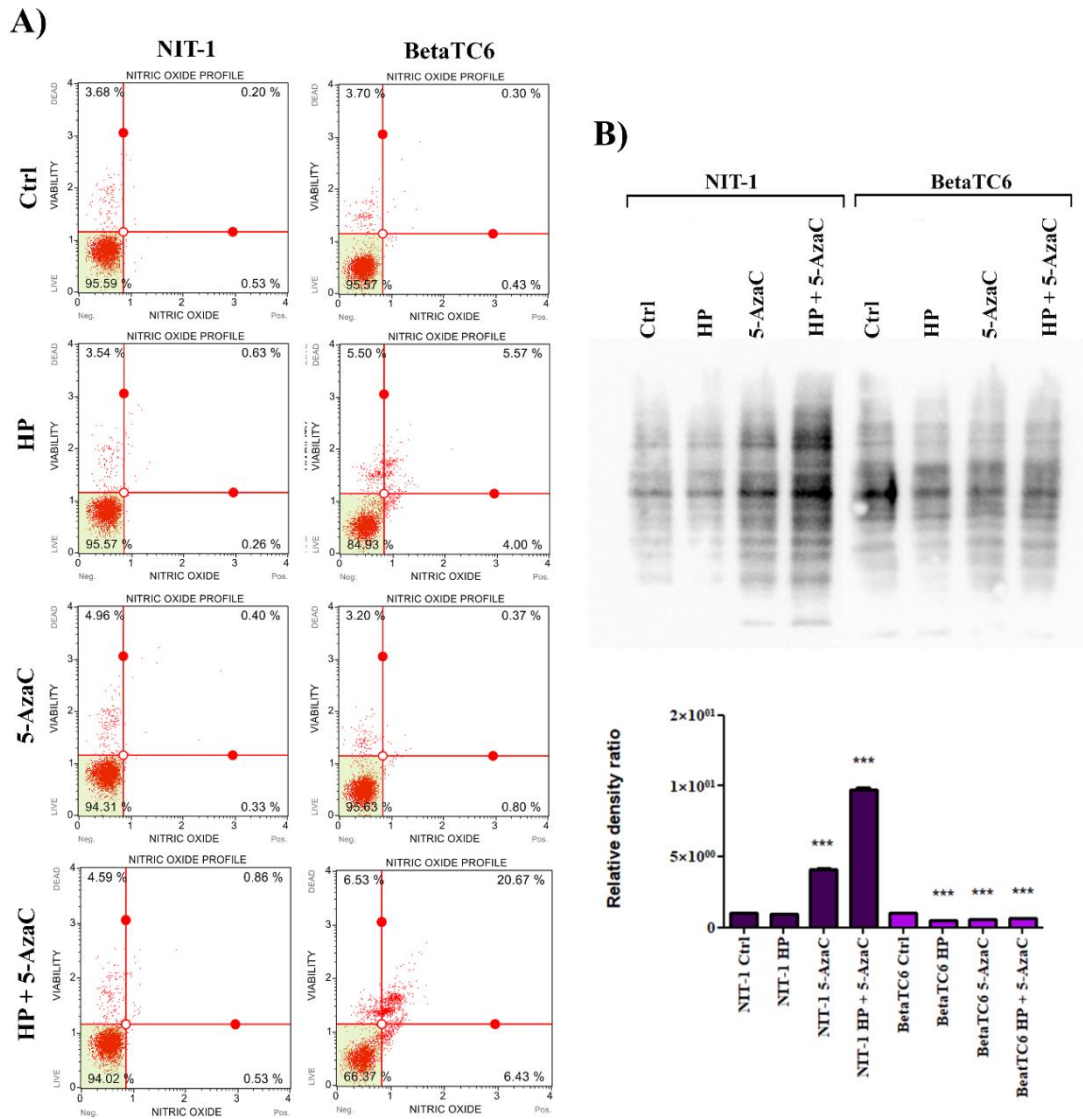


**Figure 15. 5-Azacytidine treatment under the cellular stress conditions leads to excessive NO production in BetaTC6 cell line. (A)** Nitric oxide level was measured by superoxide detection with Muse® Nitric Oxide Kit. Lower-left: live cells with no nitric oxide activity [Nitric Oxide(-) and Dead cell marker (-)]; Lower-right: live cells with nitric oxide activity [Nitric Oxide(+) and Dead cell marker (-)]; Upper-right: dead cells with nitric oxide activity [Nitric Oxide(+) and Dead cell marker (+)]; Upper-left: dead cells with no nitric oxide activity [Nitric Oxide(-) and Dead cell marker (+)] Results presented as dot plots were obtained automatically with Muse™ Nitric Oxide software module. Each dot plot displays the percentage of each detected population. **(B)** The graph presents gel quantitation measured with GelQantNET program statistical analysis done with GraphPadPrism. Bars indicate SD, n = 3, \*\*\*p < 0.001, \*\*p < 0.01, \*p < 0.05 compared to the control (ANOVA and Dunnett's *a posteriori* test).

### **4.3 HP and 5-AzaC induced apoptosis in pancreatic $\beta$ -cells**

A natural way to eliminate the unwanted cell is a process of programmed cell death, also called apoptosis. This pathway is activated during early development or in adults as a response to unrecoverable cell damage, or aging. One of the changes occurring during the first stages of apoptosis is a translocation of the phosphatidylserine (PS) normally present on the inner side of the plasma membrane, to the external layer of the cell. PS manifest a strong affinity to Annexin V, a calcium-dependent phospholipid-binding protein. Annexin V is widely used as a marker of apoptotic cell death (Vermes et al., 1995; Walton et al., 1997). Figure 16 shown Annexin V analysis and revealed significant induction of the apoptotic cell death in the BetaTC6 cell line after HP treatment. Likewise, cell proliferation has distinctly dropped. NIT-1 cell line apoptosis profile after HP and HP/5-AzaC indicated small enhancement, yet it turned out to be more resistant to the damaging action of HP since the proliferation profile was not different from the control and HP induced apoptotic pathway was notably greater in the BetaTC6 cell line than NIT-1. In both cell lines, 5-AzaC alone did not lead to apoptotic cell death.

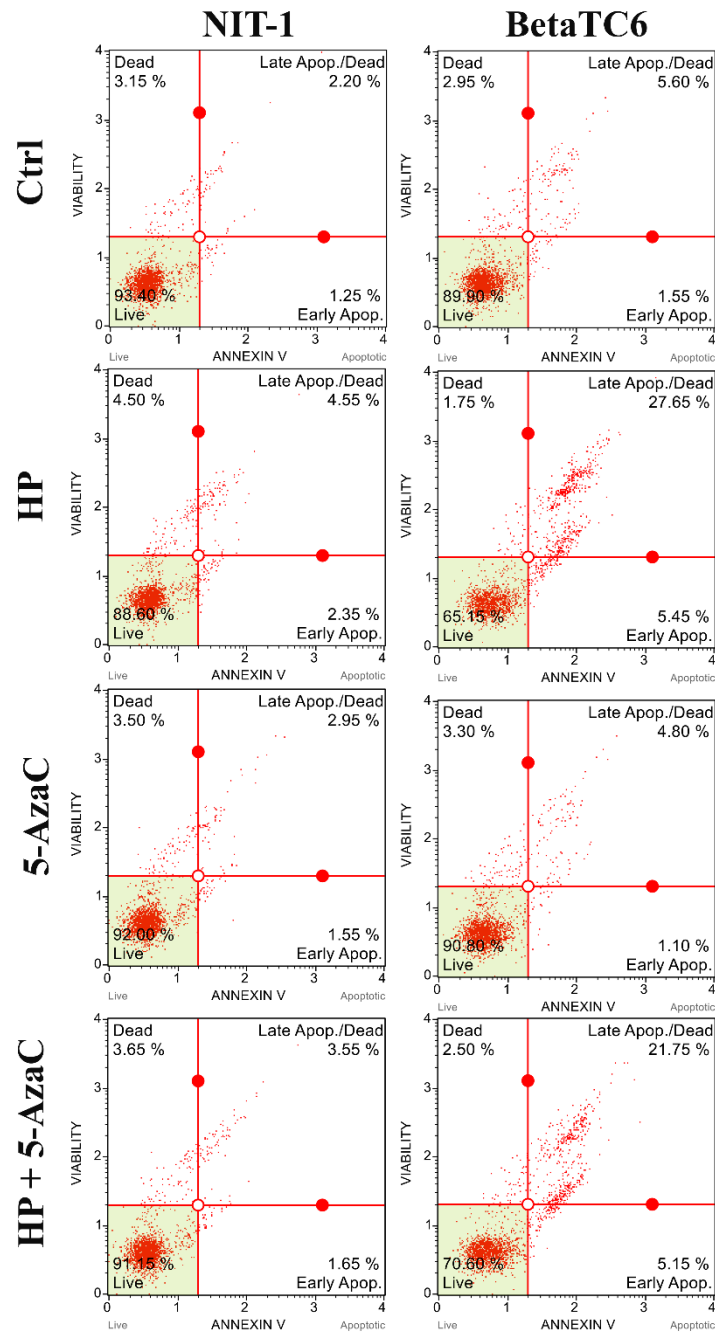


**Figure 16. Hydrogen peroxide and 5-azacitidine induced apoptosis in pancreatic  $\beta$ -cells.** Results presented as dot plots were obtained automatically with Muse™ Annexin V and Dead Cell software module. Each dot plot displays the percentage of each detected population.

## **4.4 5-Azacidine mediated alterations in protein production and localization in pancreatic $\beta$ -cells**

### **4.4.1 5-AzaC mediated activation of ER stress pathway and prevents creating protein aggregates in insulinoma**

Protein folding and maturation take place in the endoplasmic reticulum, however, the consequence of any errors in this process is the ER stress. In the response to that several pathways may be activated, like unfolded protein response (UPR) or endoplasmic reticulum-associated protein degradation (ERAD). UPR is responsible for restoring ER folding capacity and cell homeostasis. Activation of the UPR signaling pathway may take place via three different key UPR transmembrane activator proteins: IRE1, PERK, and ATF6 starting three separate response pathways (Flamment et al., 2012; Lindholm et al., 2006). The addition of the phosphor group to the protein by kinases and phosphatases is a reversible and significant post-translational modification responsible for protein activation (Ardito et al., 2017). This kind of modification concerns some of the UPR signaling transduction pathways like IRE1, eIF2 $\alpha$ , and PERK. For instance, ATF6 protein in its inactive form is localized in the ER membrane as a 90 kDa long protein. Upon ER stress cleavage of ATF6 in the process of proteolysis results in the release of an approximately 50 kDa fragment which translocates to the nucleus and activates ER chaperone genes (Haze et al., 1999).

Western blot analysis of some of the ER stress pathway markers has shown activation of this pathway by the 5-AzaC treatment (Figure 17 A). GRP78 which plays a key role in IRE-1 mediated UPR significantly increases in NIT-1 cells upon HP and 5-AzaC treatment whereas in BetaTC6 cell is downregulated in comparison to untreated control. Similarly, HP and 5-AzaC mediated upregulation of PERK expression was observed in all treated NIT-1 whole cell lysates. Moreover, in the PERK signaling pathway, phosphorylated, and thus an active form of eIF2 $\alpha$  (p-eIF2 $\alpha$ ) was also upregulated upon HP/5-AzaC treatment and significantly increased upon 5-AzaC treatment. At the same time, the levels of eIF2 $\alpha$  in all treated samples were decreased. IRE1 in the NIT-1 cell line was upregulated after 5-AzaC and HP/5-AzaC and downregulated after HP. Likewise, HP mediated pIRE1 decrease was observed, and HP/5-AzaC. Only 5-AzaC led to an increase of pIRE1 expression. Moreover, a significant expression downregulation of a third UPR transmembrane activator protein ATF6 in the NIT-1 cell line was observed. The expression of UPR protein in the BetaTC6 cell line was fairly different than in the NIT-1 cell line. In BetaTC6 cells PERK was also upregulated,

however 5-AzaC and HP/5-AzaC mediated stress induced its greater expression than in NIT-1. Furthermore, e-IF2 $\alpha$  elevated levels were detected, yet p-eIF2 $\alpha$  levels were significantly reduced. Interestingly IRE1 HP, 5-AzaC, and HP/5-AzaC mediated downregulation were detected, but more importantly, levels of activated by phosphorylation form, pIRE1, were remarkably increased (Prischi et al., 2014). ATF6 expression was upregulated was induced by HP and 5-AzaC treatment, HP/5-AzaC treatment led to decreased expression of ATF6 transmembrane activator.

In the NIT-1 cell line protein aggregation levels decrease under HP, 5-AzaC, and HP/5-AzaC treatment indicating preventing role of the UPR system. BetaTC6 cells exhibited decreased protein aggregation only upon 5-AzaC and increased upon HP treatment. HP/5-AzaC did not lead to any significant changes in a compare to the control.

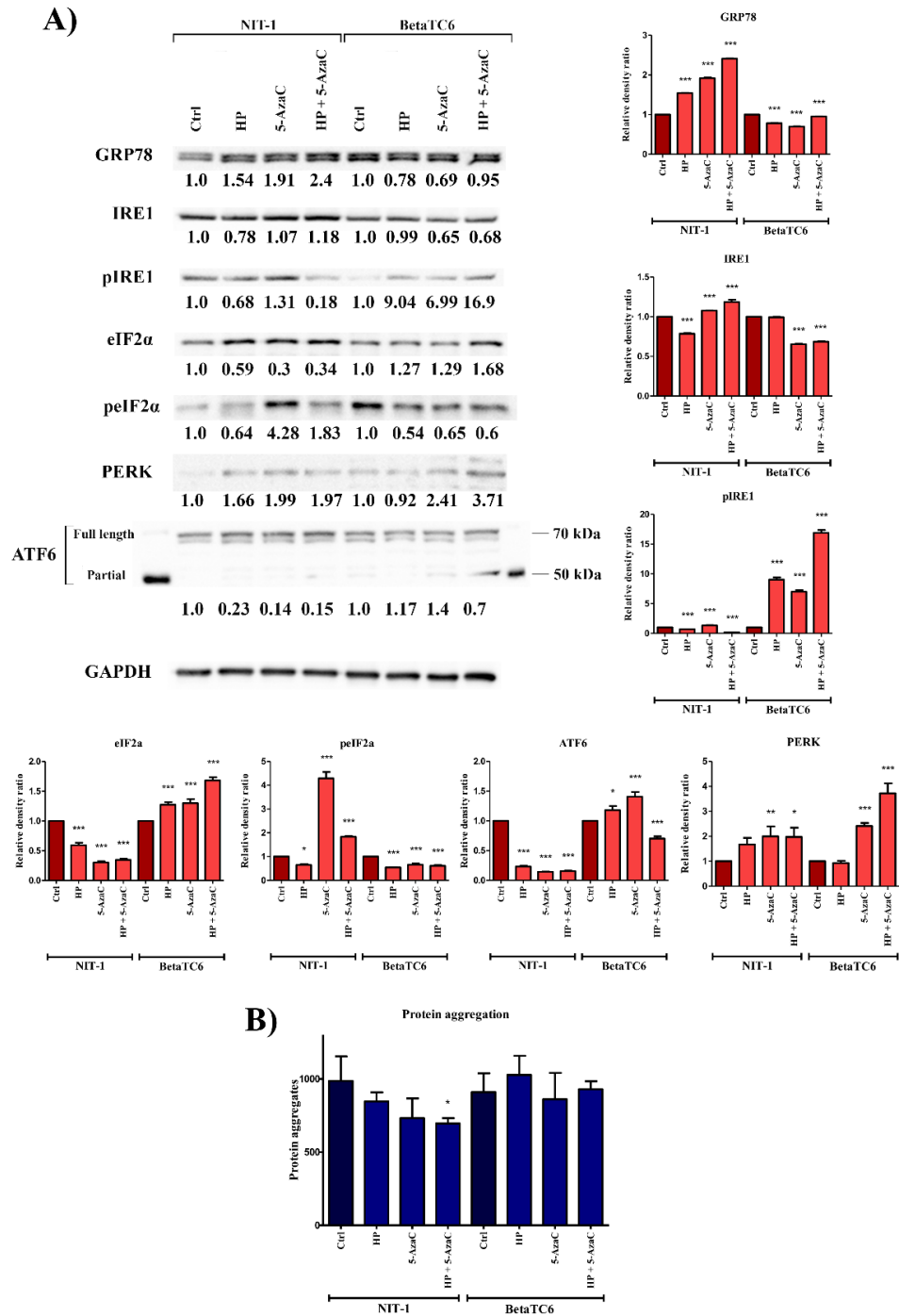


**Figure 17. Inhibition of tRNA methylation activates the endoplasmic reticulum stress pathway.**

(A) On the graph presented gel quantitation measured with GelQantNET program and statistical analysis done with GraphPadPrism. Levels of all proteins were normalized to GAPDH. Bars indicate SD, n = 3, \*\*\*p < 0.001, \*\*p < 0.01, \*p < 0.05 compared to the control (ANOVA and Dunnett's *a posteriori* test). (B) Protein aggregates were detected with PROTEOSTAT® Protein aggregation assay. Statistical analysis was done with GraphPadPrism. Bars indicate SD, n = 3, \*\*\*p < 0.001, \*\*p < 0.01, \*p < 0.05 compared to the control (ANOVA and Dunnett's *a posteriori* test).

#### **4.4.2 Autophagy mediated cell death activation in NIT-1 cell line upon HP and 5-AzaC treatment**

Autophagy is a lysosomal degradation system of damaged organelles, cell compartments, or impaired proteins. Autophagy plays an important role in lowering the ER stress, apoptosis, or aging process. There is strong crosstalk between ER stress and autophagy in which ER stress may either induce or attenuate the autophagy pathway (Mizushima, 2007). ER stress mediated autophagy promotes cell survival and prevents apoptotic cell fate. Additionally, in a process called ER-phagy autophagosomes mediated by Atg40/FAM134B complex can selectively take in ER membranes. However, as mentioned before, under some pathological circumstances, like neurodegenerative diseases, ER stress seems to trigger autophagy weakening (Rashid et al., 2015). One of the most widely used autophagy markers is LC3 due to its correlation of LC3-I to LC3-II conversion with the number of autophagosomes. To examine if the cellular stress induction and methylation inhibition trigger autophagy LC3B was detected with FlowSight Flow cytometry and Western blot protocol. Obtained results presented in figures 18 A and B indicate HP induced cellular stress and tRNA methylation inhibition activated autophagy. In the NIT-1 cell line, those results were also confirmed with Western blot analysis. Moreover, in NIT-1 cell proteasomal activity drops in treated cells, especially after combined HP/5-AzaC treatment. In opposite BetaTC6 proteasomal activity analysis shows the increased response to induced stress. The biggest enhancement appears in cells after HP mediated cellular stress.

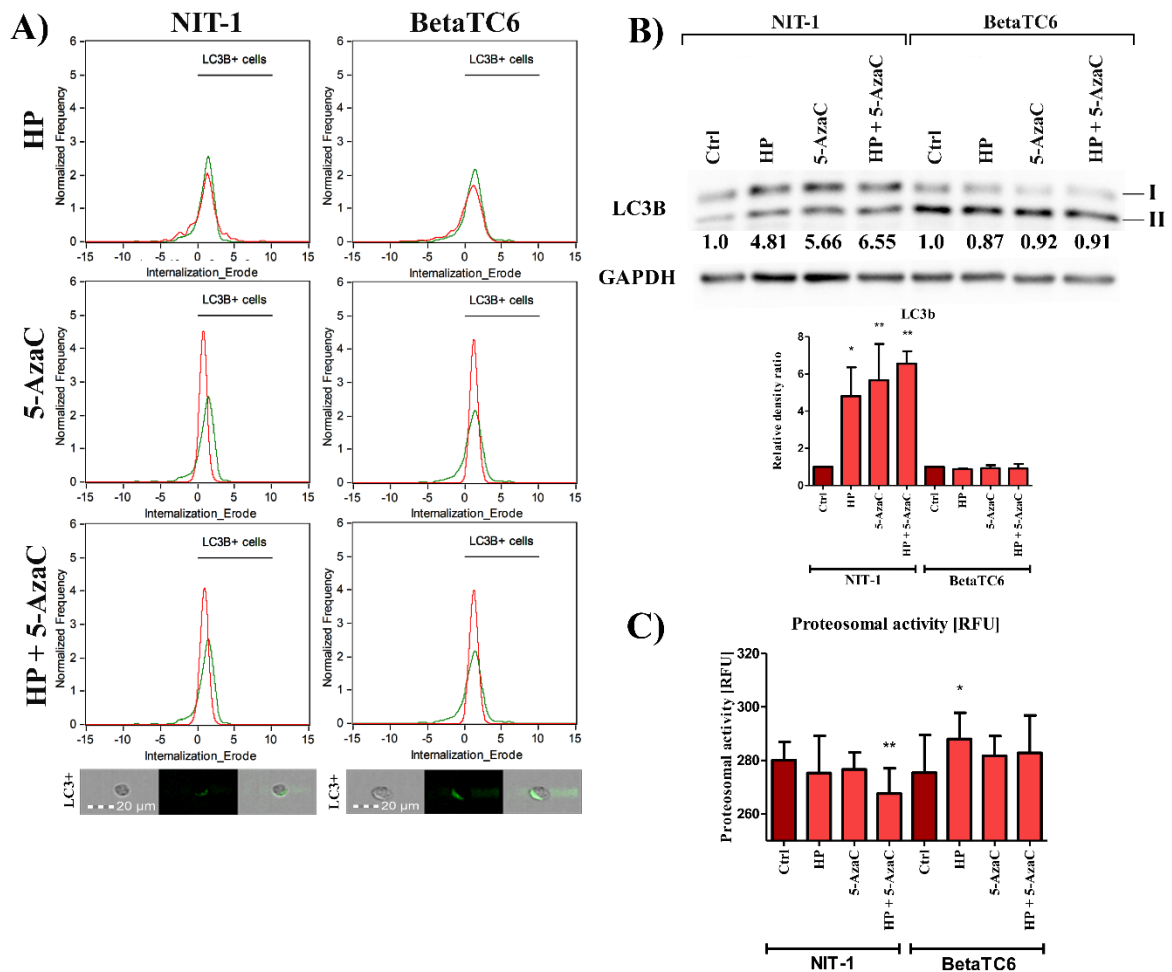


**Figure 18. Autophagy mediated cell death. Inhibition of protein aggregation is not related to proteasomal activity** (A) Level of LC3b was measured with Amnis® FlowSight® Imaging Flow Cytometer. Histograms reveal the intensity of LC3b in treated with HP and/or 5-AzaC cells (red) to compare with untreated control (green). The analysis was performed with Ideas Analysis Software. Pictures below show representative LC3b positive cells. (B) Western blot analysis of LC3b I and II expression level from the whole cell lysates. Gel quantitation was performed with GelQantNET program and statistical analysis was done with GraphPadPrism. Levels of all proteins were normalized to GAPDH. Bars indicate SD, n = 3, \*\*\*p < 0.001, \*\*p < 0.01, \*p < 0.05 compared to the control (ANOVA and Dunnett's *a posteriori* test). (C) Quantitative analysis of proteasomal activity was performed with Digital pictures were taken with IN Cell Analyzer 6500 HS, quantitative analysis was performed with HCA system IN Cell Analyzer 6500 HS and IN Carta software. Statistical analysis done with GraphPadPrism. Bars indicate SD, n = 3, \*\*\*p < 0.001, \*\*p < 0.01, \*p < 0.05 compared to the control (ANOVA and Dunnett's *a posteriori* test).



#### **4.4.3 HP and 5-AzaC mediated Phospho-S6 downregulation**

Ribosomal protein S6 (Rps6) belongs to the S6E family of ribosomal proteins and is a part of a 40S ribosomal subunit. It is a small, approximately 34 kDa, highly conserved protein occurring in yeasts and higher eukaryotes. Mammalian Rps6 may be phosphorylated at the C-terminus in 5 serine residues: Ser235, Ser236, Ser240, and Ser247. Phosphorylation of S6 ribosomal protein (Phospho-S6) is associated with an increase in translation of mRNA transcripts with 5' terminal oligopyrimidine tract (TOP mRNAs) that encode proteins involved in the cell cycle progression, cell size, and glucose homeostasis. Dephosphorylation of ribosomal protein S6 takes place at growth arrest (Ruvinsky et al., 2005). Phosphorylation of Ser235 and Ser236 is directly catalyzed by an S6 kinase (S6K). However, S6K is not the only kinase responsible for Rps6 phosphorylation at Ser235 and Ser236 sites. S6K knockdown or rapamycin treatment leading to its deactivation caused phosphorylation inhibition yet not complete abolish due to phosphorylation by (MAPK)-dependent kinase. The phosphorylation level of Rps6 can be also regulated by protein phosphatase 1 (PP1) (Hutchinson et al., 2011; Meyuhas, 2015). Lessen levels of phospho-S6 in mice skeletal muscle were found in a response to ER stress inhibitor treatment 4-phenylbutyrate (4-PBA). It has been shown that reduction of the UPR affects the activity of the Akt/mTOR pathway plus activates autophagy and the ubiquitin-proteasome system (Bohnert et al., 2016).

Results presented in figures 19 and 20 demonstrate lowered phospho-S6 levels in pancreatic  $\beta$ -cells HP and 5-AzaC. NIT-1 exhibited significantly decreased phospho-S6 regulation only upon HP mediated stress (Figure 19). The biggest decrease was observed in the BetaTC6 cell line after HP induced cellular stress and HP/5-AzaC treatment (Figure 20).

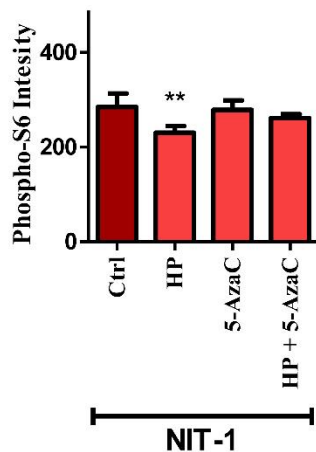
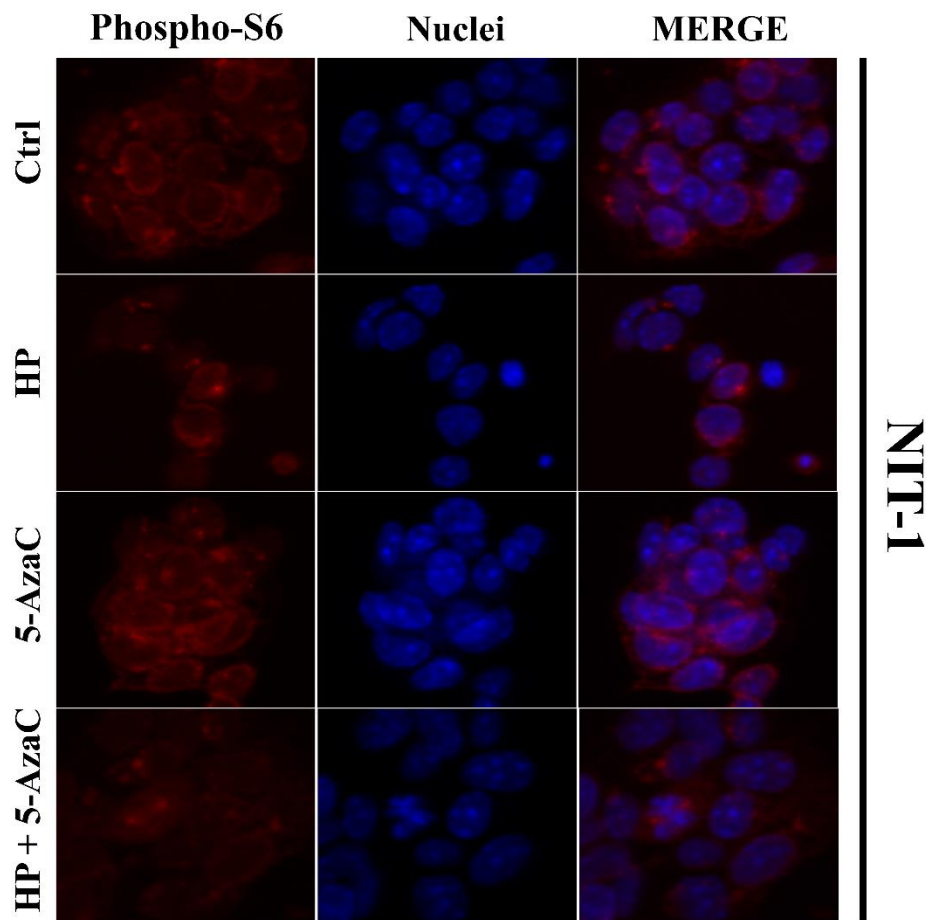


**Figure 19. Oxidative stress induction decreases Phospho-S6 (Ser235, Ser236) expression NIT-1 cell line. Representative images of staining: red fluorescence – ps6, blue fluorescence – nuclei (DAPI).** Cells were seeded onto the 96-well plate and treated with HP and/or 5-AzaC. Digital pictures were taken with IN Cell Analyzer 6500 HS, quantitative analysis was performed with HCA system IN Cell Analyzer 6500 HS and IN Carta software. Statistical analysis has been done with GraphPadPrism. Bars indicate SD, n = 3, \*\*\*p < 0.001, \*\*p < 0.01, \*p < 0.05 compared to the control (ANOVA and Dunnett’s *a posteriori* test).

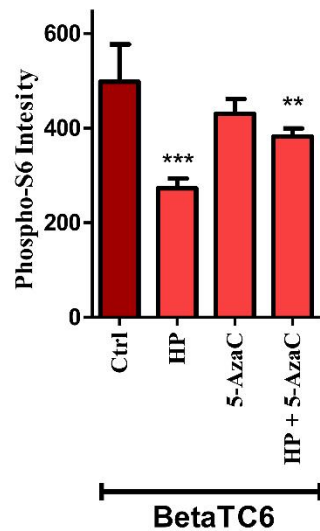
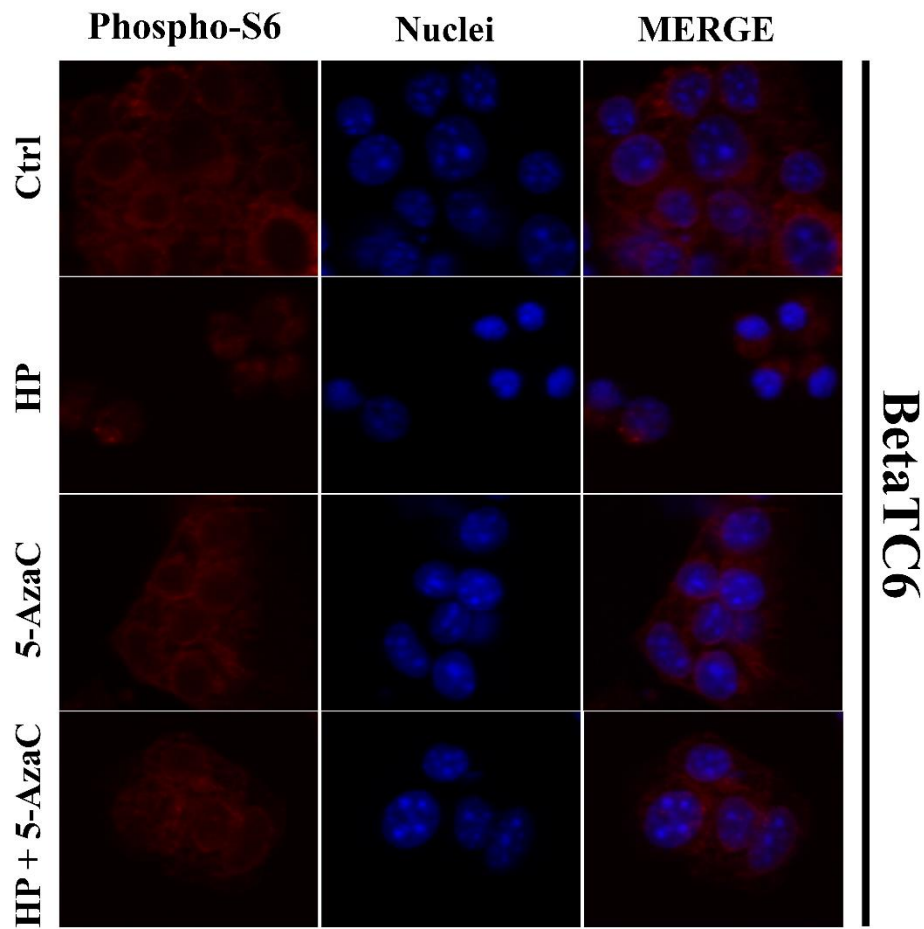


**Figure 20. Oxidative stress induction decreases expression of Phospho-S6 (Ser235, Ser236) protein in BetaTC6 cell line. Representative images of staining: red fluorescence – ps6, blue fluorescence – nuclei (DAPI).** Cells were seeded onto the 96-well plate and treated with HP and/or 5-AzaC. Digital pictures were taken with IN Cell Analyzer 6500 HS, quantitative analysis was performed with HCA system IN Cell Analyzer 6500 HS and IN Carta software. Statistical analysis was performed with InCell Analyzer 2000 analysis software and statistical analysis was done with

GraphPadPrism. Bars indicate SD, n = 3, \*\*\*p < 0.001, \*\*p < 0.01, \*p < 0.05 compared to the control (ANOVA and Dunnett's *a posteriori* test).

#### **4.4.4 Changes in Trdmt1 expression and localization in pancreatic $\beta$ -cells**

Dnmt2/Trdmt1 is a methyltransferase catalyzing the transfer of a methyl group to the C5 position of C38 in tRNA. Trdmt1 mediated methylation plays a role in protein translation regulation, ensures tRNA stability, reading frame maintenance, and controls codon-anticodon interactions (Tuorto et al., 2012). Typically Trdmt1 is located in the nucleus but it has been shown that upon the cellular stress it may be re-located to the cytoplasm (Dev et al., 2017; Thiagarajan et al., 2011).

In this study changes in Trdmt1 expression and localization has been shown with the use of the imaging flow cytometry. In control, untreated pancreatic  $\beta$ -cells supreme of the detected Trdmt1 was located in the nuclear area (Figure 21 A and B). However, HP mediated cellular stress of pancreatic insulinoma  $\beta$ -cells NIT-1 induced translocation of Trdmt1 to the cytoplasm and 5-AzaC induced increased Trdmt1 nuclear localization. Furthermore, in the BetaTC6 cell line, the augment of 5-AzaC mediated Trdmt1 biosynthesis was detected. Moreover, 5-AzaC treatment proceeded by HP induced cellular stress induces increased biosynthesis of Trdmt1 in both cell lines.

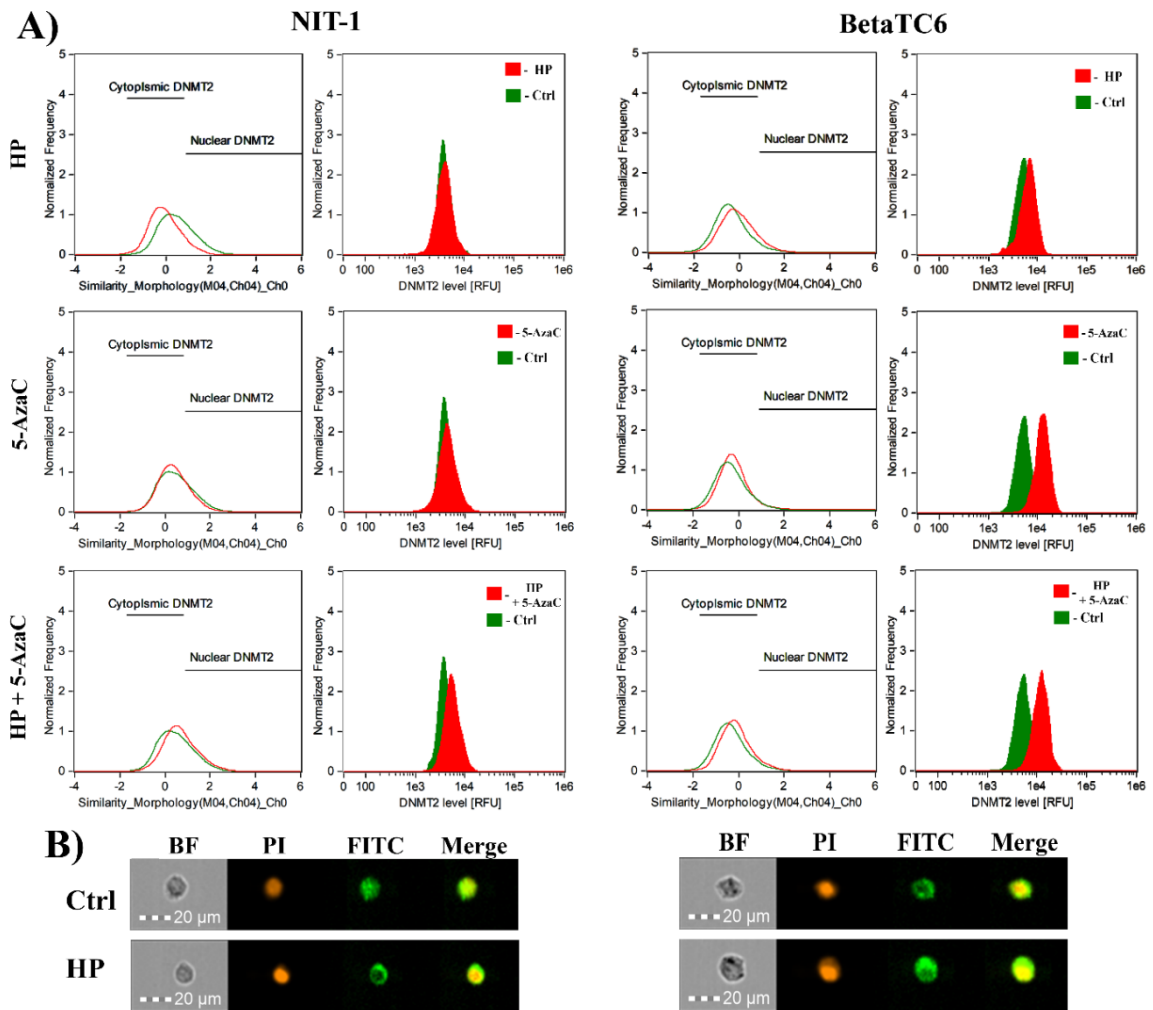


**Figure 21. 5-azaC induces changes in translocation and expression of Trdmt1 in pancreatic insulinoma  $\beta$ -cells (A)** Using Amnis® FlowSight® Imaging Flow Cytometer localization (left) and level (right) of Trdmt1 was detected in NIT-1 and BetaTC6 cell lines treated with HP and/or 5-AzaC. The analysis was performed with Ideas Analysis Software **(B)** Representative image of changes in Trdmt1 (green) level and distribution in a cell after HP treatment compared to the untreated control. Nuclei were stained with propidium iodide (red).

#### **4.4.5 Increased colocalization of Dnmt2/Trdmt1 and p-eIF2 $\alpha$ in pancreatic $\beta$ -cells under HP mediated cellular stress and tRNA methylation inhibition**

Signals detection with fluorescence microscopy allows analysis of the presence or lack of the structures/molecules, amount, and location in a cell. Estimation of the colocalization events indicates the possibility of the level of probes occupying the same cell structure and sometimes also potential interaction. A conducted experiment used two different antibodies labeled with different probes. Trdmt1 was stained in green (FITC) and p-eIF2 in red (Cy5). eIF2 $\alpha$  is one of the ER stress markers activated via phosphorylation in a PERK-dependent pathway of UPR. The main role of eIF2 $\alpha$  is protein synthesis inhibition via translation attenuation. However, eIF2 $\alpha$  phosphorylation not always leads to total translation inhibition and additionally may activate translation of the Activating Transcription Factor 4 ATF4 (Harding et al., 2000; Lu et al., 2004).

Inhibition of RNA methylation causes the endoplasmic reticulum (ER) stress and increased co-localization of Trdmt1 with p-eIF2 $\alpha$  in a BetaTC6 cell line what was shown in figure 22 B. In NIT-1 only 5-AzaC treatment lead to a small increase of Trdmt1 and p-eIF2 $\alpha$  colocalization. Moreover, presented in figure 22 D, Western blot analysis of the whole cell lysates indicates overexpression of the eIF2 $\alpha$  in the BetaTC6 cell line and decrease of its phosphorylated form. NIT-1 analysis shows downregulation of eIF2 $\alpha$  and enhanced level of p-eIF2 $\alpha$  methylation inhibition with 5-AzaC.

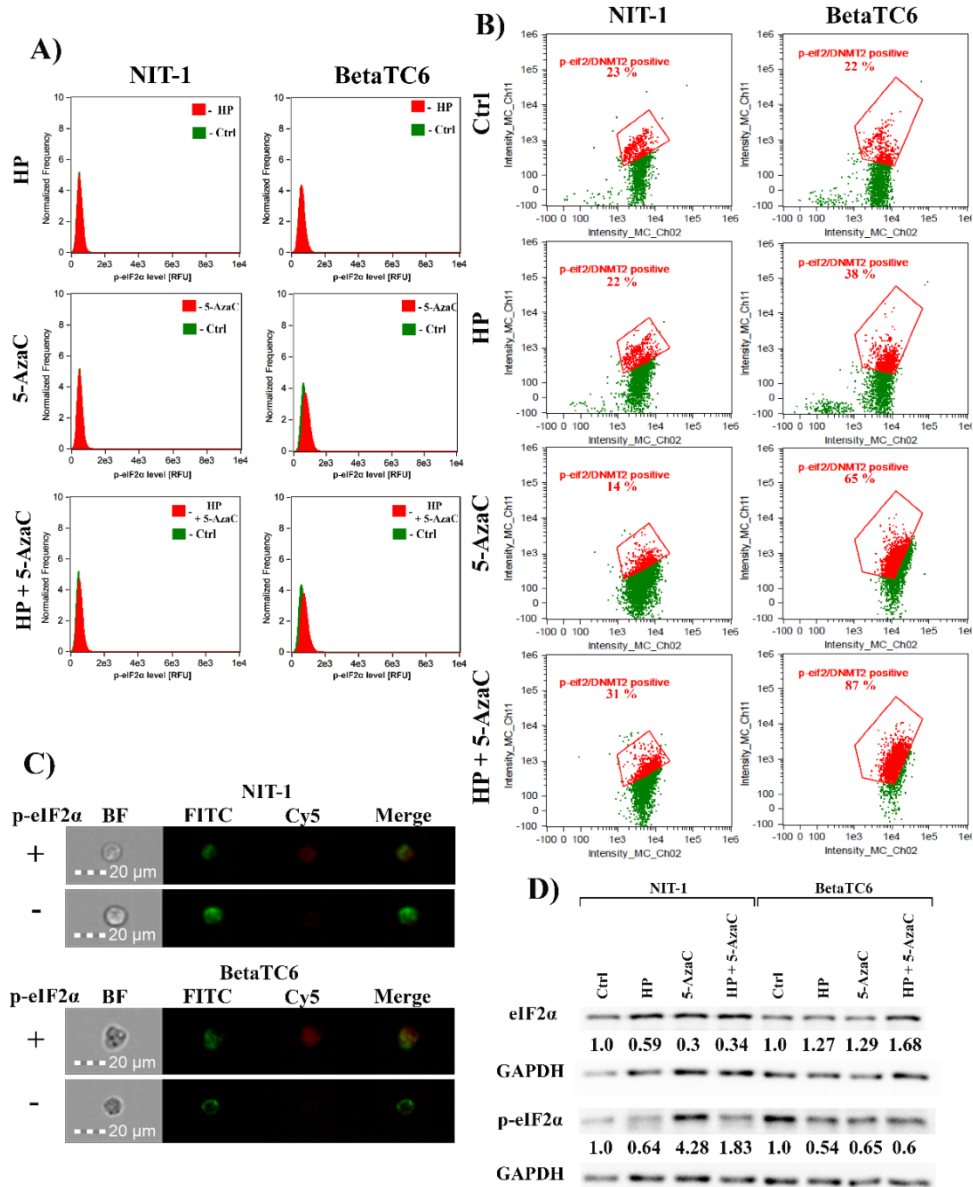


**Figure 22. Inhibition of RNA methylation causes the endoplasmic reticulum (ER) stress and increased co-localization of DNMT2 with p-eIF2α, one of the ER stress markers p-eIF2α level in NIT-1 and BetaTC6 cell lines treated with HP, 5-AzaC and combination of both was detected with Amnis® FlowSight® Imaging Flow Cytometer. The analysis was performed with Ideas Analysis Software (A) Using flow cytometry level of p-eIF2α expression in the single cell was detected. Charts present p-eIF2α fluorescence intensity (red) overlapped on its intensity in the untreated control (green). (B.) Gated units (red figure) show the percentage of p-eIF2α and DNMT2 co-localization events in the cell. (C) Representative images of staining DNMT2 (green, FITC) and p-eIF2α (red, Cy5). Upper figure (+) presents cell where p-eIF2α is expressed and lower figure (-) cell where p-eIF2α was not detected. (D) Western blot analysis of eIF2α and p-eIF2α in the whole cell lysates. Gel quantitation was performed with GelQuantNET program and statistical analysis was done with GraphPadPrism. Levels of all proteins were normalized to GAPDH. Bars indicate SD, n = 3, \*\*\*p < 0.001, \*\*p < 0.01, \*p < 0.05 compared to the control (ANOVA and Dunnett's *a posteriori* test).**

#### 4.4.6 Trdmt1 does not localize in an endoplasmic reticulum

The endoplasmic reticulum is an organelle made out of the system of membranes named cisternae. ER is responsible for protein production, modification, release, and transport to the Golgi apparatus. In this study, ER was detected with fluorescent staining by ER tracker (blue) and Trdmt1 was identified with an antibody labeled with FITC probe (green). The presented in figure 23 results of ER and Trdmt1 staining have not revealed any significant changes in the ER and Trdmt1 colocalization. Only HP and 5-AzaC treatment had a small impact on the increase ER/Trdmt1 overlapping. In other analyzed cases the Trdmt1 localization in the ER has not been observed.

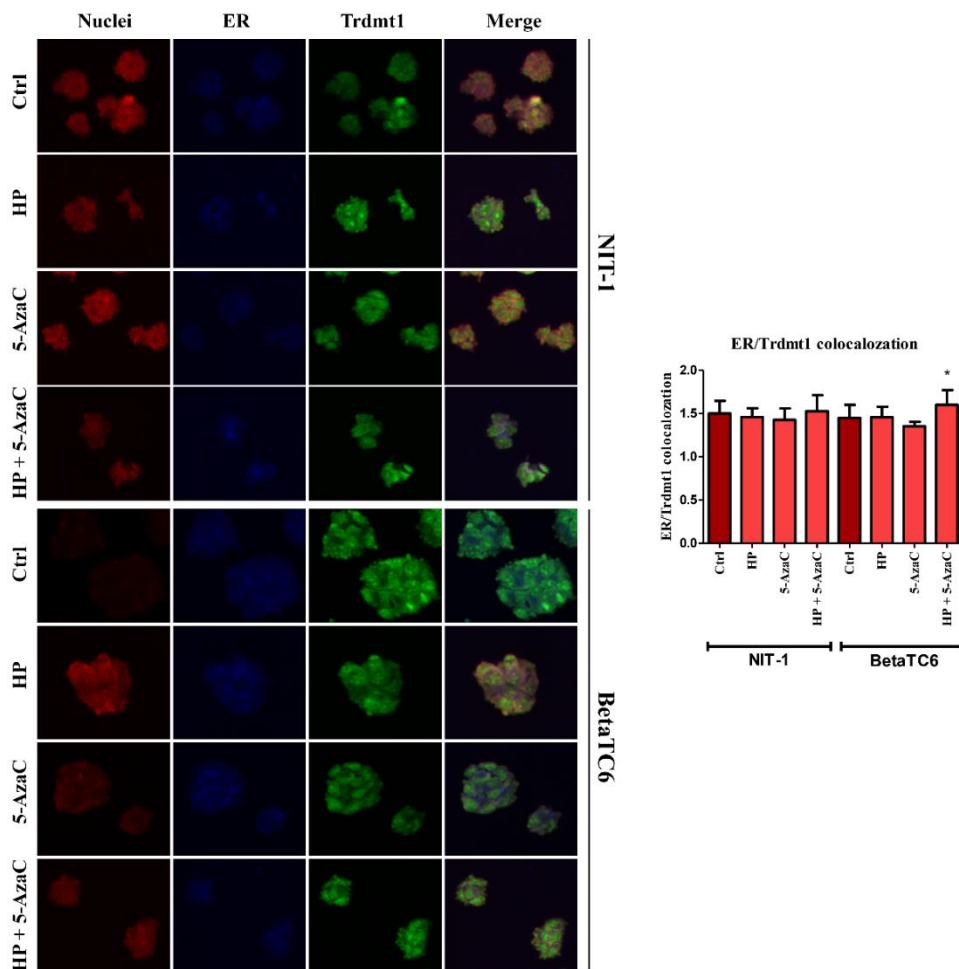


**Figure 23. ER and Trdmt1 co-localization analysis has not revealed any significant changes.** In presented representative images of the multicolor fixed-cell assay, ER was detected with ER tracker (blue fluorescence), Trdmt1 was detected with an antibody labeled with FITC (green fluorescence) and nuclei were visualized with PI (red fluorescence). Digital pictures were taken with IN Cell Analyzer 6500 HS, quantitative analysis was performed with HCA system IN Cell Analyzer 6500 HS and IN Carta software. Statistical analysis was done with GraphPadPrism. Bars indicate SD, n = 3, \*\*\*p < 0.001, \*\*p < 0.01, \*p < 0.05 compared to the control (ANOVA and Dunnett's *a posteriori* test).



#### **4.4.7 5-Azac treatment increases insulin production in pancreatic $\beta$ -cells**

Insulin is a small approximately 5.81 kDa peptide hormone translated from mRNA in the cytosol as a 110 amino-acids long single chain called pre-proinsulin. Then translocated to the ER where is modified to proinsulin and then and the active form insulin. For the insulin production in the animal body responsible are  $\beta$ -cells located in the pancreas (Weiss et al., 2000). Insulin regulates glucose level in the blood and chronic downregulation in insulin production are dangerous for the organism leading to diabetes development.

In the next step, it was taken under consideration wheatear HP-induced cellular stress and 5-AzaC mediated methylation inhibition has an impact on insulin production by pancreatic  $\beta$ -cells. To determine the level of insulin secretion conducted two analyses of NIT-1 and BetaTC6 cell lines. Using immunofluorescence technique cell nuclei were labeled with DAPI and insulin was detected with antibody conjugated with green fluorescence probe (FITC). Confocal images revealed explicit boosted insulin secretion by 5-AzaC treated NIT-1 cell line is presented in figure 24 A. Western blot analysis of insulin expression level from the whole cell lysates presented in figure 24 B has shown an increase of production in the NIT-1 cell line after tRNA methylation inhibition in comparison to untreated control. For instance, confocal imaging of BetaTC6 demonstrated significant enhancement in insulin production upon HP treatment (Figure 25 A). Western blot analysis of insulin expression level from the whole cell lysates presented in figure 25 B has shown a small increase of insulin production in the BetaTC6 cell line after 5-AzaC treatment in comparison to untreated control.

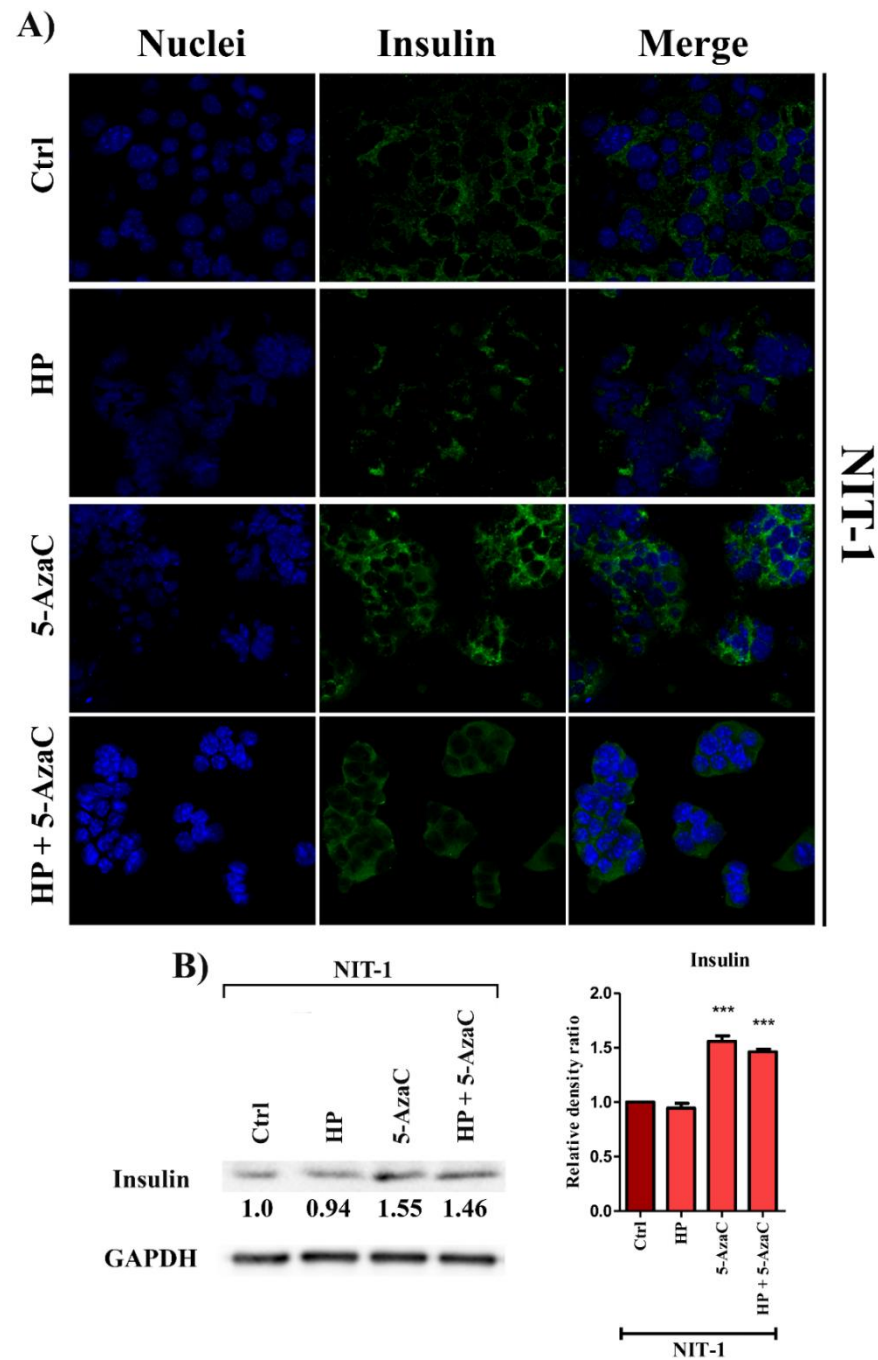


**Figure 24. Insulin production increases after 5-AzaC and HP/5-AzaC treatment in pancreatic  $\beta$ -cells NIT-1.** (A) Representative images were taken with a confocal microscope under 40x magnification. Insulin was detected with antibody conjugated with FITC (green fluorescence) and nuclei were stained with DAPI (blue fluorescence). (B) Gel quantitation was performed with GelQantNET program and statistical analysis was done with GraphPadPrism. Levels of all proteins were normalized to GAPDH. Bars indicate SD,  $n = 3$ , \*\*\* $p < 0.001$ , \*\* $p < 0.01$ , \* $p < 0.05$  compared to the control (ANOVA and Dunnett's *a posteriori* test).

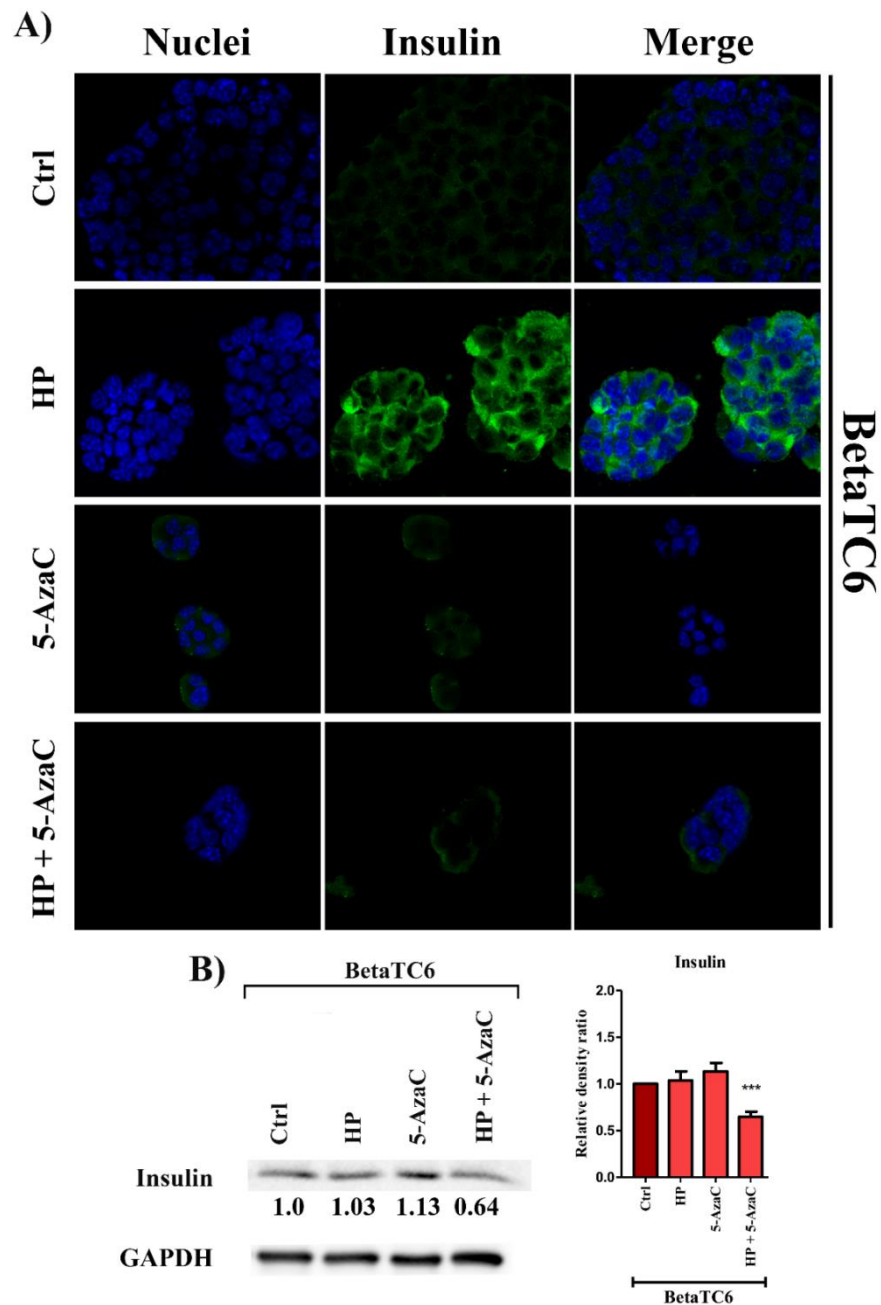


**Figure 25. BetaTC6 cells treatment with 5-AzaC stimulates insulin production and lowers its production after prior HP treatment (A)** Representative images were taken with a confocal microscope under 40x magnification. Insulin was detected with antibody conjugated with FITC (green fluorescence) and nuclei were stained with DAPI (blue fluorescence). **(B)** Gel quantitation was performed with GelQantNET program and statistical analysis was done with GraphPadPrism. Levels of all proteins were normalized to GAPDH. Bars indicate SD, n = 3, \*\*\*p < 0.001, \*\*p < 0.01, \*p < 0.05 compared to the control (ANOVA and Dunnett's *a posteriori* test).

## **5. Discussion**

Facing the urgency due to the increasing number of diabetic patients understanding the processes in the pancreatic  $\beta$ -cells seems to be crucial for the improvement of diabetes treatment and prevention. Moreover, we suspected 5-AzaC to be a factor useful in an expansion of the possibilities in insulinoma treatment of patients who cannot be qualified for surgery. To investigate the role of 5-AzaC mediated tRNA methylation inhibition in pancreatic  $\beta$ -cells, in control conditions, stress and aging were induced with a pro-oxidant, hydrogen peroxidase. To find out the role and dependence of Trdmt1, ER stress, senescence, and aging in pancreatic  $\beta$ -cells and potential implications in insulin production and senescent cell elimination.

Trdmt1 (also known as Dnmt2) protein for many years was considered as a DNA methyltransferase due to high structural and sequential similarity to proteins belonging to the DNMT family. However, Trdmt1 demonstrates a very small ability to DNA methylation and mostly methylates tRNA at the C38 position (Goll et al., 2006). Perturbations in tRNA modification can lead to errors during protein synthesis and therefore ER stress initiation (Wei et al., 2011). In a present study, we wanted to determine the potential consequences of 5-AzaC treatment on pancreatic insulinoma cells, insulin production and the potential correlation with 5-AzaC mediated tRNA methylation disruption at the Trdmt1 target site in pancreatic  $\beta$ -cells (Schaefer et al., 2009). In presented research used two cell lines delivered from mice pancreatic  $\beta$ -cells producing insulin. Both used cell lines produce insulin which is why are good models for insulin secretion. Firstly, for cellular stress induction cells were treated with hydrogen peroxide (HP) which may also increase Trdmt1 level. Furthermore, cells were incubated with media containing 5-AzaC which inhibits tRNA methylation at a Trdmt1 target site and also DNA methylation.

ROS profile analysis has shown NIT-1 cells established from transgenic nonobese diabetic (NOD/Lt) mouse is more vulnerable to an oxidative stress induction also after 5-AzaC treatment. Nevertheless, nitric oxidative profile analysis showed no changes in NO production by an NIT-1 after HP or 5-AzaC treatment. While in BetaTC6 cell line HP induced cellular stress and 5-AzaC treatment under cellular stress conditions lead to excessive NO production. Normally ROS and RNS presence is required for  $\beta$ -cell proper functioning including stimulation of insulin production (Drews et al., 2010). Yet, generally low levels and activity of antioxidant enzymes in  $\beta$ -cells provokes easy induction of oxidative stress. NO synthesis appears to be an important trigger for diabetes induction via enhanced nitric oxide synthase (iNOS) expression and thus cytokine-mediated  $\beta$ -cell death.

It has been shown that iNOS expression inhibition reduces hyperglycemia in NOD mice (Drews et al., 2010; Pierre Pirot et al., 2008). In both cell lines ROS, as well as SOD1 levels, were elevated after HP and 5-AzaC treatment nonetheless the amount of produced reactive oxygen species by NIT-1 was significantly higher. NIT-1 may be more vulnerable to excessive ROS production due to previous oxidative stress existence that is early founded in T1D NOD mice (C. W. Liu et al., 2018). Interestingly, the BetaTC6 cell line demonstrated NO excessive production. NO synthesis may be stimulated in a calcium-dependent manner what can be associated with an HP treatment since it has been shown that HP increases  $Ca^{2+}$  level (Drews et al., 2010). However, NIT-1 cell line has not demonstrated this pattern. NO production was on the very low level. Study of Wang et al. on NIT-1 cell line suggested diminished NO production mediated by GRP78 elevated levels. In GRP78 transfected NIT-1 cell line after treatment with streptozotocin detected decreased level of NO, SOD upregulation and apoptosis reduction (M. Wang et al., 2007). In this study NIT-1 cell line exhibited similar pattern after cellular stress induction with HP and 5-AzaC what may confirm GRP78 mediated prevention from excessive NO production and apoptotic cell death. BetaTC6 cell line has not responded to a cellular stress induction in the same way. Possibly due to observed GRP78 downregulation NO and apoptotic cell death levels were elevated.

In the presented study we observed that HP mediated inhibition of the G2/M and phases and HP/5-AzaC mediated S phase inhibition in the NIT-1 cell line. In BetaTC6 cells, we demonstrated S phase inhibition after HP and HP/5-AzaC treatment. Along with the S phase, cell cycle arrest in BetaTC6 increased apoptosis was detected. This can be supported by other studies indicating that ROS induces DNA damage which can stimulate either cell cycle arrest in the G1 or G2/M phase, and apoptosis of cells in the S phase or senescence-like growth arrest (CHEN et al., 2000; Shackelford et al., 2000). Whereas, NIT-1 HP mediated cell cycle arrest was greater in a G2/M phase than S phase and apoptotic cell death induction was only slightly increased in comparison to BetaTC6. Moreover, the BetaTC6 cell line proliferation profile was remarkably lowered by HP and HP/5-AzaC treatment. The loss of the proliferation capability may indicate cell senescence. Cellular growth rate decrease related to senescence is a hallmark of both stress conditions and aging thus it is a standard mechanism preventing aberrant cell division. Molecules with the ability to inhibit senescent cell anti-apoptotic pathways (SCAPs) are called senolytic. Another type of molecule which action focus on senescence cells is senostatics (senomorphic). Those drugs in opposite to

senolytic do not promote senescence cell removal but suppress SASP. Both sorts of drugs can delay aging and prevent diseases related to age, like diabetes (Muñoz-Espin & Demaria, 2020; Niedernhofer & Robbins, 2018). In the conducted experiment in both cell combined treatment with HP and 5-AzaC in NIT-1 as well as in BetaTC6 cell line significantly changed the morphology of  $\beta$ -cells. Cells of both cell lines did not aged, did not proliferate but were not also dead what indicates 5-AzaC senolytic activity - selective death induction of senescent cells. All senescent cells were killed and the cell cycle of others was inhibited. HP treatment led to premature senescence which indicates its senostatic activity – inhibited signaling and blocked proliferation of senescent cells. BetaTC6 cellular senescence mediated by a prooxidant and 5-AzaC might be also an indicative of accelerated aging process. Similarly, as in Tan et. al study of age-related changes in monkey chondrocytes, BetaTC6 decreased chaperone level, here GRP78, and upregulation of ER stress marker pIRE1, accompanied by apoptosis activation (Tan et al., 2020).

Taken together an elevated level of NO observed in BetaTC6 cell suggest NO-mediated apoptotic death of BetaTC6  $\beta$ -cells what may indicate that HP induced increased level of the  $Ca^{2+}$  in cytosol triggers NO production, ER stress, and related induction of apoptosis preceded by the cell cycle inhibition in S phase.

Besides, one of the factors of cell cycle suppression, apoptosis, and autophagy regulation, FOXO3a was found to increase in HP and HP/5-AzaC treated NIT-1 cells. At the same time, essential for FOXO3a action translocation to the nucleus in NIT-1 has not been observed (Nho, 2014). In contrast, BetaTC6 cells demonstrated HP-mediated FOXO3a downregulation but HP and HP/5-AzaC induced translocation to the nucleus. Some studies indicate ER stress and UPR crosstalk in FOXO3a activation. Coronary artery selective PERK inhibition led to decreased FOXO3a nuclear localization (Sun et al., 2017). Research on neuronal cells indicates CHOP direct interaction with FOXO3a in a response to tunicamycin induced ER stress, increased active nuclear FOXO3a, and apoptosis induction (Ghosh et al., 2012). BetaTC6 demonstrated FOXO3a translocation, PERK upregulation, and apoptosis induction upon HP and HP/5-AzaC treatment. Considering FOXO3a apoptosis promoting activity during oxidative stress and the lack of survival factors (Lehtinen et al., 2006), obtained results indicate UPR PERK/CHOP mediated FOXO3a activation by increased nuclear localization in BetaTC6 cells and thus promotes apoptotic cell death. Moreover, FOXO3a protects the cell from ROS-mediated damage through the regulation of antioxidant enzymes, including SODs (Kops et al., 2002). A low level of

FOXO3a explains a low response to oxidative stress and a low level of SOD1. Similarly, the upregulation of SOD1 in NIT-1 cells explains the increased expression of FOXO3a (Marinkovic et al., 2007).

Iodine propide staining revealed increased expression and/or translocation of Trdmt1 protein upon cellular stress induction in pancreatic  $\beta$ -cells. Trdmt1 is mainly cytoplasmic protein but can also occur in the nucleus. Schaefer et. al in their research on *Drosophila* suggested Trdmt1 translocation to the nuclei only during particular cell cycle phases (Schaefer et al., 2008). It has been shown that cellular stress induces Trdmt1 translocation from the nucleus to the cytoplasm where takes part in RNA processing (Thiagarajan et al., 2011). Flow cytometry analysis revealed induced by 5-AzaC increased Trdmt1 expression in BetaTC6 cells and HP mediated translocation to the cytoplasm in NIT-1 cells. Shown results may indicate the role of Trdmt1 in the response to cellular stress. A study on human fibroblasts shows that Trdmt1 silencing leads to increased HP-mediated increased apoptosis and senescence (Lewinska et al., 2017). Here, used 5-AzaC may cause tRNA demethylation mediated by Trdmt1, so to compensate for this state as a response more Trdmt1 is synthesized by BetaTC6 cells. NIT-1 cell line flow cytometry assay revealed increased Trdmt1 translocation upon cellular stress. Trdmt1 may help to cope with the cellular stress induction either by its increased biosynthesis or augmented translocation to the cytoplasm that was observed in the NIT-1 cell line. Moreover, flow cytometry analysis of Trdmt1 and p-eIF2 $\alpha$  localization and expression showed in NIT-1 cells 5-AzaC mediated upregulation of p-eIF2 $\alpha$  expression and HP and HP/5-AzaC mediated increased p-eIF2 $\alpha$ /Trdmt1 co-localization what may be correlated with the increased level of cytoplasmic Trdmt1 content. Using FlowSight flow cytometry level of LC3B was measured as one of the autophagy markers. In the performed experiment, 5-AzaC activated autophagy mediated cell death. However, only in NIT-1 cells, those results were also confirmed with Western blot analysis. Western blot of whole BetaTC6 cell lysates has not shown significant changes. Strengthened autophagy in a response to not only HP-induced cellular stress but also mediated by 5-AzaC reveals the need to cell survival promotion and apoptotic cell fate prevention. Comparing those results to apoptosis analysis it is clear that the NOD cell line responded to 5-AzaC treatment by activating the autophagy pathway and thus maintaining proliferation rate whereas BetaTC6 cells appeared to be more vulnerable to stress which triggered apoptosis and proliferation decrease. Furthermore, ER stress mediated autophagy promotes cell survival and prevents apoptotic cell fate (Rashid et al., 2015), and in NIT-1 cells 5-AzaC



treatment activated ER stress. This led to UPR stimulation via one of the transmembrane ER stress sensor PERK which is responsible for eIF2 $\alpha$  phosphorylation. Even though Western blot did not show enhanced expression of eIF2 $\alpha$ , yet its phosphorylated form (p-eIF2 $\alpha$ ) was on a significantly higher level. This indicates ER stress mediated autophagy activation which protected NIT-1 cells from apoptotic cell death (Rashid et al., 2015). Moreover, proteasomal activity in NIT-1 drops after HP and/or 5-AzaC treatment can be supported by potential crosstalk between ubiquitin-proteasome system and autophagy. Proteasome system inhibition may result in the compensatory activation of autophagy through ER stress and UPR activation (Ding et al., 2007; Ji & Kwon, 2017). Additionally, in NOD cell line carbonylation increases together with the lower level of protein aggregates. Stimulated pathways seemed to be efficient due to exhibited successive elimination of protein aggregates in NIT-1 by autophagy in a process mediated by 5-AzaC. At the same time, BetaTC6 cells as well as NIT-1 demonstrated upregulation of the UPR proteins like pIRE and PERK but increased proteasomal activity, thus suggesting BetaTC6 cell line ER stress induction was not related to UPS inhibition. IRE1 promotion of autophosphorylation in a response to ER stress generated pIRE1 acts as ribonuclease and splices of Xbp-1 mRNA (Xbp-1s). Spliced Xbp1 upregulates ER chaperones and genes related to ERAD (Kemp et al., 2013; Lin & Stone, 2020). Moreover, in BetaTC6 cells, the number of protein aggregates was elevated. Those results indicate non-5-AzaC dependent ERAD activation in BetaTC6 due to the accumulated protein aggregates, however not effective enough what resulted in apoptotic cell death augment.

In both pancreatic  $\beta$ -cells detected HP and 5-AzaC induced phospho-S6 downregulation. The greatest augment was observed in the BetaTC6 cell line after HP and HP/5-AzaC treatment. Phospho-S6 reduced levels are contributed to UPR weakening and UPS activation (Bohnert et al., 2016). Indeed, in the BetaTC6 cell line increased proteasomal activity was detected. Moreover, dephosphorylation of ribosomal protein S6 takes place at growth arrest which great increase in the S phase was observed in BetaTC6 HP mediated cellular stress (Ruvinsky et al., 2005).

One of the most important parts of the conducted study was to check the effect of the potential correlation with 5-AzaC mediated tRNA methylation disruption at the Trdmt1 target site in pancreatic  $\beta$ -cells and insulin production. Immunostaining has shown a high increase of insulin secretion NIT-1 cells after 5-AzaC in comparison to untreated control. Similarly, Western blot analysis of insulin expression level from the whole cell lysates has

shown an increase of production in the NIT-1 cell line after 5-AzaC and HP/5-AzaC treatment, which presents 5-AzaC as a factor that prevents T1D. Furthermore, an increase in insulin production correlates with Trdmt1 inhibition. For instance, confocal imaging of BetaTC6 demonstrated significant enhancement in insulin production upon HP treatment. Western blot analysis of insulin expression level from the whole cell lysates indicated a small increase of insulin production in the BetaTC6 cell line after 5-AzaC treatment and a decrease after HP/5-AzaC treatment. Here, BetaTC6 cells 5-AzaC treatment led to decreased insulin production and upregulated Trdmt1 level.

It has been reported that HP transiently induces insulin secretion in rat pancreatic  $\beta$ -cells and the same dependence was reported here in the BetaTC6 cell line (Maechler et al., 1999). However, NIT-1 did not respond in the same way, demonstrating the same insulin expression level as in untreated control.

Some recent studies describe cases of glycemic homeostasis disorder haematologic malignancies in patients treated with 5-Azacytidine. In reported cases, patients developed hyperglycaemia in a response to 5-AzaC. The authors explain this state suggesting 5-AzaC DNA hypomethylation activity leading to either glucocorticoids upregulation or pancreatic  $\beta$ -cells impairment (Morton, 2019; Ponard et al., 2018). Here, BetaTC6 upon HP/5-AzaC also indicated decreased level of insulin secretion. Yet, it is important to notice that the treatment has been done in vitro on only one type of cells, therefore glucocorticoid dysregulation, in this case, can be excluded. The reason for this decrease may be inhibition of tRNA methylation at the Trdmt1 target site leading to disturbance in insulin production, ER stress, and induced cell senescence. However, as mentioned before 5-AzaC is also a DNA hypomethylating agent and may be implicated in the regulation of some genes like *CDKN1A*, *PDE7B*, or *SEPT9* that are directly involved in insulin secretion (Dayeh et al., 2014). Surprisingly, 5-AzaC treatment enhanced insulin production in the nonobese diabetic cell line. It has been previously reported that pancreatic adenocarcinoma cell treatment with 5-AzaC yields insulin production. Furthermore, it also led to inhibition of pancreatic adenocarcinoma cell growth and increased vulnerability to anticancer drugs (Gailhouste et al., 2018).

Yet, it has to be taken under consideration that 5-Azacytidine is not the exclusive tRNA methylation inhibitor but also inhibits DNA methylation. 5-methylcytosine formed by the transfer of a methyl group onto the DNA cytosine regulates gene expression (Moore et al., 2013). Inflammation response in the NOD mice induces insulin DNA methylation altering

insulin gene expression during T1D development (Rui et al., 2016). The study on the mouse embryonic stem cells revealed the importance of the insulin gene *Ins2* promoter demethylation for proper cell differentiation and insulin secretion (Kuroda et al., 2009). Those mechanisms were not investigated in this study thus the direct effect of 5-AzaC on pancreatic  $\beta$ -cells is not well known and requires further investigation. Showed responses, activated pathways, and final cell fate as a result of 5-Azacytidine treatment differ between insulinoma pancreatic cell lines what has been displayed in figures 26 and 27. Furthermore, 5-Azacytidine did not lead to decreased insulin productions, as suspected in the beginning but insulinoma Non Obese Diabetic NIT-1 cells and BetaTC6 cell line increased insulin production. However, it is not sure if the released hormone is functional. Increased apoptosis and senescence in the BetaTC6 insulinoma cell line gives the prospective of 5-AzaC in cancer therapy what agrees with the most recent study of Sugisawa et al. on pancreatic cancer. In the trial, they used triple methyl blockade where one of the used inhibitors was 5-Azacytidine, which showed the potential in pancreatic treatment via tumor growth arrest (Sugisawa et al., 2021).

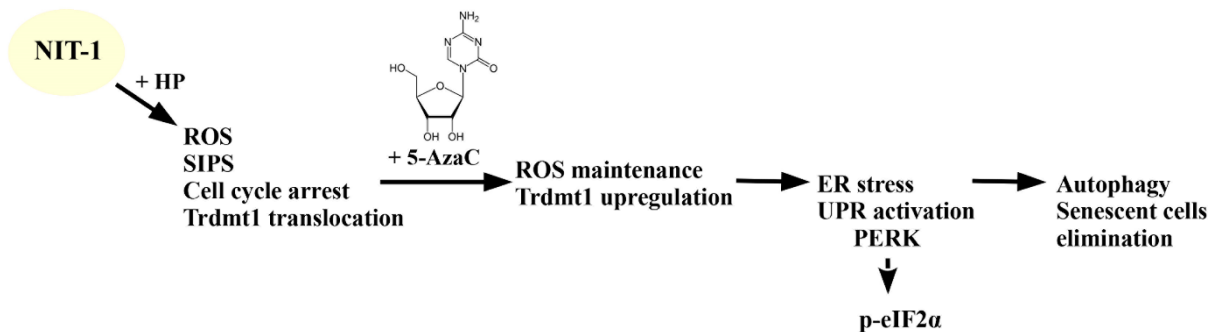


**Figure 26. 5-Azacytidine mediated response during cellular stress NIT-1 insulinoma cell line.** The 5-Azacytidine treatment leads to oxidative stress maintenance, Trdmt1 upregulation, and ER stress leading to autophagy and senescent cells elimination.

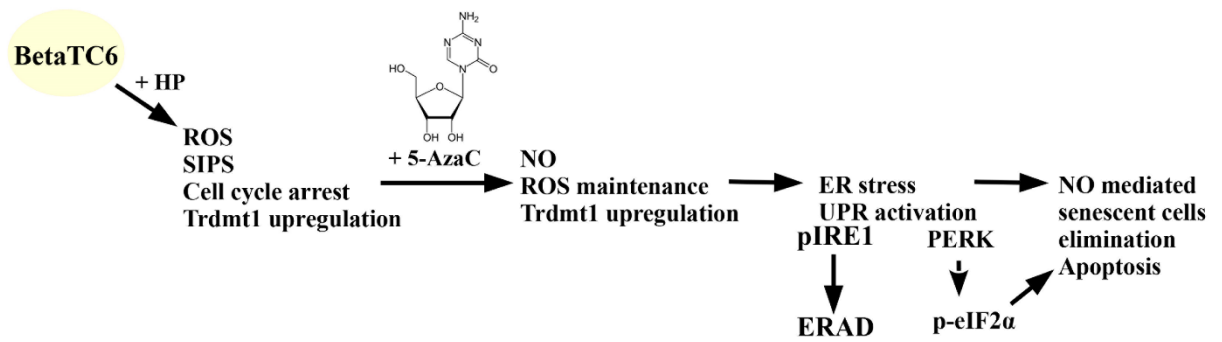


**Figure 27. 5-Azacididine mediated response during cellular stress BeatTC6 insulinoma cell line.** The 5-Azacididine treatment leads to nitrosative stress, oxidative stress maintenance, Trdmt1 increased expression, ER stress activation, and nitrosative stress mediated apoptosis and senescent cells elimination.

# Conclusions

- Stress-induced premature senescence reduces insulinoma cell growth
- SIPS insulinoma cells are associated with increased Trdmt1 level and/or altered intracellular localization
- Senescent cells elimination is correlated to 5-AzaC mediated oxidative and ER stress induction, and/or nitrosative stress activation
- 5-AzaC induces insulinoma senescent cells elimination proceeded by HP mediated cell cycle inhibition
- 5-AzaC inhibits adaptative response related to cellular stress mediated Trdmt1 upregulation
- 5-AzaC modulates insulin secretion by senescent insulinoma cells
- The combined therapy of prooxidants and 5-AzaC may be considered in the future as a novel potential therapeutic in insulinoma treatment
- 5-AzaC mediated enhanced insulin production in NOD cell line as a factor preventing T1D

# Literature

1. Adams, C. J., Kopp, M. C., Larburu, N., Nowak, P. R., & Ali, M. M. U. (2019). Structure and molecular mechanism of ER stress signaling by the unfolded protein response signal activator IRE1. In *Frontiers in Molecular Biosciences*. <https://doi.org/10.3389/fmolb.2019.00011>
2. Ahima, R. S. (2009). Connecting obesity, aging and diabetes. In *Nature Medicine*. <https://doi.org/10.1038/nm0909-996>
3. Aimiwu, J., Wang, H., Chen, P., Xie, Z., Wang, J., Liu, S., Klisovic, R., Mims, A., Blum, W., Marcucci, G., & Chan, K. K. (2012). RNA-dependent inhibition of ribonucleotide reductase is a major pathway for 5-azacytidine activity in acute myeloid leukemia. *Blood*. <https://doi.org/10.1182/blood-2011-11-382226>
4. Ali, D. M., Ansari, S. S., Zepp, M., Knapp-Mohammady, M., & Berger, M. R. (2019). Optineurin downregulation induces endoplasmic reticulum stress, chaperone-mediated autophagy, and apoptosis in pancreatic cancer cells. *Cell Death Discovery*. <https://doi.org/10.1038/s41420-019-0206-2>
5. Anderson, R. M., & Weindruch, R. (2012). The caloric restriction paradigm: Implications for healthy human aging. *American Journal of Human Biology*. <https://doi.org/10.1002/ajhb.22243>
6. Ardito, F., Giuliani, M., Perrone, D., Troiano, G., & Muzio, L. Lo. (2017). The crucial role of protein phosphorylation in cell signaling and its use as targeted therapy (Review). In *International Journal of Molecular Medicine* (Vol. 40, Issue 2, pp. 271–280). Spandidos Publications. <https://doi.org/10.3892/ijmm.2017.3036>
7. Avril, T., Vauléon, E., & Chevet, E. (2017). Endoplasmic reticulum stress signaling and chemotherapy resistance in solid cancers. *Oncogenesis*, 6(8), e373–e373. <https://doi.org/10.1038/oncsis.2017.72>
8. Baar, M. P., Brandt, R. M. C., Putavet, D. A., Klein, J. D. D., Derks, K. W. J., Bourgeois, B. R. M., Stryeck, S., Rijksen, Y., van Willigenburg, H., Feijtel, D. A., van der Pluijm, I., Essers, J., van Cappellen, W. A., van IJcken, W. F., Houtsmuller, A. B., Pothof, J., de Bruin, R. W. F., Madl, T., Hoeijmakers, J. H. J., ... de Keizer, P. L. J. (2017). Targeted Apoptosis of Senescent Cells Restores Tissue Homeostasis in Response to Chemotoxicity and Aging. *Cell*. <https://doi.org/10.1016/j.cell.2017.02.031>
9. Baekkeskov, S., Aanstoot, H. J., Christgai, S., Reetz, A., Solimena, M., Cascalho, M.,

- Folli, F., Richter-Olesen, H., & Camilli, P. De. (1990). Identification of the 64K autoantigen in insulin-dependent diabetes as the GABA-synthesizing enzyme glutamic acid decarboxylase. *Nature*. <https://doi.org/10.1038/347151a0>
10. Baeshen, N. A., Baeshen, M. N., Sheikh, A., Bora, R. S., Ahmed, M. M. M., Ramadan, H. A. I., Saini, K. S., & Redwan, E. M. (2014). Cell factories for insulin production. *Microbial Cell Factories*. <https://doi.org/10.1186/s12934-014-0141-0>
  11. Barnosky, A. R., Hoddy, K. K., Unterman, T. G., & Varady, K. A. (2014). Intermittent fasting vs daily calorie restriction for type 2 diabetes prevention: A review of human findings. In *Translational Research*. <https://doi.org/10.1016/j.trsl.2014.05.013>
  12. Barnum, K. J., & O'Connell, M. J. (2014). Cell cycle regulation by checkpoints. *Methods in Molecular Biology*, 1170, 29–40. [https://doi.org/10.1007/978-1-4939-0888-2\\_2](https://doi.org/10.1007/978-1-4939-0888-2_2)
  13. Beger, H. G., Warshaw, A. L., Büchler, M. W., Kozarek, R. A., Lerch, M. M., Neoptolemos, J. P., Shiratori, K., Whitcomb, D. C., & Rau, B. M. (2009). The Pancreas: An Integrated Textbook of Basic Science, Medicine, and Surgery: Second Edition. In *The Pancreas: An Integrated Textbook of Basic Science, Medicine, and Surgery: Second Edition*. <https://doi.org/10.1002/9781444300123>
  14. Bell, G. I., Horita, S., & Karam, J. H. (1984). A Polymorphic Locus Near the Human Insulin Gene Is Associated with Insulin-dependent Diabetes Mellitus. *Diabetes*. <https://doi.org/10.2337/diab.33.2.176>
  15. Blanco, S., & Frye, M. (2014). Role of RNA methyltransferases in tissue renewal and pathology. In *Current Opinion in Cell Biology*. <https://doi.org/10.1016/j.ceb.2014.06.006>
  16. Bohnert, K. R., Gallot, Y. S., Sato, S., Xiong, G., Hindi, S. M., & Kumar, A. (2016). Inhibition of ER stress and unfolding protein response pathways causes skeletal muscle wasting during cancer cachexia. *The FASEB Journal*, 30(9), 3053–3068. <https://doi.org/10.1096/fj.201600250RR>
  17. Bottazzo, G. F., Florin-Christensen, A., & Doniach, D. (1974). ISLET-CELL ANTIBODIES IN DIABETES MELLITUS WITH AUTOIMMUNE POLYENDOCRINE DEFICIENCIES. *The Lancet*. [https://doi.org/10.1016/S0140-6736\(74\)90140-8](https://doi.org/10.1016/S0140-6736(74)90140-8)
  18. Bottini, N., Musumeci, L., Alonso, A., Rahmouni, S., Nika, K., Rostamkhani, M., MacMurray, J., Meloni, G. F., Lucarelli, P., Pellicchia, M., Eisenbarth, G. S., Comings,

- D., & Mustelin, T. (2004). A functional variant of lymphoid tyrosine phosphatase is associated with type I diabetes. *Nature Genetics*. <https://doi.org/10.1038/ng1323>
19. Boucher, J., Kleinridders, A., & Ronald Kahn, C. (2014). Insulin receptor signaling in normal and insulin-resistant states. *Cold Spring Harbor Perspectives in Biology*. <https://doi.org/10.1101/cshperspect.a009191>
20. Bruckdorfer, R. (2005). The basics about nitric oxide. In *Molecular Aspects of Medicine* (Vol. 26, Issues 1-2 SPEC. ISS., pp. 3–31). Elsevier Ltd. <https://doi.org/10.1016/j.mam.2004.09.002>
21. Bujnicki, J. M., Feder, M., Ayres, C. L., & Redman, K. L. (2004). Sequence-structure-function studies of tRNA:m5C methyltransferase Trm4p and its relationship to DNA:m5C and RNA:m5U methyltransferases. *Nucleic Acids Research*. <https://doi.org/10.1093/nar/gkh564>
22. Chen, L. H., Chiou, G. Y., Chen, Y. W., Li, H. Y., & Chiou, S. H. (2010). MicroRNA and aging: A novel modulator in regulating the aging network. In *Ageing Research Reviews*. <https://doi.org/10.1016/j.arr.2010.08.002>
23. CHEN, Q. M., LIU, J., & MERRETT, J. B. (2000). Apoptosis or senescence-like growth arrest: influence of cell-cycle position, p53, p21 and bax in H<sub>2</sub>O<sub>2</sub> response of normal human fibroblasts. *Biochemical Journal*, 347(2), 543–551. <https://doi.org/10.1042/bj3470543>
24. Cheng, X., Liu, H., Jiang, C. C., Fang, L., Chen, C., Zhang, X. D., & Jiang, Z. W. (2014). Connecting endoplasmic reticulum stress to autophagy through IRE1/JNK/beclin-1 in breast cancer cells. *International Journal of Molecular Medicine*. <https://doi.org/10.3892/ijmm.2014.1822>
25. Christman, J. K. (2002). 5-Azacytidine and 5-aza-2'-deoxycytidine as inhibitors of DNA methylation: Mechanistic studies and their implications for cancer therapy. In *Oncogene*. <https://doi.org/10.1038/sj.onc.1205699>
26. Cipak Gasparovic, A., Zarkovic, N., Zarkovic, K., Semen, K., Kaminsky, D., Yelisyeyeva, O., & Bottari, S. P. (2017). Biomarkers of oxidative and nitro-oxidative stress: conventional and novel approaches. In *British Journal of Pharmacology*. <https://doi.org/10.1111/bph.13673>
27. Clayton, D. G. (2009). Prediction and interaction in complex disease genetics: Experience in type 1 diabetes. In *PLoS Genetics*. <https://doi.org/10.1371/journal.pgen.1000540>



28. Coelho, M., Oliveira, T., & Fernandes, R. (2013). *Biochemistry of adipose tissue: an endocrine organ*. <https://doi.org/10.5114/aoms.2013.33181>
29. Cole, S. P. C. (1986). Rapid chemosensitivity testing of human lung tumor cells using the MTT assay. *Cancer Chemotherapy and Pharmacology*. <https://doi.org/10.1007/BF00256695>
30. Copps, K. D., & White, M. F. (2012). Regulation of insulin sensitivity by serine/threonine phosphorylation of insulin receptor substrate proteins IRS1 and IRS2. In *Diabetologia*. <https://doi.org/10.1007/s00125-012-2644-8>
31. Costa, I. S., Medeiros, A. F., Piuvezam, G., Medeiros, G. C. B. S., Maciel, B. L. L., & Morais, A. H. A. (2020). Insulin-like proteins in plant sources: A systematic review. In *Diabetes, Metabolic Syndrome and Obesity: Targets and Therapy*. <https://doi.org/10.2147/DMSO.S256883>
32. Cuervo, A. M., & Wong, E. (2014). Chaperone-mediated autophagy: Roles in disease and aging. In *Cell Research*. <https://doi.org/10.1038/cr.2013.153>
33. Dalle-Donne, I., Rossi, R., Giustarini, D., Milzani, A., & Colombo, R. (2003). Protein carbonyl groups as biomarkers of oxidative stress. In *Clinica Chimica Acta*. [https://doi.org/10.1016/S0009-8981\(03\)00003-2](https://doi.org/10.1016/S0009-8981(03)00003-2)
34. Dayeh, T., Volkov, P., Salö, S., Hall, E., Nilsson, E., Olsson, A. H., Kirkpatrick, C. L., Wollheim, C. B., Eliasson, L., Rönn, T., Bacos, K., & Ling, C. (2014). Genome-Wide DNA Methylation Analysis of Human Pancreatic Islets from Type 2 Diabetic and Non-Diabetic Donors Identifies Candidate Genes That Influence Insulin Secretion. *PLoS Genetics*, *10*(3), e1004160. <https://doi.org/10.1371/journal.pgen.1004160>
35. Dev, R. R., Ganji, R., Singh, S. P., Mahalingam, S., Banerjee, S., & Khosla, S. (2017). Cytosine methylation by DNMT2 facilitates stability and survival of HIV-1 RNA in the host cell during infection. *Biochemical Journal*, *474*(12), 2009–2026. <https://doi.org/10.1042/BCJ20170258>
36. Diagnosis and classification of diabetes mellitus. (2013). In *Diabetes Care*. <https://doi.org/10.2337/dc13-S067>
37. Dice, J. F. (2007). Chaperone-mediated autophagy. In *Autophagy*. <https://doi.org/10.4161/auto.4144>
38. DiMeglio, L. A., Evans-Molina, C., & Oram, R. A. (2018). Type 1 diabetes. In *The Lancet*. [https://doi.org/10.1016/S0140-6736\(18\)31320-5](https://doi.org/10.1016/S0140-6736(18)31320-5)
39. Dimri, G. P., Lee, X., Basile, G., Acosta, M., Scott, G., Roskelley, C., Medrano, E. E.,

- Linskens, M., Rubelj, I., Pereira-Smith, O., Peacocke, M., & Campisi, J. (1995). A biomarker that identifies senescent human cells in culture and in aging skin in vivo. *Proceedings of the National Academy of Sciences of the United States of America*. <https://doi.org/10.1073/pnas.92.20.9363>
40. Ding, W. X., Ni, H. M., Gao, W., Yoshimori, T., Stolz, D. B., Ron, D., & Yin, X. M. (2007). Linking of autophagy to ubiquitin-proteasome system is important for the regulation of endoplasmic reticulum stress and cell viability. *American Journal of Pathology*, *171*(2), 513–524. <https://doi.org/10.2353/ajpath.2007.070188>
41. Dong, A., Yoder, J. A., Zhang, X., Zhou, L., Bestor, T. H., & Cheng, X. (2001). Structure of human DNMT2, an enigmatic DNA methyltransferase homolog that displays denaturant-resistant binding to DNA. *Nucleic Acids Research*, *29*(2), 439–448. <https://doi.org/10.1093/nar/29.2.439>
42. Drews, G., Krippeit-Drews, P., & Duifer, M. (2010). Oxidative stress and beta-cell dysfunction. In *Pflugers Archiv European Journal of Physiology* (Vol. 460, Issue 4, pp. 703–718). <https://doi.org/10.1007/s00424-010-0862-9>
43. Ellgaard, L., Molinari, M., & Helenius, A. (1999). Setting the standards: Quality control in the secretory pathway. In *Science*. <https://doi.org/10.1126/science.286.5446.1882>
44. Erbaykent Tepedelen, B., & Ballar Kirmizibayrak, P. (2019). Endoplasmic Reticulum-Associated Degradation (ERAD). In *Endoplasmic Reticulum*. <https://doi.org/10.5772/intechopen.82043>
45. Flamment, M., Hajdich, E., Ferré, P., & Foufelle, F. (2012). New insights into ER stress-induced insulin resistance. In *Trends in Endocrinology and Metabolism*. <https://doi.org/10.1016/j.tem.2012.06.003>
46. Furmli, S., Elmasry, R., Ramos, M., & Fung, J. (2018). Therapeutic use of intermittent fasting for people with type 2 diabetes as an alternative to insulin. *BMJ Case Reports*. <https://doi.org/10.1136/bcr-2017-221854>
47. Furukawa-Hibi, Y., Kobayashi, Y., Chen, C., & Motoyama, N. (2005). FOXO transcription factors in cell-cycle regulation and the response to oxidative stress. In *Antioxidants and Redox Signaling* (Vol. 7, Issues 5–6, pp. 752–760). <https://doi.org/10.1089/ars.2005.7.752>
48. Gabbouj, S., Ryhänen, S., Marttinen, M., Wittrahm, R., Takalo, M., Kempainen, S., Martiskaine, H., Tanila, H., Haapasalo, A., Hiltunen, M., & Natunen, T. (2019). Altered insulin signaling in Alzheimer’s disease brain-special emphasis on pi3k-akt pathway.

In *Frontiers in Neuroscience*. <https://doi.org/10.3389/fnins.2019.00629>

49. Gailhouste, L., Liew, L. C., Hatada, I., Nakagama, H., & Ochiya, T. (2018). Epigenetic reprogramming using 5-azacytidine promotes an anti-cancer response in pancreatic adenocarcinoma cells. *Cell Death and Disease*, 9(5), 1–12. <https://doi.org/10.1038/s41419-018-0487-z>
50. Ge, P., Luo, Y., Liu, C. L., & Hu, B. (2007). Protein aggregation and proteasome dysfunction after brain ischemia. *Stroke*. <https://doi.org/10.1161/STROKEAHA.107.487108>
51. Ghanbarian, H., Wagner, N., Polo, B., Baudouy, D., Kiani, J., Michiels, J. F., Cuzin, F., Rassoulzadegan, M., & Wagner, K. D. (2016). Dnmt2/Trdmt1 as mediator of RNA polymerase II transcriptional activity in cardiac growth. *PLoS ONE*. <https://doi.org/10.1371/journal.pone.0156953>
52. Ghosh, A. P., Klocke, B. J., Ballestas, M. E., & Roth, K. A. (2012). CHOP Potentially Co-Operates with FOXO3a in Neuronal Cells to Regulate PUMA and BIM Expression in Response to ER Stress. *PLoS ONE*, 7(6), e39586. <https://doi.org/10.1371/journal.pone.0039586>
53. Goll, M. G., Kirpekar, F., Maggert, K. A., Yoder, J. A., Hsieh, C. L., Zhang, X., Golic, K. G., Jacobsen, S. E., & Bestor, T. H. (2006). Methylation of tRNA<sup>Asp</sup> by the DNA methyltransferase homolog Dnmt2. *Science*. <https://doi.org/10.1126/science.1120976>
54. Grant, C. S. (2005). Insulinoma. *Best Practice and Research: Clinical Gastroenterology*, 19(5 SPEC. ISS.), 783–798. <https://doi.org/10.1016/j.bpg.2005.05.008>
55. Greenberg, A. S., & Obin, M. S. (2006). Obesity and the role of adipose tissue in inflammation and metabolism. *American Journal of Clinical Nutrition*. <https://doi.org/10.1093/ajcn/83.2.461s>
56. Ha, D. P., & Lee, A. S. (2020). Insulin-like growth factor 1-receptor signaling stimulates GRP78 expression through the PI3K/AKT/mTOR/ATF4 axis. *Cellular Signalling*, 75, 109736. <https://doi.org/10.1016/j.cellsig.2020.109736>
57. Halim, M., & Halim, A. (2019). The effects of inflammation, aging and oxidative stress on the pathogenesis of diabetes mellitus (type 2 diabetes). In *Diabetes and Metabolic Syndrome: Clinical Research and Reviews*. <https://doi.org/10.1016/j.dsx.2019.01.040>
58. Halliwell, B., & Aruoma, O. I. (1991). DNA damage by oxygen-derived species Its mechanism and measurement in mammalian systems. In *FEBS Letters*.

[https://doi.org/10.1016/0014-5793\(91\)80347-6](https://doi.org/10.1016/0014-5793(91)80347-6)

59. Hamaguchi, K., Gaskins, H. R., & Leiter, E. H. (1991). NIT-1, a pancreatic  $\beta$ -cell line established from a transgenic NOD/Lt mouse. *Diabetes*, 40(7), 842–849. <https://doi.org/10.2337/diab.40.7.842>
60. Harding, H. P., Novoa, I., Zhang, Y., Zeng, H., Wek, R., Schapira, M., & Ron, D. (2000). Regulated translation initiation controls stress-induced gene expression in mammalian cells. *Molecular Cell*. [https://doi.org/10.1016/S1097-2765\(00\)00108-8](https://doi.org/10.1016/S1097-2765(00)00108-8)
61. Haschek, W. M., Rousseaux, C. G., & Wallig, M. A. (2009). Fundamentals of Toxicologic Pathology: Second Edition. In *Fundamentals of Toxicologic Pathology: Second Edition*. <https://doi.org/10.1016/C2009-0-02051-0>
62. Haze, K., Yoshida, H., Yanagi, H., Yura, T., & Mori, K. (1999). Mammalian transcription factor ATF6 is synthesized as a transmembrane protein and activated by proteolysis in response to endoplasmic reticulum stress. *Molecular Biology of the Cell*, 10(11), 3787–3799. <https://doi.org/10.1091/mbc.10.11.3787>
63. Holczer, M., Márton, M., Kurucz, A., Bánhegyi, G., & Kapuy, O. (2015). A comprehensive systems biological study of autophagy-apoptosis crosstalk during endoplasmic reticulum stress. *BioMed Research International*. <https://doi.org/10.1155/2015/319589>
64. Hollenbach, P. W., Nguyen, A. N., Brady, H., Williams, M., Ning, Y., Richard, N., Krushel, L., Aukerman, S. L., Heise, C., & MacBeth, K. J. (2010). A comparison of azacitidine and decitabine activities in acute myeloid leukemia cell lines. *PLoS ONE*. <https://doi.org/10.1371/journal.pone.0009001>
65. Hollien, J., Lin, J. H., Li, H., Stevens, N., Walter, P., & Weissman, J. S. (2009). Regulated Ire1-dependent decay of messenger RNAs in mammalian cells. *Journal of Cell Biology*. <https://doi.org/10.1083/jcb.200903014>
66. Hori, H. (2014). Methylated nucleosides in tRNA and tRNA methyltransferases. In *Frontiers in Genetics*. <https://doi.org/10.3389/fgene.2014.00144>
67. Horne, B. D., Grajower, M. M., & Anderson, J. L. (2020). Limited Evidence for the Health Effects and Safety of Intermittent Fasting among Patients with Type 2 Diabetes. In *JAMA - Journal of the American Medical Association*. <https://doi.org/10.1001/jama.2020.3908>
68. Hoseki, J., Ushioda, R., & Nagata, K. (2010). Mechanism and components of endoplasmic reticulum-associated degradation. In *Journal of Biochemistry*.

<https://doi.org/10.1093/jb/mvp194>

69. Høyer-Hansen, M., & Jäättelä, M. (2007). Connecting endoplasmic reticulum stress to autophagy by unfolded protein response and calcium. In *Cell Death and Differentiation*. <https://doi.org/10.1038/sj.cdd.4402200>
70. Hu, Y., Gao, Y., Zhang, M., Deng, K. Y., Singh, R., Tian, Q., Gong, Y., Pan, Z., Liu, Q., Boisclair, Y. R., & Long, Q. (2019). Endoplasmic reticulum–associated degradation (ERAD) has a critical role in supporting glucose-stimulated insulin secretion in pancreatic B-cells. *Diabetes*. <https://doi.org/10.2337/db18-0624>
71. Huang, X., Liu, G., Guo, J., & Su, Z. Q. (2018). The PI3K/AKT pathway in obesity and type 2 diabetes. In *International Journal of Biological Sciences*. <https://doi.org/10.7150/ijbs.27173>
72. Huber, A. L., Lebeau, J., Guillaumot, P., Pétrilli, V., Malek, M., Chilloux, J., Fauvet, F., Payen, L., Kfoury, A., Renno, T., Chevet, E., & Manié, S. N. (2013). P58IPK-Mediated Attenuation of the Proapoptotic PERK-CHOP Pathway Allows Malignant Progression upon Low Glucose. *Molecular Cell*. <https://doi.org/10.1016/j.molcel.2013.01.009>
73. Hutchinson, J. A., Shanware, N. P., Chang, H., & Tibbetts, R. S. (2011). Regulation of ribosomal protein S6 phosphorylation by casein kinase 1 and protein phosphatase 1. *Journal of Biological Chemistry*, 286(10), 8688–8696. <https://doi.org/10.1074/jbc.M110.141754>
74. Ibrahim, I. M., Abdelmalek, D. H., & Elfiky, A. A. (2019). GRP78: A cell's response to stress. In *Life Sciences* (Vol. 226, pp. 156–163). Elsevier Inc. <https://doi.org/10.1016/j.lfs.2019.04.022>
75. IDF Diabetes Atlas 9th edition. (2019). IDF Diabetes Atlas 9th edition 2019. In *International Diabetes Federation Diabetes Atlas, Ninth Edition*.
76. Inageda, K. (2010). Insulin modulates induction of glucose-regulated protein 78 during endoplasmic reticulum stress via augmentation of ATF4 expression in human neuroblastoma cells. *FEBS Letters*, 584(16), 3649–3654. <https://doi.org/10.1016/j.febslet.2010.07.040>
77. Itahana, K., Itahana, Y., & Dimri, G. P. (2013). Colorimetric detection of senescence-associated  $\beta$  galactosidase. *Methods in Molecular Biology*. [https://doi.org/10.1007/978-1-62703-239-1\\_8](https://doi.org/10.1007/978-1-62703-239-1_8)
78. Jeltsch, A., Ehrenhofer-Murray, A., Jurkowski, T. P., Lyko, F., Reuter, G., Ankri, S.,

- Nellen, W., Schaefer, M., & Helm, M. (2017). Mechanism and biological role of Dnmt2 in Nucleic Acid Methylation. In *RNA Biology*. <https://doi.org/10.1080/15476286.2016.1191737>
79. Jeon, M., Choi, H., Lee, S. I., Kim, J. S., Park, M., Kim, K., Lee, S., & Byun, S. J. (2016). GRP78 is required for cell proliferation and protection from apoptosis in chicken embryo fibroblast cells. *Poultry Science*. <https://doi.org/10.3382/ps/pew016>
80. Ji, C. H., & Kwon, Y. T. (2017). Crosstalk and interplay between the ubiquitin-proteasome system and autophagy. In *Molecules and Cells* (Vol. 40, Issue 7, pp. 441–449). Korean Society for Molecular and Cellular Biology. <https://doi.org/10.14348/molcells.2017.0115>
81. Jonkers, Y. M. H., Ramaekers, F. C. S., & Speel, E. J. M. (2007). Molecular alterations during insulinoma tumorigenesis. In *Biochimica et Biophysica Acta - Reviews on Cancer* (Vol. 1775, Issue 2, pp. 313–332). Elsevier. <https://doi.org/10.1016/j.bbcan.2007.05.004>
82. Jurkowski, T. P., Meusbürger, M., Phalke, S., Helm, M., Nellen, W., Reuter, G., & Jeltsch, A. (2008). Human DNMT2 methylates tRNA<sup>Asp</sup> molecules using a DNA methyltransferase-like catalytic mechanism. *RNA*. <https://doi.org/10.1261/rna.970408>
83. Kahn, C. R., & White, M. F. (1988). The insulin receptor and the molecular mechanism of insulin action. In *Journal of Clinical Investigation*. <https://doi.org/10.1172/JCI113711>
84. Kania, E., Roest, G., Vervliet, T., Parys, J. B., & Bultynck, G. (2017). IP3 receptor-mediated calcium signaling and its role in autophagy in cancer. In *Frontiers in Oncology*. <https://doi.org/10.3389/fonc.2017.00140>
85. Kemp, K. L., Lin, Z., Zhao, F., Gao, B., Song, J., Zhang, K., & Fang, D. (2013). The serine-threonine kinase inositol-requiring enzyme 1 $\alpha$  (IRE1 $\alpha$ ) promotes IL-4 production in T helper cells. *Journal of Biological Chemistry*, 288(46), 33272–33282. <https://doi.org/10.1074/jbc.M113.493171>
86. Kilarski, W. (2005). Strukturalne podstawy biologii komórki. In *Strukturalne podstawy biologii komórki*.
87. Kim, D. S., Kim, J. H., Lee, G. H., Kim, H. T., Lim, J. M., Chae, S. W., Chae, H. J., & Kim, H. R. (2010). p38 mitogen-activated protein kinase is involved in endoplasmic reticulum stress-induced cell death and autophagy in human gingival fibroblasts. *Biological and Pharmaceutical Bulletin*. <https://doi.org/10.1248/bpb.33.545>

88. Kooner, J. S., Saleheen, D., Sim, X., Sehmi, J., Zhang, W., Frossard, P., Been, L. F., Chia, K. S., Dimas, A. S., Hassanali, N., Jafar, T., Jowett, J. B. M., Li, X., Radha, V., Rees, S. D., Takeuchi, F., Young, R., Aung, T., Basit, A., ... Chambers, J. C. (2011). Genome-wide association study in individuals of South Asian ancestry identifies six new type 2 diabetes susceptibility loci. *Nature Genetics*. <https://doi.org/10.1038/ng.921>
89. Kops, G. J. P. L., Dansen, T. B., Polderman, P. E., Saarloos, I., Wirtz, K. W. A., Coffey, P. J., Huang, T. T., Bos, J. L., Medema, R. H., & Burgering, B. M. T. (2002). Forkhead transcription factor FOXO3a protects quiescent cells from oxidative stress. *Nature*, *419*(6904), 316–321. <https://doi.org/10.1038/nature01036>
90. Kuroda, A., Rauch, T. A., Todorov, I., Ku, H. T., Al-Abdullah, I. H., Kandeel, F., Mullen, Y., Pfeifer, G. P., & Ferreri, K. (2009). Insulin Gene Expression Is Regulated by DNA Methylation. *PLoS ONE*, *4*(9), e6953. <https://doi.org/10.1371/journal.pone.0006953>
91. Lee, E., Nichols, P., Spicer, D., Groshen, S., Yu, M. C., & Lee, A. S. (2006). GRP78 as a novel predictor of responsiveness to chemotherapy in breast cancer. *Cancer Research*. <https://doi.org/10.1158/0008-5472.CAN-06-1660>
92. Lehtinen, M. K., Yuan, Z., Boag, P. R., Yang, Y., Villén, J., Becker, E. B. E., DiBacco, S., de la Iglesia, N., Gygi, S., Blackwell, T. K., & Bonni, A. (2006). A Conserved MST-FOXO Signaling Pathway Mediates Oxidative-Stress Responses and Extends Life Span. *Cell*, *125*(5), 987–1001. <https://doi.org/10.1016/j.cell.2006.03.046>
93. Levine, A. B., Punihale, D., & Levine, T. B. (2012). Characterization of the role of nitric oxide and its clinical applications. *Cardiology (Switzerland)*, *122*(1), 55–68. <https://doi.org/10.1159/000338150>
94. Lewinska, A., Adamczyk-Grochala, J., Kwasniewicz, E., Deregowska, A., Semik, E., Zabek, T., & Wnuk, M. (2018). Reduced levels of methyltransferase DNMT2 sensitize human fibroblasts to oxidative stress and DNA damage that is accompanied by changes in proliferation-related miRNA expression. *Redox Biology*. <https://doi.org/10.1016/j.redox.2017.08.012>
95. Lewinska, A., Adamczyk-Grochala, J., Kwasniewicz, E., & Wnuk, M. (2017). Downregulation of methyltransferase Dnmt2 results in condition-dependent telomere shortening and senescence or apoptosis in mouse fibroblasts. *Journal of Cellular Physiology*. <https://doi.org/10.1002/jcp.25848>
96. Li, L. H., Olin, E. J., Buskirk, H. H., & Reineke, L. M. (1970). Cytotoxicity and Mode

- of Action of 5-Azacytidine on L1210 Leukemia. *Cancer Research*.
97. Li, R., Yang, Y., Hong, P., Zhang, Z., Li, L., Hui, J., & Zheng, X. (2020).  $\beta$ -carotene attenuates weaning-induced apoptosis via inhibition of PERK-CHOP and IRE1-JNK/p38 MAPK signalling pathways in piglet jejunum. *Journal of Animal Physiology and Animal Nutrition*. <https://doi.org/10.1111/jpn.13216>
  98. Li, W., Yang, Q., & Mao, Z. (2018). Signaling and induction of chaperone-mediated autophagy by the endoplasmic reticulum under stress conditions. In *Autophagy*. <https://doi.org/10.1080/15548627.2018.1444314>
  99. Li, W., Zhu, J., Dou, J., She, H., Tao, K., Xu, H., Yang, Q., & Mao, Z. (2017). Phosphorylation of LAMP2A by p38 MAPK couples ER stress to chaperone-mediated autophagy. *Nature Communications*. <https://doi.org/10.1038/s41467-017-01609-x>
  100. Lin, W., & Stone, S. (2020). Unfolded protein response in myelin disorders. In *Neural Regeneration Research* (Vol. 15, Issue 4, pp. 636–645). Wolters Kluwer Medknow Publications. <https://doi.org/10.4103/1673-5374.266903>
  101. Lindholm, D., Wootz, H., & Korhonen, L. (2006). ER stress and neurodegenerative diseases. In *Cell Death and Differentiation*. <https://doi.org/10.1038/sj.cdd.4401778>
  102. Lipson, K. L., Fonseca, S. G., Ishigaki, S., Nguyen, L. X., Foss, E., Bortell, R., Rossini, A. A., & Urano, F. (2006). Regulation of insulin biosynthesis in pancreatic beta cells by an endoplasmic reticulum-resident protein kinase IRE1. *Cell Metabolism*. <https://doi.org/10.1016/j.cmet.2006.07.007>
  103. Lipson, K. L., Ghosh, R., & Urano, F. (2008). The role of IRE1 $\alpha$  in the degradation of insulin mRNA in pancreatic  $\beta$ -cells. *PLoS ONE*. <https://doi.org/10.1371/journal.pone.0001648>
  104. Liu, B., Hutchison, A. T., Thompson, C. H., Lange, K., Wittert, G. A., & Heilbronn, L. K. (2020). Effects of Intermittent Fasting or Calorie Restriction on Markers of Lipid Metabolism in Human Skeletal Muscle. *The Journal of Clinical Endocrinology & Metabolism*. <https://doi.org/10.1210/clinem/dgaa707>
  105. Liu, C. W., Bramer, L., Webb-Robertson, B. J., Waugh, K., Rewers, M. J., & Zhang, Q. (2018). Temporal expression profiling of plasma proteins reveals oxidative stress in early stages of Type 1 Diabetes progression. *Journal of Proteomics*, 172, 100–110. <https://doi.org/10.1016/j.jprot.2017.10.004>
  106. Liu, Y., Santi, D. V., & Walsh, C. T. (2000). m<sup>5</sup>C RNA and m<sup>5</sup>C DNA methyl



- transferases use different cysteine residues as catalysts Scheme 1. Proposed mechanism for methylation of cytosine nucleotides. In *PNAS July*.
107. Longnecker, D. S. (2021). Anatomy and Histology of the Pancreas. *Pancreapedia: The Exocrine Pancreas Knowledge Base*. <https://doi.org/10.3998/PANC.2021.01>
  108. Lu, P. D., Harding, H. P., & Ron, D. (2004). Translation reinitiation at alternative open reading frames regulates gene expression in an integrated stress response. *Journal of Cell Biology*. <https://doi.org/10.1083/jcb.200408003>
  109. Maechler, P., Jornot, L., & Wollheim, C. B. (1999). Hydrogen peroxide alters mitochondrial activation and insulin secretion in pancreatic beta cells. *Journal of Biological Chemistry*, 274(39), 27905–27913. <https://doi.org/10.1074/jbc.274.39.27905>
  110. Małeckki, M. T. (2006). Otyłość – insulinooporność – cukrzyca typu 2. *Kardiologia Polska*.
  111. Marinkovic, D., Zhang, X., Yalcin, S., Luciano, J. P., Brugnara, C., Huber, T., & Ghaffari, S. (2007). Foxo3 is required for the regulation of oxidative stress in erythropoiesis. *Journal of Clinical Investigation*, 117(8), 2133–2144. <https://doi.org/10.1172/JCI31807>
  112. Meyuhis, O. (2015). Ribosomal Protein S6 Phosphorylation: Four Decades of Research. *International Review of Cell and Molecular Biology*, 320, 41–73. <https://doi.org/10.1016/bs.ircmb.2015.07.006>
  113. Mizushima, N. (2007). Autophagy: Process and function. In *Genes and Development*. <https://doi.org/10.1101/gad.1599207>
  114. Molfino, A., Cascino, A., Conte, C., Ramaccini, C., Rossi Fanelli, F., & Laviano, A. (2010). Caloric restriction and L-carnitine administration improves insulin sensitivity in patients with impaired glucose metabolism. *Journal of Parenteral and Enteral Nutrition*. <https://doi.org/10.1177/0148607109353440>
  115. Moore, L. D., Le, T., & Fan, G. (2013). DNA methylation and its basic function. In *Neuropsychopharmacology* (Vol. 38, Issue 1, pp. 23–38). Nature Publishing Group. <https://doi.org/10.1038/npp.2012.112>
  116. Morton, A. (2019). Azacitidine-induced hyperglycaemia. *BMJ Case Reports*, 12(11), e231903. <https://doi.org/10.1136/bcr-2019-231903>
  117. Müller, A., & Florek, M. (2010). 5-Azacytidine/Azacitidine. In *Recent Results*

- in Cancer Research*. [https://doi.org/10.1007/978-3-642-01222-8\\_11](https://doi.org/10.1007/978-3-642-01222-8_11)
118. Muñoz-Espin, D., & Demaria, M. (Eds.). (2020). *Senolytics in Disease, Ageing and Longevity* (Vol. 11). Springer International Publishing. <https://doi.org/10.1007/978-3-030-44903-2>
  119. Murray, R. K., Granner, D. K., & Rodwell, V. W. (2015). *Biochemia Harpera*. In *Pzwl*.
  120. Nastos, C., Giannouloupoulos, D., Dellaportas, D., Mizamtsidi, M., Dafnios, N., Klonaris, N., Kalogeris, N., & Vryonidou, A. (2020). Sudden ‘cure’ of type two diabetes due to pancreatic insulinoma: A case report. *Molecular and Clinical Oncology*, *12*(2), 174–178. <https://doi.org/10.3892/mco.2019.1957>
  121. Nelson 1942-, D. L. (David L. (2005). *Lehninger principles of biochemistry*. Fifth edition. New York : W.H. Freeman, 2005. <https://search.library.wisc.edu/catalog/999964334502121>
  122. Nho, R. S. (2014). FoxO3a and disease progression. *World Journal of Biological Chemistry*, *5*(3), 346. <https://doi.org/10.4331/wjbc.v5.i3.346>
  123. Niedernhofer, L. J., & Robbins, P. D. (2018). Senotherapeutics for healthy ageing. In *Nature Reviews Drug Discovery* (Vol. 17, Issue 5, p. 377). Nature Publishing Group. <https://doi.org/10.1038/nrd.2018.44>
  124. Nishimura, M., Obayashi, H., Maruya, E., Ohta, M., Tegoshi, H., Fukui, M., Hasegawa, G., Shigeta, H., Kitagawa, Y., Nakano, K., Saji, H., & Nakamura, N. (2000). Association between type 1 diabetes age-at-onset and intercellular adhesion molecule-1 (ICAM-1) gene polymorphism. *Human Immunology*. [https://doi.org/10.1016/S0198-8859\(00\)00101-4](https://doi.org/10.1016/S0198-8859(00)00101-4)
  125. Nisticò, L., Buzzetti, R., Pritchard, L. E., Van Der Auwera, B., Giovannini, C., Bosi, E., Martinez Larrad, M. T., Rios, M. S., Chow, C. C., Cockram, C. S., Jacobs, K., Mijovic, C., Bain, S. C., Barnett, A. H., Vandewalle, C. L., Schuit, F., Gorus, F. K., Tosi, R., Pozzilli, P., & Todd, J. A. (1996). The CTLA-4 gene region of chromosome 2q33 is linked to, and associated with, type 1 diabetes. *Human Molecular Genetics*. <https://doi.org/10.1093/hmg/5.7.1075>
  126. Noda, T., Fujita, N., & Yoshimori, T. (2009). The late stages of autophagy: How does the end begin? In *Cell Death and Differentiation*. <https://doi.org/10.1038/cdd.2009.54>
  127. Novosyadlyy, R., Kurshan, N., Lann, D., Vijayakumar, A., Yakar, S., &

- LeRoith, D. (2008). Insulin-like growth factor-I protects cells from ER stress-induced apoptosis via enhancement of the adaptive capacity of endoplasmic reticulum. *Cell Death and Differentiation*. <https://doi.org/10.1038/cdd.2008.52>
128. Nuss, J. E., Choksi, K. B., DeFord, J. H., & Papaconstantinou, J. (2008). Decreased enzyme activities of chaperones PDI and BiP in aged mouse livers. *Biochemical and Biophysical Research Communications*. <https://doi.org/10.1016/j.bbrc.2007.10.194>
129. Nykiforuk, C. L., Boothe, J. G., Murray, E. W., Keon, R. G., Goren, H. J., Markley, N. A., & Moloney, M. M. (2006). Transgenic expression and recovery of biologically active recombinant human insulin from *Arabidopsis thaliana* seeds. *Plant Biotechnology Journal*. <https://doi.org/10.1111/j.1467-7652.2005.00159.x>
130. Ogata, M., Hino, S., Saito, A., Morikawa, K., Kondo, S., Kanemoto, S., Murakami, T., Taniguchi, M., Tanii, I., Yoshinaga, K., Shiosaka, S., Hammarback, J. A., Urano, F., & Imaizumi, K. (2006). Autophagy Is Activated for Cell Survival after Endoplasmic Reticulum Stress. *Molecular and Cellular Biology*. <https://doi.org/10.1128/mcb.01453-06>
131. Okabayashi, T., Shima, Y., Sumiyoshi, T., Kozuki, A., Ito, S., Ogawa, Y., Kobayashi, M., & Hanazaki, K. (2013). Diagnosis and management of insulinoma. In *World Journal of Gastroenterology* (Vol. 19, Issue 6, pp. 829–837). Baishideng Publishing Group Co. <https://doi.org/10.3748/wjg.v19.i6.829>
132. Okano, M., Xie, S., & Li, E. (1998). Dnmt2 is not required for de novo and maintenance methylation of viral DNA in embryonic stem cells. *Nucleic Acids Research*. <https://doi.org/10.1093/nar/26.11.2536>
133. Palmer, J. P., Asplin, C. M., Clemons, P., Lyen, K., Tatpati, O., Raghu, P. K., & Paquette, T. L. (1983). Insulin antibodies in insulin-dependent diabetics before insulin treatment. *Science*. <https://doi.org/10.1126/science.6362005>
134. Pardo, P. S., Hajira, A., Boriek, A. M., & Mohamed, J. S. (2017). MicroRNA-434-3p regulates age-related apoptosis through eIF5A1 in the skeletal muscle. *Aging*. <https://doi.org/10.18632/aging.101207>
135. Park, S., Yoo, K. M., Hyun, J. S., & Kang, S. (2017). Intermittent fasting reduces body fat but exacerbates hepatic insulin resistance in young rats regardless of high protein and fat diets. *Journal of Nutritional Biochemistry*. <https://doi.org/10.1016/j.jnutbio.2016.10.003>

136. Paula, P. C., Oliveira, J. T. A., Sousa, D. O. B., Alves, B. G. T., Carvalho, A. F. U., Franco, O. L., & Vasconcelos, I. M. (2017). Insulin-like plant proteins as potential innovative drugs to treat diabetes—The *Moringa oleifera* case study. *New Biotechnology*. <https://doi.org/10.1016/j.nbt.2016.10.005>
137. Pearson, J. A., Wong, F. S., & Wen, L. (2016). The importance of the Non Obese Diabetic (NOD) mouse model in autoimmune diabetes. In *Journal of Autoimmunity* (Vol. 66, pp. 76–88). Academic Press. <https://doi.org/10.1016/j.jaut.2015.08.019>
138. Pickart, C. M. (1997). Targeting of substrates to the 26S proteasome. *The FASEB Journal*. <https://doi.org/10.1096/fasebj.11.13.9367341>
139. Pirot, P., Naamane, N., Libert, F., Magnusson, N. E., Ørntoft, T. F., Cardozo, A. K., & Eizirik, D. L. (2007). Global profiling of genes modified by endoplasmic reticulum stress in pancreatic beta cells reveals the early degradation of insulin mRNAs. *Diabetologia*. <https://doi.org/10.1007/s00125-007-0609-0>
140. Pirot, Pierre, Cardozo, A. K., & Eizirik, D. L. (2008). Mediators and mechanisms of pancreatic beta-cell death in type 1 diabetes. In *Arquivos Brasileiros de Endocrinologia e Metabologia* (Vol. 52, Issue 2, pp. 156–165). ABE&M. <https://doi.org/10.1590/S0004-27302008000200003>
141. Pískala, A., & Šorm, F. (1964). Nucleic acids components and their analogues. LI. Synthesis of 1-glycosyl derivatives of 5-azauracil and 5-azacytosine. *Collection of Czechoslovak Chemical Communications*. <https://doi.org/10.1135/cccc19642060>
142. Pociot, F., & Lernmark, Å. (2016). Genetic risk factors for type 1 diabetes. In *The Lancet*. [https://doi.org/10.1016/S0140-6736\(16\)30582-7](https://doi.org/10.1016/S0140-6736(16)30582-7)
143. Poitout, V., Stout, L. E., Armstrong, M. B., Walseth, T. F., Sorenson, R. L., & Robertson, R. P. (1995). Morphological and functional characterization of  $\beta$ TC-6 cells - An insulin-secreting cell line derived from transgenic mice. *Diabetes*, 44(3), 306–313. <https://doi.org/10.2337/diab.44.3.306>
144. Ponard, A., Ferreira-Maldent, N., Ertault, M., Delain, M., Amraoui, K., Regina, S., Jonville-Béra, A. P., Hérault, O., Colombat, P., & Gyan, E. (2018). Glycemic dysregulation in a patient with type 2 diabetes treated with 5-azacitidine: A case report. *Journal of Medical Case Reports*, 12(1), 1–4. <https://doi.org/10.1186/s13256-018-1690-3>
145. Popkin, B. M. (2015). Nutrition Transition and the Global Diabetes Epidemic. In *Current Diabetes Reports*. <https://doi.org/10.1007/s11892-015-0631-4>

146. Prischi, F., Nowak, P. R., Carrara, M., & Ali, M. M. U. (2014). Phosphoregulation of Ire1 RNase splicing activity. *Nature Communications*, 5(1), 1–11. <https://doi.org/10.1038/ncomms4554>
147. Raasi, S., & Wolf, D. H. (2007). Ubiquitin receptors and ERAD: A network of pathways to the proteasome. In *Seminars in Cell and Developmental Biology*. <https://doi.org/10.1016/j.semcdb.2007.09.008>
148. Raddatz, G., Guzzardo, P. M., Olova, N., Fantappiè, M. R., Rampp, M., Schaefer, M., Reik, W., Hannon, G. J., & Lyko, F. (2013). Dnmt2-dependent methylomes lack defined DNA methylation patterns. *Proceedings of the National Academy of Sciences of the United States of America*, 110(21), 8627–8631. <https://doi.org/10.1073/pnas.1306723110>
149. Rai, K., Chidester, S., Zavala, C. V., Manos, E. J., James, S. R., Karpf, A. R., Jones, D. A., & Cairns, B. R. (2007). Dnmt2 functions in the cytoplasm to promote liver, brain, and retina development in zebrafish. *Genes and Development*. <https://doi.org/10.1101/gad.1472907>
150. Rashid, H. O., Yadav, R. K., Kim, H. R., & Chae, H. J. (2015). ER stress: Autophagy induction, inhibition and selection. *Autophagy*, 11(11), 1956–1977. <https://doi.org/10.1080/15548627.2015.1091141>
151. Reed, M. J., & Scribner, K. A. (1999). In-vivo and in-vitro models of type 2 diabetes in pharmaceutical drug discovery. In *Diabetes, Obesity and Metabolism*. <https://doi.org/10.1046/j.1463-1326.1999.00014.x>
152. Reinhardt, H. C., & Schumacher, B. (2012). The p53 network: Cellular and systemic DNA damage responses in aging and cancer. In *Trends in Genetics*. <https://doi.org/10.1016/j.tig.2011.12.002>
153. Rodier, F., Campisi, J., & Bhaumik, D. (2007). Two faces of p53: Aging and tumor suppression. *Nucleic Acids Research*. <https://doi.org/10.1093/nar/gkm744>
154. Rui, J., Deng, S., Lebastchi, J., Clark, P. L., Usmani-Brown, S., & Herold, K. C. (2016). Methylation of insulin DNA in response to proinflammatory cytokines during the progression of autoimmune diabetes in NOD mice. *Diabetologia*, 59(5), 1021–1029. <https://doi.org/10.1007/s00125-016-3897-4>
155. Runwal, G., Stamatakou, E., Siddiqi, F. H., Puri, C., Zhu, Y., & Rubinsztein, D. C. (2019). LC3-positive structures are prominent in autophagy-deficient cells. *Scientific Reports*. <https://doi.org/10.1038/s41598-019-46657-z>

156. Ruvinsky, I., Sharon, N., Lerer, T., Cohen, H., Stolovich-Rain, M., Nir, T., Dor, Y., Zisman, P., & Meyuhass, O. (2005). Ribosomal protein S6 phosphorylation is a determinant of cell size and glucose homeostasis. *Genes and Development*. <https://doi.org/10.1101/gad.351605>
157. Sandow, J., Landgraf, W., Becker, R., & Seipke, G. (2015). Equivalent recombinant human insulin preparations and their place in therapy. *European Endocrinology*. <https://doi.org/10.17925/ee.2015.11.01.10>
158. Sano, R., & Reed, J. C. (2013). ER stress-induced cell death mechanisms. In *Biochimica et Biophysica Acta - Molecular Cell Research*. <https://doi.org/10.1016/j.bbamcr.2013.06.028>
159. Schaefer, M., Hagemann, S., Hanna, K., & Lyko, F. (2009). Azacytidine inhibits RNA methylation at DNMT2 target sites in human cancer cell lines. *Cancer Research*. <https://doi.org/10.1158/0008-5472.CAN-09-0458>
160. Schaefer, M., & Lyko, F. (2010). Solving the Dnmt2 enigma. In *Chromosoma*. <https://doi.org/10.1007/s00412-009-0240-6>
161. Schaefer, M., Steringer, J. P., & Lyko, F. (2008). The Drosophila Cytosine-5 Methyltransferase Dnmt2 Is Associated with the Nuclear Matrix and Can Access DNA during Mitosis. *PLoS ONE*, 3(1), e1414. <https://doi.org/10.1371/journal.pone.0001414>
162. Schmid, I., Uittenbogaart, C., & Jamieson, B. D. (2007). Live-cell assay for detection of apoptosis by dual-laser flow cytometry using Hoechst 33342 and 7-amino-actinomycin D. *Nature Protocols*. <https://doi.org/10.1038/nprot.2006.458>
163. Schröder, M. (2008). Endoplasmic reticulum stress responses. In *Cellular and Molecular Life Sciences*. <https://doi.org/10.1007/s00018-007-7383-5>
164. Shackelford, R. E., Kaufmann, W. K., & Paules, R. S. (2000). Oxidative stress and cell cycle checkpoint function. *Free Radical Biology and Medicine*, 28(9), 1387–1404. [https://doi.org/10.1016/S0891-5849\(00\)00224-0](https://doi.org/10.1016/S0891-5849(00)00224-0)
165. Shanmugam, R., Aklujkar, M., Schäfer, M., Reinhardt, R., Nickel, O., Reuter, G., Lovley, D. R., Ehrenhofer-Murray, A., Nellen, W., Ankri, S., Helm, M., Jurkowski, T. P., & Jeltsch, A. (2014a). The Dnmt2 RNA methyltransferase homolog of *Geobacter sulfurreducens* specifically methylates tRNA-Glu. *Nucleic Acids Research*. <https://doi.org/10.1093/nar/gku256>
166. Shanmugam, R., Aklujkar, M., Schäfer, M., Reinhardt, R., Nickel, O., Reuter, G., Lovley, D. R., Ehrenhofer-Murray, A., Nellen, W., Ankri, S., Helm, M., Jurkowski,

- T. P., & Jeltsch, A. (2014b). The Dnmt2 RNA methyltransferase homolog of *Geobacter sulfurreducens* specifically methylates tRNA-Glu. *Nucleic Acids Research*, *42*(10), 6487–6496. <https://doi.org/10.1093/nar/gku256>
167. Shen, J., Chen, X., Hendershot, L., & Prywes, R. (2002). ER stress regulation of ATF6 localization by dissociation of BiP/GRP78 binding and unmasking of golgi localization signals. *Developmental Cell*. [https://doi.org/10.1016/S1534-5807\(02\)00203-4](https://doi.org/10.1016/S1534-5807(02)00203-4)
168. Shin, J. J., Gorden, P., & Libutti, S. K. (2010). Insulinoma: pathophysiology, localization and management. In *Future oncology (London, England)* (Vol. 6, Issue 2, pp. 229–237). <https://doi.org/10.2217/fon.09.165>
169. Shlush, L. I., Itzkovitz, S., Cohen, A., Rutenberg, A., Berkovitz, R., Yehezkel, S., Shahar, H., Selig, S., & Skorecki, K. (2011). Quantitative digital in situ senescence-associated  $\beta$ -galactosidase assay. *BMC Cell Biology*. <https://doi.org/10.1186/1471-2121-12-16>
170. Soare, A., Weiss, E. P., & Pozzilli, P. (2014). Benefits of caloric restriction for cardiometabolic health, including type 2 diabetes mellitus risk. In *Diabetes/Metabolism Research and Reviews*. <https://doi.org/10.1002/dmrr.2517>
171. Song, S., Tan, J., Miao, Y., Li, M., & Zhang, Q. (2017). Crosstalk of autophagy and apoptosis: Involvement of the dual role of autophagy under ER stress. In *Journal of Cellular Physiology*. <https://doi.org/10.1002/jcp.25785>
172. Sugisawa, N., Yamamoto, J., Han, Q., Tan, Y., Tashiro, Y., Nishino, H., Inubushi, S., Hamada, K., Kawaguchi, K., Unno, M., Bouvet, M., & Hoffman, R. M. (2021). Triple-Methyl Blockade With Recombinant Methioninase, Cycloleucine, and Azacitidine Arrests a Pancreatic Cancer Patient-Derived Orthotopic Xenograft Model. *Pancreas*, *50*(1), 93–98. <https://doi.org/10.1097/MPA.0000000000001709>
173. Sun, W. T., Wang, X. C., Mak, S. K., He, G. W., Liu, X. C., Underwood, M. J., & Yang, Q. (2017). Activation of PERK branch of ER stress mediates homocysteine-induced BKCa channel dysfunction in coronary artery via FoxO3-dependent regulation of atrogin-1. *Oncotarget*, *8*(31), 51462–51477. <https://doi.org/10.18632/oncotarget.17721>
174. Suzuki, M., & Boothman, D. A. (n.d.). *Stress-induced Premature Senescence (SIPS)-Influence of SIPS on Radiotherapy*. <https://doi.org/10.1269/jrr.07081>
175. T. Hamilton, R. (2012). Mouse Models of Oxidative Stress Indicate a Role for

- Modulating Healthy Aging. *Journal of Clinical & Experimental Pathology*.  
<https://doi.org/10.4172/2161-0681.s4-005>
176. Tan, L., Register, T. C., & Yammani, R. R. (2020). Age-related decline in expression of molecular chaperones induces endoplasmic reticulum stress and chondrocyte apoptosis in articular cartilage. *Aging and Disease*.  
<https://doi.org/10.14336/AD.2019.1130>
177. Tanida, I. (2011). Autophagy basics. In *Microbiology and Immunology*.  
<https://doi.org/10.1111/j.1348-0421.2010.00271.x>
178. *The Biology of the Cell Cycle - J. M. Mitchison - Google Books*. (n.d.). Retrieved March 25, 2021, from  
[https://books.google.it/books?hl=en&lr=&id=VFw4AAAAIAAJ&oi=fnd&pg=PA1&dq=cell+cycle+&ots=IRhvr0eGd2&sig=UJdUJ9iVmvoZklztseMNL7sVae8&redir\\_esc=y#v=onepage&q=cell cycle&f=false](https://books.google.it/books?hl=en&lr=&id=VFw4AAAAIAAJ&oi=fnd&pg=PA1&dq=cell+cycle+&ots=IRhvr0eGd2&sig=UJdUJ9iVmvoZklztseMNL7sVae8&redir_esc=y#v=onepage&q=cell cycle&f=false)
179. *The Pancreas: An Integrated Textbook of Basic Science, Medicine, and Surgery - Google Books*. (n.d.). Retrieved April 2, 2021, from  
[https://books.google.it/books?hl=en&lr=&id=uq9FDwAAQBAJ&oi=fnd&pg=PA10&dq=pancreas+anatomy+and+histology&ots=nrjDYye4ES&sig=lxRUyOv7GnxNtu1Ds gpt8EjyIk&redir\\_esc=y#v=onepage&q=pancreas anatomy and histology&f=false](https://books.google.it/books?hl=en&lr=&id=uq9FDwAAQBAJ&oi=fnd&pg=PA10&dq=pancreas+anatomy+and+histology&ots=nrjDYye4ES&sig=lxRUyOv7GnxNtu1Ds gpt8EjyIk&redir_esc=y#v=onepage&q=pancreas anatomy and histology&f=false)
180. Thiagarajan, D., Dev, R. R., & Khosla, S. (2011). The DNA methyltransferase Dnmt2 participates in RNA processing during cellular stress. *Epigenetics*, 6(1), 103–113. <https://doi.org/10.4161/epi.6.1.13418>
181. Toussaint, O., Medrano, E. E., & Von Zglinicki, T. (2000). Cellular and molecular mechanisms of stress-induced premature senescence (SIPS) of human diploid fibroblasts and melanocytes. In *Experimental Gerontology* (Vol. 35, Issue 8, pp. 927–945). Pergamon. [https://doi.org/10.1016/S0531-5565\(00\)00180-7](https://doi.org/10.1016/S0531-5565(00)00180-7)
182. Toussaint, Olivier, Royer, V., Salmon, M., & Remacle, J. (2002). Stress-induced premature senescence and tissue ageing. *Biochemical Pharmacology*, 64(5–6), 1007–1009. [https://doi.org/10.1016/S0006-2952\(02\)01170-X](https://doi.org/10.1016/S0006-2952(02)01170-X)
183. Tuorto, F., Herbst, F., Alerasool, N., Bender, S., Popp, O., Federico, G., Reitter, S., Liebers, R., Stoecklin, G., Gröne, H., Dittmar, G., Glimm, H., & Lyko, F. (2015). The tRNA methyltransferase Dnmt2 is required for accurate polypeptide synthesis during haematopoiesis. *The EMBO Journal*. <https://doi.org/10.15252/embj.201591382>
184. Tuorto, F., Liebers, R., Musch, T., Schaefer, M., Hofmann, S., Kellner, S., Frye,



- M., Helm, M., Stoecklin, G., & Lyko, F. (2012). RNA cytosine methylation by Dnmt2 and NSun2 promotes tRNA stability and protein synthesis. *Nature Structural and Molecular Biology*, *19*(9), 900–905. <https://doi.org/10.1038/nsmb.2357>
185. Urano, F., Wang, X. Z., Bertolotti, A., Zhang, Y., Chung, P., Harding, H. P., & Ron, D. (2000). Coupling of stress in the ER to activation of JNK protein kinases by transmembrane protein kinase IRE1. *Science*. <https://doi.org/10.1126/science.287.5453.664>
186. Vella, A., Cooper, J. D., Lowe, C. E., Walker, N., Nutland, S., Widmer, B., Jones, R., Ring, S. M., McArdle, W., Pembrey, M. E., Strachan, D. P., Dunger, D. B., Twells, R. C. J., Clayton, D. G., & Todd, J. A. (2005). Localization of a type 1 diabetes locus in the IL2RA/CD25 region by use of tag single-nucleotide polymorphisms. *American Journal of Human Genetics*. <https://doi.org/10.1086/429843>
187. Vermes, I., Haanen, C., Steffens-Nakken, H., & Reutelingsperger, C. (1995). A novel assay for apoptosis Flow cytometric detection of phosphatidylserine expression on early apoptotic cells using fluorescein labelled Annexin V. *Journal of Immunological Methods*. [https://doi.org/10.1016/0022-1759\(95\)00072-1](https://doi.org/10.1016/0022-1759(95)00072-1)
188. Vicencio, J. M., Ortiz, C., Criollo, A., Jones, A. W. E., Kepp, O., Galluzzi, L., Joza, N., Vitale, I., Morselli, E., Tailleur, M., Castedo, M., Maiuri, M. C., Molgó, J., Szabadkai, G., Lavandro, S., & Kroemer, G. (2009). The inositol 1,4,5-trisphosphate receptor regulates autophagy through its interaction with Beclin 1. *Cell Death and Differentiation*. <https://doi.org/10.1038/cdd.2009.34>
189. Walton, M., Sirimanne, E., Reutelingsperger, C., Williams, C., Gluckman, P., & Dragunow, M. (1997). Annexin V labels apoptotic neurons following hypoxia-ischemia. *NeuroReport*. <https://doi.org/10.1097/00001756-199712220-00007>
190. Wang, M., Zhao, X. R., Wang, P., Li, L., Dai, Y., Huang, H., Lei, P., Zhu, H. F., & Shen, G. X. (2007). Glucose regulated proteins 78 protects insulinoma cells (NIT-1) from death induced by streptozotocin, cytokines or cytotoxic T lymphocytes. *International Journal of Biochemistry and Cell Biology*, *39*(11), 2076–2082. <https://doi.org/10.1016/j.biocel.2007.05.022>
191. Wang, Miao, Wey, S., Zhang, Y., Ye, R., & Lee, A. S. (2009). Role of the unfolded protein response regulator GRP78/BiP in development, cancer, and neurological disorders. In *Antioxidants and Redox Signaling*. <https://doi.org/10.1089/ars.2009.2485>

192. Wang, Q., & Zou, M. H. (2018). Measurement of reactive oxygen species (ROS) and mitochondrial ROS in AMPK knockout mice blood vessels. In *Methods in Molecular Biology*. [https://doi.org/10.1007/978-1-4939-7598-3\\_32](https://doi.org/10.1007/978-1-4939-7598-3_32)
193. Watanabe, M., Hayasaki, H., Tamayama, T., & Shimada, M. (1998). Histologic distribution of insulin and glucagon receptors. *Brazilian Journal of Medical and Biological Research*. <https://doi.org/10.1590/S0100-879X1998000200008>
194. Wei, F. Y., Suzuki, T., Watanabe, S., Kimura, S., Kaitsuka, T., Fujimura, A., Matsui, H., Atta, M., Michiue, H., Fontecave, M., Yamagata, K., Suzuki, T., & Tomizawa, K. (2011). Deficit of tRNA<sup>Lys</sup> modification by Cdkal1 causes the development of type 2 diabetes in mice. *Journal of Clinical Investigation*. <https://doi.org/10.1172/JCI58056>
195. Wei, F. Y., & Tomizawa, K. (2011). Functional loss of Cdkal1, a novel tRNA modification enzyme, causes the development of type 2 diabetes. In *Endocrine Journal*. <https://doi.org/10.1507/endocrj.EJ11-0099>
196. Wei, F. Y., & Tomizawa, K. (2012). Development of type 2 diabetes caused by a deficiency of a tRNA lys modification. *Islets*. <https://doi.org/10.4161/isl.4.1.18262>
197. Weiss, M., Steiner, D. F., & Philipson, L. H. (2000). Insulin Biosynthesis, Secretion, Structure, and Structure-Activity Relationships. In *Endotext*.
198. Wiesenborn, D. S., Menon, V., Zhi, X., Do, A., Gesing, A., Wang, Z., Bartke, A., Altomare, D. A., & Masternak, M. M. (2014). The effect of calorie restriction on insulin signaling in skeletal muscle and adipose tissue of Ames dwarf mice. *Aging*. <https://doi.org/10.18632/aging.100700>
199. Xie, Z., & Klionsky, D. J. (2007). Autophagosome formation: Core machinery and adaptations. In *Nature Cell Biology*. <https://doi.org/10.1038/ncb1007-1102>
200. Xue, S., Xu, H., Sun, Z., Shen, H., Chen, S., Ouyang, J., Zhou, Q., Hu, X., & Cui, H. (2019). Depletion of TRDMT1 affects 5-methylcytosine modification of mRNA and inhibits HEK293 cell proliferation and migration. *Biochemical and Biophysical Research Communications*. <https://doi.org/10.1016/j.bbrc.2019.09.098>
201. Yamamoto, K., Sato, T., Matsui, T., Sato, M., Okada, T., Yoshida, H., Harada, A., & Mori, K. (2007). Transcriptional Induction of Mammalian ER Quality Control Proteins Is Mediated by Single or Combined Action of ATF6 $\alpha$  and XBP1. *Developmental Cell*. <https://doi.org/10.1016/j.devcel.2007.07.018>
202. Yao, J., Weng, Y., Dickey, A., & Wang, K. Y. (2015). Plants as factories for

- human pharmaceuticals: Applications and challenges. In *International Journal of Molecular Sciences*. <https://doi.org/10.3390/ijms161226122>
203. Yaribeygi, H., Atkin, S. L., Ramezani, M., & Sahebkar, A. (2019). A review of the molecular pathways mediating the improvement in diabetes mellitus following caloric restriction. In *Journal of Cellular Physiology*. <https://doi.org/10.1002/jcp.27760>
204. Yoshida, H. (2007). ER stress and diseases. In *FEBS Journal*. <https://doi.org/10.1111/j.1742-4658.2007.05639.x>
205. Yoshida, H., Matsui, T., Yamamoto, A., Okada, T., & Mori, K. (2001). XBP1 mRNA is induced by ATF6 and spliced by IRE1 in response to ER stress to produce a highly active transcription factor. *Cell*. [https://doi.org/10.1016/S0092-8674\(01\)00611-0](https://doi.org/10.1016/S0092-8674(01)00611-0)
206. Yuan, Q., Pan, A., Fu, Y., & Dai, Y. (2021). Anatomy and physiology of the pancreas. In *Integrative Pancreatic Intervention Therapy*. <https://doi.org/10.1016/b978-0-12-819402-7.00001-2>
207. Zelko, I. N., Mariani, T. J., & Folz, R. J. (2002). Superoxide dismutase multigene family: A comparison of the CuZn-SOD (SOD1), Mn-SOD (SOD2), and EC-SOD (SOD3) gene structures, evolution, and expression. In *Free Radical Biology and Medicine* (Vol. 33, Issue 3, pp. 337–349). Elsevier Inc. [https://doi.org/10.1016/S0891-5849\(02\)00905-X](https://doi.org/10.1016/S0891-5849(02)00905-X)
208. Zhan, H. X., Cong, L., Zhao, Y. P., Zhang, T. P., Chen, G., Zhou, L., & Guo, J. C. (2012). Activated mTOR/P70S6K signaling pathway is involved in insulinoma tumorigenesis. *Journal of Surgical Oncology*, 106(8), 972–980. <https://doi.org/10.1002/jso.23176>
209. Zhao, J., Brault, J. J., Schild, A., Cao, P., Sandri, M., Schiaffino, S., Lecker, S. H., & Goldberg, A. L. (2007). FoxO3 Coordinately Activates Protein Degradation by the Autophagic/Lysosomal and Proteasomal Pathways in Atrophying Muscle Cells. *Cell Metabolism*, 6(6), 472–483. <https://doi.org/10.1016/j.cmet.2007.11.004>
210. Zheng, Y., Tu, J., Wang, X., Yu, Y., Li, J., Jin, Y., & Wu, J. (2019). The therapeutic effect of melatonin on GC by inducing cell apoptosis and autophagy induced by endoplasmic reticulum stress. *Oncotargets and Therapy*. <https://doi.org/10.2147/OTT.S226140>
211. Zhu, Q. (2020). The ER stress-autophagy axis: Implications for cognitive dysfunction in diabetes mellitus. In *Clinical Science*.

<https://doi.org/10.1042/CS20200235>